

DISCLAIMER

"This book was prepared as an account of work sponsored by an agency of the United States Government. Neither the United States Government nor any agency thereof, nor any of their employees, makes any warranty, express or implied, or assumes any legal liability or responsibility for the accuracy, completeness, or usefulness of any information, apparatus, product, or process disclosed, or represents that its use would not infringe privately owned rights. Reference herein to any specific commercial product, process, or service by trade name, trademark, manufacturer, or otherwise, does not necessarily constitute or imply its endorsement, recommendation, or favoring by the United States Government or any agency thereof. The views and opinions of authors expressed herein do not necessarily state or reflect those of the United States Government or any agency thereof."

Available from the National Technical Information Service, U.S. Department of Commerce, Springfield, Virginia 22161.

NTIS price codes

Paper copy: \$9.00
Microfiche copy: \$3.50

IN-SITU COMBUSTION MODELS FOR THE
STEAM PLATEAU AND FOR FIELDWIDE OIL RECOVERY

SUPRI-TR-11

By

A. Satman, W.E. Brigham and H.J. Ramey, Jr.
Stanford University Petroleum Research Institute
Stanford, California 94305
415/497-0691

H.J. Lechtenberg, *Technical Project Officer*
San Francisco Operations Office
Fossil Energy Division
1333 Broadway
Oakland, California 94612
415/273-7951

Date Published—June 1981

Work Performed for the Department of Energy
Under Contract No. DE-AC03-76ET12056

U.S. DEPARTMENT OF ENERGY

TABLE OF CONTENTS

LIST OF FIGURES v

LIST OF TABLES vii

ACKNOWLEDGEMENT viii

ABSTRACT ix

1. INTRODUCTION 1

2. LITERATURE SURVEY. 4

 2.1 Mathematical Studies of Hot Fluid Injection
 and the Steam Plateau 4

 2.2 Experimental Studies of In-Situ Combustion. 7

 2.3 Studies of Oil Recovery Prediction for
 In-Situ Combustion Processes. 8

3. THEORY OF THE IN-SITU COMBUSTION PROCESS 11

4. THE STEAM PLATEAU MODEL. 15

 4.1 Conceptual Model of the Steam Plateau 15

 4.2 Mathematical Formulation of the Steam Plateau 17

 4.3 Solution to the Governing Equation Using
 the Method of Characteristics 25

 4.4 Application of the Steam Plateau Model
 to the Laboratory Runs. 30

5. EXPERIMENTAL EQUIPMENT 39

 5.1 Experimental Procedure. 44

Table of Contents, continued

5.2	Experimental Method and Results	45
5.2.1	Preparation of Pack.	45
5.2.2	Combustion Characteristics	46
5.2.3	Analysis of Products and Results	53
6.	RECOVERY CORRELATIONS FOR IN-SITU COMBUSTION PROCESSES.	61
6.1	Parameters Affecting Combustion Performance	61
6.2	In-Situ Combustion Correlation Efforts.	64
6.3	Correlation Technique	69
6.4	Case History Analysis of Fieldwide Dry In-Situ Combustion Tests.	70
6.5	Case History Analysis of Pilot Dry Combustion Tests.	84
6.6	Case History Analysis of Wet Combustion Tests	90
6.7	Application of Correlations	90
6.7.1	Bartlesville Sand Reservoir, Kansas.	91
6.7.2	The Sloss Field, Nebraska.	93
6.7.3	The South Belridge Field, California	94
7.	CONCLUSIONS.	98
	NOMENCLATURE	101
	REFERENCES	103
	APPENDICES	106
A	Derivation of Energy Balance in the Steam Plateau Region	106

20	CUMULATIVE INCREMENTAL OIL PRODUCTION VS CUMULATIVE AIR INJECTION FOR FIELDWIDE COMBUSTION TESTS	71
21	DIMENSIONLESS CUMULATIVE INCREMENTAL OIL VS AIR INJECTION FOR FIELDWIDE COMBUSTION TESTS	72
22	EFFECTS OF FUEL BURNED, ROCK VOLUME, AND OXYGEN UTILIZATION ON CUMULATIVE INCREMENTAL OIL VS AIR INJECTION FOR FIELD-WIDE COMBUSTION TESTS	75
23	EFFECT OF MULTIPLE LINEAR REGRESSION ANALYSIS ON DATA ON FIG. 22	77
24	FIRST CORRELATION CURVE	78
25	DATA FOR THE SECOND CORRELATION	81
26	SECOND CORRELATION CURVE	82
27	CUMULATIVE INCREMENTAL OIL PRODUCTION VS CUMULATIVE AIR INJECTION FOR PILOT DRY COMBUSTION TESTS	85
28	EFFECTS OF FUEL BURNED, ROCK VOLUME, AND OXYGEN INJECTION FOR PILOT DRY COMBUSTION TESTS	87
29	APPLICATION OF THE SECOND CORRELATION TO PILOT DRY COMBUSTION TESTS	88
30	APPLICATION OF THE SECOND CORRELATION TO BARTLESVILLE SAND	92
31	APPLICATION OF THE SECOND CORRELATION TO THE SOUTH BELRIDGE FIELD	96
32	RESULTS OF THE APPLICATION OF THE SECOND CORRELATION TO THE SOUTH BELRIDGE FIELD	97

LIST OF FIGURES

1	SCHEMATIC DIAGRAM OF IN-SITU COMBUSTION PROCESS (AFTER MCNIEL AND MOSS ³⁰)	12
2	MOVEMENT OF FLUID AND ROCK MATRIX RELATIVE TO X-COORDINATE SYSTEM	19
3	BEHAVIOR OF THE STEAM PLATEAU MODEL AND PROPAGATION PROFILES FOR CONSTANT MASS INJECTION RATE, CONSTANT INJECTION TEMPERATURE, AND CONSTANT THERMAL PROPERTIES	28
4	THE EFFECT OF OVERALL HEAT TRANSFER COEFFICIENT ON THE SOLUTION	29
5	THE EFFECT OF MASS FLUX INTO THE STEAM PLATEAU ON THE SOLUTION	29
6	COMPARISON OF THE CALCULATED AND EXPERIMENTAL RESULTS FOR RUN 78-2	31
7	GROWTH OF THE STEAM PLATEAU DURING RUN 78-2	33
8	COMPARISON OF THE CALCULATED AND EXPERIMENTAL RESULTS FOR ONE TRAVERSE OF RUN 78-2	36
9	SCHEMATIC TEMPERATURE PROFILE	38
10	SCHEMATIC DIAGRAM OF THE COMBUSTION TUBE APPARATUS	40
11	COMBUSTION TUBE ASSEMBLY	42
12	PRODUCED GAS RATE VS RUN TIME FOR RUN 78-4	48
13	PRODUCED GAS COMPOSITION VS RUN TIME FOR RUN 78-3	49
14	TEMPERATURE PROFILES FOR RUN 78-2	50
15	CUMULATIVE LIQUID PRODUCTION DATA FOR RUN 78-2	51
16	THE BURNING FRONT AND STEAM PLATEAU LOCATIONS FOR RUN 78-2	52
17	TEMPERATURE PROFILES FOR RUN 78-4	57
18	EFFECT OF AIR INJECTION PRESSURE ON THE STEAM PLATEAU TEMPERATURE.	58
19	EFFECT OF AIR FLUX ON THE STEAM PLATEAU GROWTH	59

Table of Contents, continued

B	Temperature Distribution in the Steam Plateau Under Adiabatic Conditions	108
C	Calculations of the Amount of Water Vaporized in the Region Between the Burning Front and Steam Plateau.	110

LIST OF TABLES

TABLE

1	Parts of the Combustion Tube Apparatus Shown on Figure 10.	41
2	Initial Pack Condition for Tube Runs.	47
3	Summary of Combustion Tube Results.	55
4A	In-Situ Combustion Test General Characteristics	66
4B	In-Situ Combustion Test Rock and Fluid Properties	67
4C	In-Situ Combustion Test Results	68

ACKNOWLEDGEMENT

The author would like to express his sincere appreciation to Professor William E. Brigham, for his guidance, understanding and encouragement as research advisor. His invaluable assistance was extremely helpful during the execution of this study. His constructive, critical review of the manuscript is also acknowledged.

The author is indebted to Professor Henry J. Ramey, Jr. co-research advisor, for his assistance and guidance pertaining to the steam plateau part of this work. Professors Ramey, Brigham, S.S. Marsden and F.G. Miller have given the author valuable insights into the petroleum engineering discipline.

Thanks are due to Professor Heber L. Cinco for his helpful discussions. The author is also indebted to Professors J. Oliger of the Computer Sciences Department, A. Acrivos, and G.M. Homsy of the Chemical Engineering Department, and Allen F. Moench of the USGS for their assistance in the mathematical part of the steam plateau problem.

Discussions with my colleagues, Abdullah Atalar, Roland Horne and Mohamed Soliman are sincerely appreciated.

The financial support from the Ministry of National Education of Turkey and SUPRI are gratefully acknowledged.

I would like to express my sincere thanks to Professor Aytin Göktekin of the Technical University of Istanbul, for his encouragement in my pursuit of the Ph.D. degree.

Finally, the author is forever indebted to his Mother, Şükriye, his Father, Mehmet, and his brother, Mustafa, whose inspiration made this study possible. The author dedicates this work to the three of them.

ABSTRACT

In this study, two interrelated parts of the in-situ combustion oil recovery process have been investigated.

The steam plateau region of laboratory combustion tube experiments was studied and heat transfer modes describing the steam plateau were defined. The combustion parameters affecting the steam plateau were also studied and evaluated. This part of the study points out some of the design problems and considerations important to the operation of the combustion tube and the interpretation of the results related to the steam plateau. An analytical heat model was developed which describes the movement of the steam plateau axially along a cylinder with heat loss through an annular insulation. The behavior of the solution was studied to determine the interaction of the heat transfer mechanisms in laboratory cores. The results of laboratory combustion tube runs were used to verify the theory set forth by the heat model. The agreement between experimental laboratory temperature profiles and those computed by model were satisfactory.

In the second part of the study, correlations were developed to predict field scale recovery of dry in-situ combustion processes. Basically, a case history analysis was made on field tests as a first step. The recovery histories of those field systems were studied. A combination of an engineering and a statistical approach was used to develop the correlations. The parameters that appeared promising from heat and material balance analysis were included to reach the first step for correlation. For the final step, multiple linear regression analysis was used to include those

additional variables judged to be important. After developing the correlations, their validity was tested. The match between the correlations and field test results was also satisfactory. The number of wet combustion projects were small compared to the dry combustion cases and therefore no attempt was made to develop recovery correlations for these cases. However, the study shows that the recovery correlations developed for dry combustion processes may be used for the recovery prediction of the wet combustion test in which the air-water injected ratio is high. This study also indicated that air injection and/or oil migration losses are important factors affecting the recovery mechanisms of a pilot project. Thus in pilot projects, for the same air injection, the recovery is somewhat less than found in fieldwide cases. The extension of one of the correlations to pilot dry in-situ combustion projects shows that the correlation parameters used to predict field scale recovery appeared to be reasonable as correlating parameters for dry pilot projects.

1. INTRODUCTION

During the last three decades, the injection of a heat-bearing fluid into a reservoir has gained considerable usage as an enhanced oil recovery mechanism. The low-API gravity, high-viscosity crude oils do not respond satisfactorily to conventional recovery processes. Since oil viscosity is highly temperature dependent, the performance of these reservoirs can be significantly improved by raising the reservoir temperature through the application of heat.

During dry forward in-situ combustion, air is injected to burn a part of the in-place hydrocarbons. Combustion gas and a steam plateau ahead of the combustion front displace oil toward the production well. The heat is transferred ahead of the combustion front by the convection of combustion gases, by vaporization and recondensation of connate water and by conduction.

A steam plateau is usually observed to move ahead of the combustion front. This region is characterized by a nearly flat temperature profile if pressure drop is small. Here the temperature level appears to be controlled by phase behavior. That is, the temperature level is related to the partial pressure of water in the gas phase and to the vapor pressure-temperature characteristics of water.

Describing the movement of heat and fluids analytically or numerically during the in-situ combustion process has been a subject of interest to numerous investigators. The results of field tests and of laboratory combustion tube studies have been reported. However, there is no complete

model which describes the movement of heat and fluids analytically. The complexity of the process has forced investigators to study the process in parts. Penberthy and Ramey¹⁸ have developed an analytical model to represent the temperature profiles behind and ahead of the burning front for combustion tube studies. They were able to match laboratory experimental data with that heat model. The other parts of the combustion process to be still investigated are the steam plateau, heat movement ahead of the steam plateau, and the burning front itself.

In the combustion process, the steam plateau starts growing immediately after ignition takes place. Since it plays an important role on the transportation of heat ahead of the burning front, it is important to obtain a reasonable estimate of the size and temperature of this plateau as a function of time. The availability of a mathematical model to describe the size of the steam plateau and the temperature distribution is of value for the better understanding of the in-situ combustion process. Another significant value to having a mathematical model for the steam plateau is that it will help complete the analytical description of the combustion tube studies when it is connected with Penberthy's¹⁸ model.

Numerical modelling has been an alternate way of describing the in-situ combustion process. However, the complexity of the process inherently causes problems in numerical modelling. The major problems in modelling are related to distillation and condensation, cracking, oxidation at various temperature levels, multiphase flow, heat transfer and gravity affects. If the model includes all these mechanisms, it becomes too cumbersome to run routinely. On the other hand, if many of the above items are neglected, one worries about the validity of recovery predictions made from such a model.

Oil recovery predictions for simple engineering calculations for in-situ combustion projects provide a basis for calculating air-oil ratios, oil rates, oil recovery, and economic limits. Although there are some screening guides²⁰⁻²⁵ in the literature which attempt to define which projects may be successes or failures, either these guides only make a yes/no evaluation or they are only applicable to certain fields. Therefore there is a clear need to develop a model to predict the oil recovery to be expected from an in-situ combustion process.

This study has focused on the following objectives:

1. to develop a simplified mathematical model of the multiphase nonisothermal fluid flow in the steam plateau,
2. to examine the importance of various parameters on the behavior of the model,
3. to study the possibility of developing new correlations to predict field scale recovery of in-situ combustion processes,
4. to relate these correlations to any additional field data available to test their validity.

2. LITERATURE SURVEY

Estimating the thermal behavior during hot fluid injection, and predicting the oil recovery mechanism of the in-situ combustion process have been two major subjects for investigators. In the following, studies which are pertinent to the stated objectives of this study are reviewed.

2.1 Mathematical Studies of Hot Fluid Injection and The Steam Plateau

In the published literature initial attempts were directed toward an analytical treatment of hot fluid injection mechanisms. Perhaps the most widely known solution is due to Lauwerier.¹ It includes heat losses to the impermeable strata surrounding the reservoir. He assumed that heat is transferred only by forced convection in the porous injection interval, and heat losses take place only by vertical conduction to the adjacent strata. His solution has been successfully applied to problems where hot water is injected into an oil bearing layer. In his model Lauwerier assumed that there was no vertical temperature gradient within the porous strata where the hot fluid is flowing. Thus the heat losses from the strata are overestimated to some extent. This has been called the "Lauwerier assumption" by Prats⁴¹ and others. This same assumption was used in the Marx-Langenheim work.²

Marx and Langenheim studied a similar problem in which the injection of a heat bearing fluid into a reservoir was investigated. They formulated an energy balance equation for heated area growth as a function of time. They defined a step temperature function for the heated zone and used the

solution for the cooling of a semi-infinite slab for vertical heat loss from the heated zone. Rather than solving for temperature distributions in the reservoir, they considered the total area of the heated reservoir to be at constant temperature, proceeded to develop an expression for the area heated as a function of time, provided the flow of heat from the hot fluid into the liquid zone ahead of the condensation front is neglected. Their method can be used to estimate thermal invasion rates and theoretical limits for sustained hot-fluid injection at a constant rate into an idealized reservoir.

Ramey³ extended the Marx-Langenheim work to the case of variable heat injection rate, and pointed out that the solution should be most appropriate for steam injection rather than hot water injection, because heat losses would not necessarily cause steam to cool.

Rubinstein⁴² developed an analytical solution for heat losses during hot fluid injection. He did not use Lauwerier assumption, and he allowed for isothropic thermal conductivity in both the fluid reservoir and surrounding formation. Ramey⁴³ determined that the heating efficiencies of the Lauwerier and Marx-Langenheim models were the same. The heating efficiency is defined as the fraction of heat injected into the reservoir that still remains in it. Ramey also showed that the Rubinstein's model gave somewhat smaller heat losses.

Ersoy⁴ both mathematically and experimentally studied hot water injection into a linear flow system with radial heat losses into the surrounding insulating medium. Both analytical and numerical formulations were made to approximate the experimental system. He used the same assumptions used by Lauwerier for his analytical solution. However, he

concluded that his finite difference solution, which included an effective thermal conductivity in the direction of fluid flow, was more useful for examining the experimental results.

Atkinson⁵ developed a series of mathematical models to describe heat transfer in laboratory experiments made by Arihara.⁶ He used the method of characteristics to extract an analytical solution for either hot or cold water injection. His model considered heat transfer by convection of fluids and heat loss into the surroundings. He found the method characteristics solution could be used to describe the temperature distribution in the core for hot or cold water injection with variable injection temperature. However his model did not give reasonable fit with experimental data for those cases where the injection temperature was constant. He concluded that this was due to the fact that the effective axial thermal conductivity had a major effect on the character of transient temperature profiles for those cases with constant injection temperature.

Holst and Karra⁷ presented a numerical method for calculating the size of the steam plateau as a function of time. Their equations describing the physical system were designed in a manner analogous to the Marx-Langenheim derivation for hot fluid injection. The main difference between the formulations was that they assumed that an optimal wet combustion was taking place in the reservoir so that the temperature behind the burning front was the same as the steam plateau temperature. The results of the investigation were presented as a function of the important dimensionless groups.

Chu⁸ investigated numerically the forward combustion process using a one-dimensional linear mathematical model, taking into consideration the effect of the vaporization and condensation which occurs in the steam plateau.

He concluded that the vaporization-condensation phenomenon did not induce an appreciable change in the temperature at the combustion front, and its primary effect was to create a steam plateau and to increase the length of the heated zone ahead of the combustion front.

Thus only preliminary and unsatisfactory attempts have been made to describe the steam plateau. The existence and importance of the steam plateau have not been completely understood as yet. Therefore, investigation of steam plateau phenomena became an important objective of this study.

2.2 Experimental Studies of In-Situ Combustion

There have been many laboratory experiments on in-situ combustion dating from the 1950's. In general, however, the investigators did not give a great deal of attention to the steam plateau which is associated with the forward-combustion process. The steam plateau is a region immediately ahead of the burning front wherein the temperature appears to be controlled by phase equilibrium due to vaporization of water.

Willman, et al.⁹ reported the results of an investigation into the use of steam as a recovery agent. The injection of cold water, hot water, and steam was studied systematically for a variety of rocks, oils, and injection temperatures. Mechanisms for enhanced oil recovery due to steam injection were deduced.

Szasz¹⁰ suggested that both lighter hydrocarbons and water are vaporized on the leading edge of the burning front, are carried forward in the gas stream, and are then condensed to create banks of oil and water. Various investigators¹¹⁻¹⁶ studied the various aspects of the in-situ combustion process in small-scale tube run experiments. Boussaid and Ramey¹⁷ presented experimental results on the oxidation reaction kinetics in the forward

combustion oil recovery process. Penberthy and Ramey¹⁸ developed an analytical heat model of movement of the burning front axially along a cylinder with heat loss through an annulus insulation. They used this model to match the results of their laboratory combustion tube experiments. They also demonstrated the existence of the steam plateau in forward combustion oil recovery.¹⁹

2.3 Studies of Oil Recovery Predictions for In-Situ Combustion Processes

During the early years of combustion application several industry experts studied the field results of in-situ combustion tests to determine the reservoir and fluid properties suitable for fireflooding. Poetmann²⁰ and Geffen²¹ were among them. Both of them suggested some screening guides for successful fire flood projects. Poetmann suggested a minimum value of the porosity-oil saturation product (ϕS_o) equal 0.10 and a permeability of 100 md as a lower limit for the reservoir in order to achieve a successful fireflood project. Geffen proposed ϕS_o greater than 0.05 for wet combustion and also mentioned that for Combinations Of Forward Combustion And Waterflooding, COFCAW, kh/μ_o needs to be over 100 md-ft/cp. Bleakley²² and Farouq Ali²³ surveyed the combustion projects. F. Ali concluded that in-situ combustion was feasible under a variety of field conditions, however it needed more engineering. He then reported that a well designed fireflood could be expected to recover fifty percent of the oil in place, and could make a profit, especially if simultaneous or intermittent water injection with air is employed.

Chu²⁴ reviewed many firefloods, developed equations relating fireflood performance to reservoir properties, and established criteria for screening

prospects for the application of the fireflood process. Two different approaches were used to establish screening guides for firefloods. He applied those two screening guides to 39 firefloods and concluded that they should be useful for pointing out reservoirs that show promise of being economic successes.

Gates and Ramey²⁵ suggested that the oil recovery/volume burned method of making engineering calculations for in-situ combustion projects would provide a means for calculating air-oil ratios, oil rates, oil recovery, and economic limits. They developed a number of curves based on laboratory combustion tube study results to estimate oil recovery as a function of volume burned with gas saturation as a variable. They showed that their method worked better than frontal displacement calculations for the South Belridge field. They indicated that other oil recovery mechanisms in conjunction with in-situ combustion cause an increased oil recovery. These include hot water drive, steam drive, hot gas drive, miscible phase displacement, oil expansion, and gravity drainage. As a result, the oil recovery/burned volume method predicts higher oil recovery and lower air-oil ratios than are predicted from frontal displacement calculations. They also emphasized that the early application of in-situ combustion would maximize the economics.

Satman, et al.²⁶ described a new correlation developed to predict field scale recovery of dry in-situ combustion processes. Their approach was different than Gates and Ramey's in the sense that their correlation curve was based on a case history analysis made on actual field tests rather than laboratory combustion tube run results. A combination of an engineering and a statistical approach was used to develop the correlation

They concluded that the correlation was accurate enough to use as a rapid and simplified approach toward recovery prediction.

The second objective of this study was concerned with developing simplified and convenient models for predicting oil recovery from in-situ combustion processes.

The preceding has discussed previous studies related to the objectives of this study. The next section discusses the theory of the in-situ combustion process. The following two sections discuss a simplified analytical model describing the temperature distribution in the steam plateau and then describe laboratory in-situ combustion tube experiments. The succeeding section describes the development of oil recovery correlations for dry in-situ combustion processes and also discusses the results of case history analyses made on pilot tests. The last two sections discuss the application of these correlations to additional field data and then the conclusions from this study.

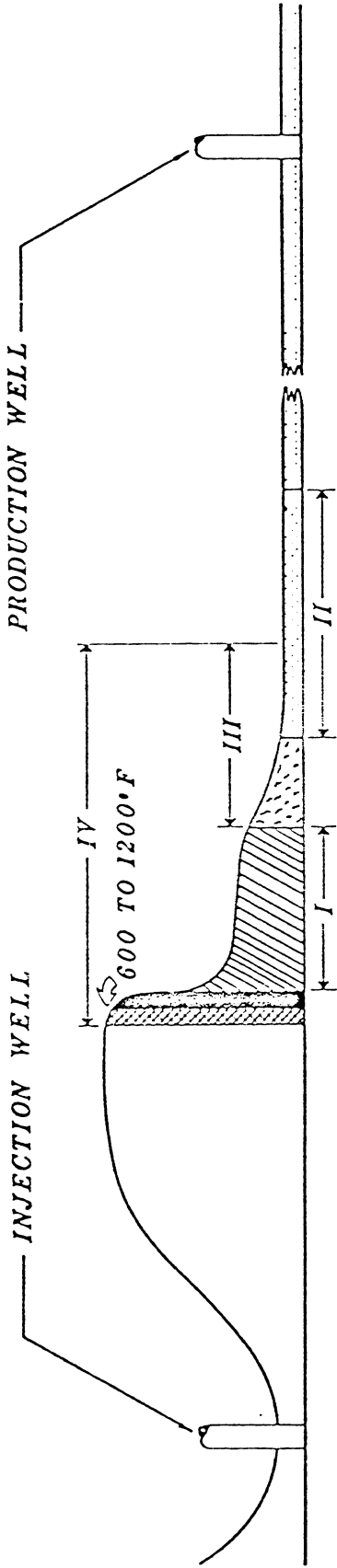
3. THEORY OF THE IN-SITU COMBUSTION PROCESS

In the forward in-situ combustion recovery process, air is injected into a well, ignition is initiated at the input well, and a combustion zone is propagated within the reservoir rock toward nearby producing wells.

The process is initiated by injecting air for a short period so as to establish a continuous gas phase between the injecting and producing wells. In many reservoirs this could lead to ignition of the reservoir oil, which is known as spontaneous ignition. If spontaneous ignition does not occur, heat can be introduced into the injecting well (or the producing well in reverse combustion) to achieve ignition. Usually, even if the reservoir will spontaneously ignite, it is better to add heat at the injection well for a controlled ignition. This assures a more uniform ignition. As air injection continues, the burning front gradually progresses further from the well.

Figure 1 shows a schematic of the forward in-situ combustion process. The upper portion of this figure presents the temperature distribution from the injection well to the producing well. There is a burned region from the injection well to the burning front. Near the injection well, the air is at the injected air temperature. With increasing distance from the injection well, air temperature increases to a maximum temperature at the burning front. Continued air injection recuperates heat from the burned sand and moves it towards the burning front. The burned region is completely void of liquid and consists of hot dry sand. The burning zone is usually at a temperature of 600° to 1200°F. All residual fuel deposited as a result of thermal cracking of the crude oil ahead of the burning front is consumed in this region.

TEMPERATURE DISTRIBUTION



CROSS-SECTION OF FORMATION

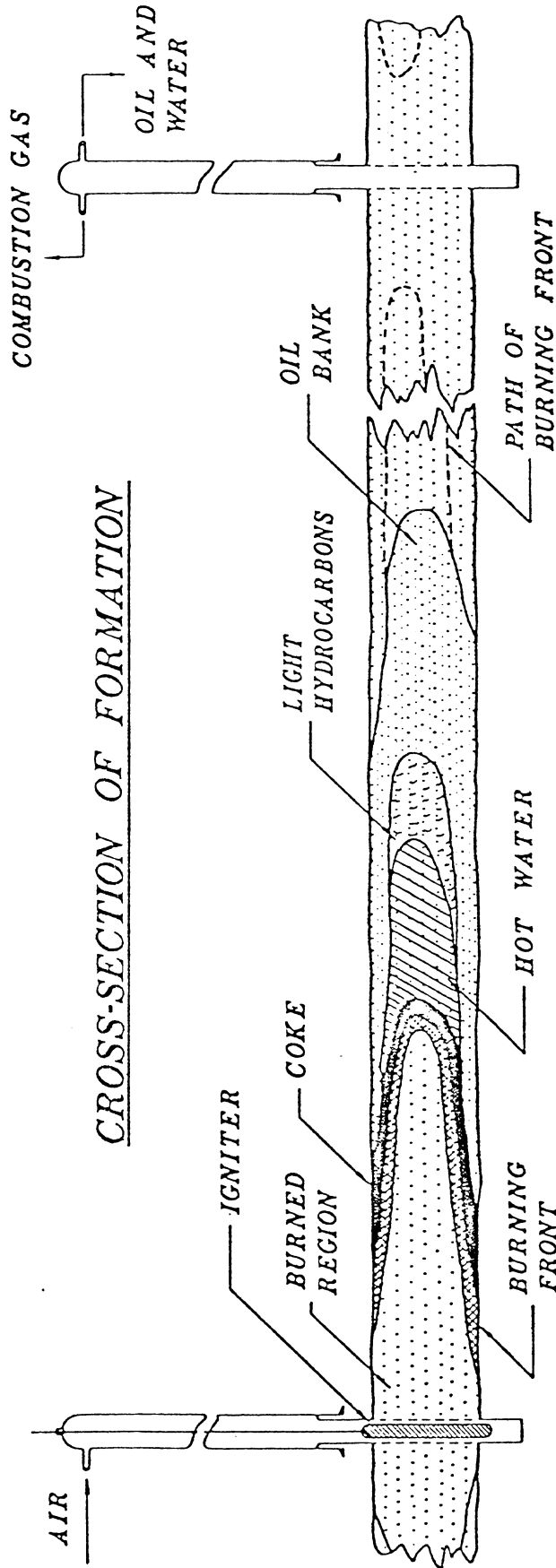


FIG. 1: SCHEMATIC DIAGRAM OF IN-SITU COMBUSTION PROCESS (AFTER MCNIEL AND MOSS³⁰)

Immediately ahead of the burning front, temperature decreases rapidly through the cracking and evaporation zone. In this zone, all liquid water and light components of crude oil are vaporized.

Ahead of the cracking and evaporation zone is the condensing steam zone which is also known as a steam plateau and it is recognized by a flat temperature distribution. This zone consists of steam, combustion gases, vaporized oil, and liquid water and oil which move through the region. Experimental results and the steam plateau model developed in this study indicate that the temperature of the steam plateau is determined primarily by the air injection pressure and the water saturation; its growth may be controlled by air flux, initial formation temperature, and/or heat loss. Ahead of the steam plateau, temperature drops gradually to the initial formation temperature. The lower temperatures ahead of the steam plateau cause the steam and vaporized oil to condense; therefore a condensed water and light oil bank is identified immediately ahead of the steam plateau. Ahead of the light hydrocarbon zone is an oil bank resulting from the oil being pushed ahead by the burning front. Then, ahead of the oil bank is the substantially undisturbed formation at its original temperature.

The in-situ combustion process has generally been applied as one of three techniques, namely dry forward combustion, wet forward combustion and reverse combustion. As implied from the name, ignition starts near the injection well and the burning front moves toward the producing wells during dry forward combustion. Oil displacement in the forward combustion process is a result of a combination of the following four mechanisms:

1. Viscosity reduction primarily due to heat and secondarily due to CO₂ solubility,

2. Vaporization due to heat,
3. Displacement improvement resulting from the three-phase emulsion ahead of the burning front,
4. Pressure gradient imposed by injected air.

In the wet combustion process, air and water are injected either simultaneously or alternately. Adding water to the injection stream increases the sensible heat of the injected stream so that more heat is recuperated from the burned region. Transfer of this heat toward to the unburned portions of the reservoir increases the oil displacement efficiency of the process.

In the reverse combustion case, ignition begins near the producing well and the burning front moves countercurrent to the flow of the injected air. Reverse combustion was attempted early and proved inferior to the other combustion techniques. The main reason for consideration of this process was that it appeared to be a potentially operable scheme for heavy tar deposits by developing some mobility to the tar.

4. THE STEAM PLATEAU MODEL

The following discusses the derivation of the steam plateau model and its application to the laboratory combustion tube experiment results.

4.1 Conceptual Model of The Steam Plateau

A steam plateau is conceptualized as a flat temperature region which takes place ahead of the burning front. It is mainly formed as a result of the burning front which gives off heat as it moves through a porous medium. The total heat is due to sensible heat and latent heat transfer. Sensible heat is the result of hot, noncondensable gases (N_2 , CO_2 , CO , CH_4 , ...), while the latent heat is due to the water vapor formed during combustion, and that which results from boiling residual water over the interval immediately ahead of the combustion front.

Laboratory combustion tube runs and numerical models indicate that steam, noncondensable gases, water and oil exist in the steam plateau. The model described here assumes that steam and noncondensable gases are flowing and mass transfer due to condensation of steam occurs to build up a water saturation. However, it is also assumed that water and oil are not flowing, although they are considered for the heat storage capacity of the combustion tube. Assuming a constant oil saturation in the steam plateau is in agreement with the experimental saturation-distance profile that was presented by Martin, et al.¹¹ Actually it is true that oil and water in the steam plateau move due to hot gas drive, steam drive, miscible phase displacement, and pressure gradient, but for practical purposes their dynamic effects on the heat balance in the steam plateau can be neglected

since latent heat is the dominant factor.

The steam plateau starts with a constant steam plateau temperature which can be related to the vapor fraction of the steam in the gas phase, since the steam plateau is assumed to be under equilibrium conditions. Experimental results indicate that the steam fraction in the gas phase in the steam plateau is considerably higher than the amount of steam formed due to burning which can be determined by using the stoichiometric equations. This difference may be explained by the vaporizing mechanism which occurs ahead of the burning front in the region between the burning front and steam plateau. It provides a source of steam under proper conditions of temperature and pressure.

The temperature in the steam plateau decreases due to heat loss to the surroundings. But latent heat due to condensation compensates for the heat loss and provides the latent-heat content of the steam plateau.

Important conclusions concerning the steam plateau phenomena may be gained by the use of a simplified heat-transfer model associated with the movement of hot fluids in a linear system. The problem to be considered involves heat transfer by convection, condensation and heat loss. It is assumed that:

1. The beginning of the steam plateau moves at constant velocity and temperature in a cylindrical system due to constant air flux. As a first approximation, this velocity is assumed to be the same as the velocity of the burning front.
2. The temperature is constant radially within the combustion tube,
3. The condensation of steam and the associated latent heat is considered,

4. Heat loss is considered at the circumference of the cylinder by steady-state radial convective heat flow,
5. The pressure gradient across the steam plateau is negligible. Thus the temperature depends only on the partial pressure of water,
6. Heat transfer by conduction is neglected,
7. The vaporization-condensation effects of crude oil are neglected,
8. Heat transfer by liquid flow is negligible,
9. Thermal and physical properties are independent of temperature,
10. The convection coefficient between the fluids and sand is considered to be infinitely large. Therefore at any location, fluids and solids have the same local temperature.

The injected fluid is basically air. As it is known, air contains oxygen. The oxygen is gradually consumed in the combustion process and replaced by carbon oxides and water. The carbon oxides formed by combustion have approximately the same mass and specific heat as the oxygen consumed. The physical properties of the non-condensable gas are therefore assumed not to change as a result of combustion. They are identical to those of the injected air.

The assumption (7) may not always be reasonable; however, the large majority of combustion projects involve very heavy crude oil. The composition of these crudes is such that distillation of the crude oil at steam-plateau temperatures and pressures is negligible.

4.2 Mathematical Formulation of the Steam Plateau

The experimental equipment represents a linear fluid flow model, with radial heat losses through a surrounding formation of effectively an infinite extent. The air injection interval is a long cylindrical core in which the steam plateau moves in an axial direction. As hot steam and

non-condensable gases enter the cylindrical core, radial heat losses take place in the surrounding annular space. The heat is transferred from the system to the surroundings by combined conduction and convection. However, a convection equation form is used, as follows,

$$q = UA(T-T_e) \tag{1}$$

This model does not properly describe heat loss in a reservoir, since such heat loss is governed by conduction through the overburden and underburden. However, Equation 1 is a reasonable approximation for the heat loss mechanism occurring in non-adiabatic laboratory tube experiments.³³

The analytical formulation of this model has been considered in order to match the temperature behavior of the steam plateau in the core.

In the formulation of the problem, the beginning of the steam plateau is assumed moving with a constant velocity, v_{sp} , in the direction of fluid flow. This means that in a coordinate system, x , moving at a velocity v_{sp} , the temperature and fluid distributions are fixed. In actual practice the velocity v_{sp} is very nearly equal to the burning front velocity. It is not quite the same; in an actual laboratory combustion, there is some conduction ahead of the burning front which causes the beginning of the steam plateau to move slightly faster than the burning front. This can be seen in the experimental temperature profiles of combustion tube runs.

Let us consider a differential element of thickness dx moving with velocity v_{sp} (Fig. 2). Through this element fluid and rock matrix move in counterflow, the fluid in positive x direction with a Darcy velocity u_g , and the matrix in the opposite direction with velocity $-v_{sp}$. This indicates a moving coordinate system so that the steam plateau always starts at an x -coordinate of zero. In deriving the equations for this system, first the basic partial differential equations will be derived in the static coordinate

HEAT LOSS, $q = UA\Delta T$

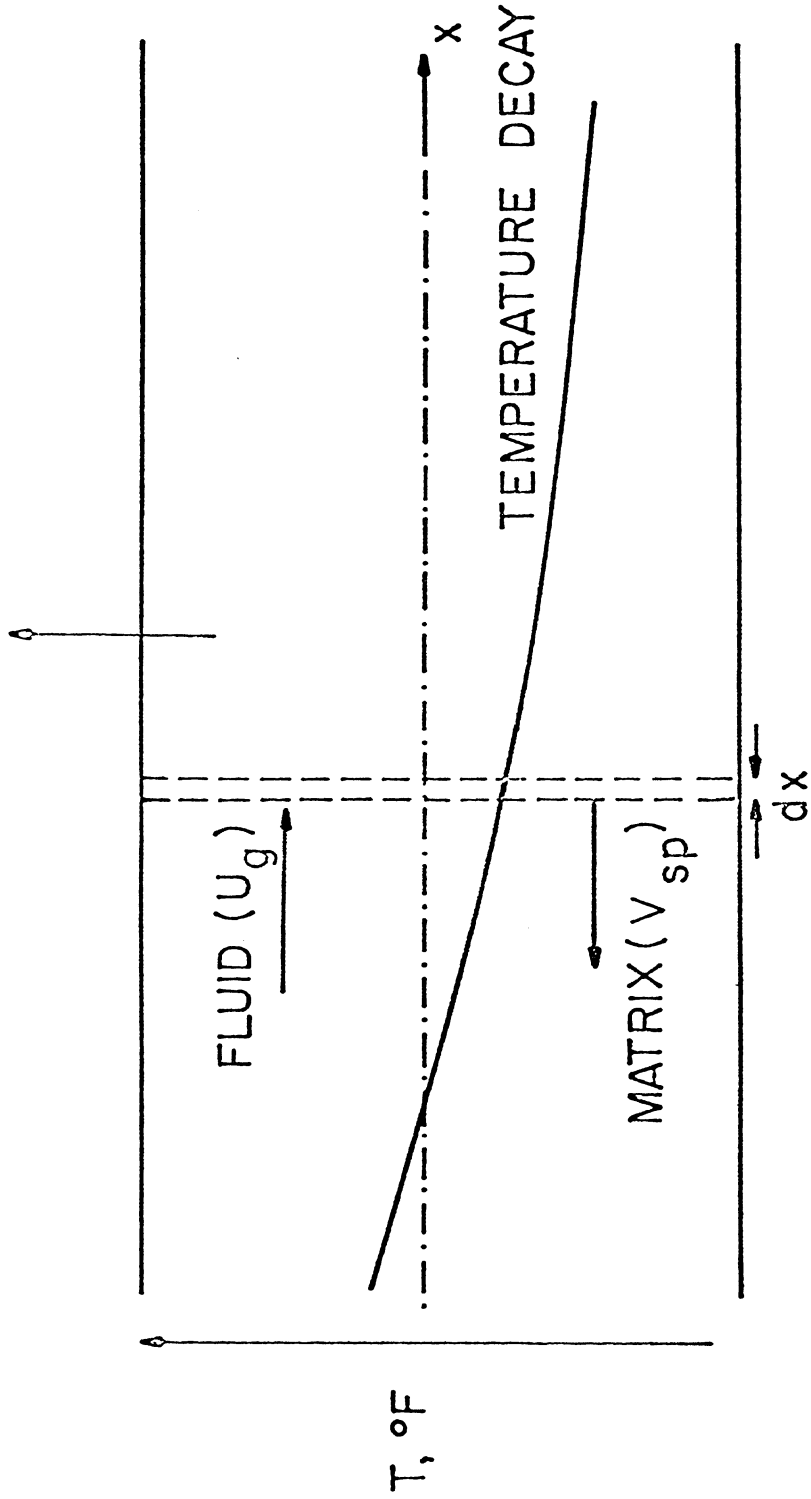


FIG. 2: MOVEMENT OF FLUID AND ROCK MATRIX RELATIVE TO X-COORDINATE SYSTEM

system, then a variable transformation will be used to change the equations to the moving coordinate system.

The fluid entering into the steam plateau consists of non-condensable gas saturated with water vapor. The non-condensable gas initially contains N_2 , CO_2 , CO , and traces of CH_4 and other gases. The water vapor is gradually condensed in the steam plateau to build up the water saturation.

The formulation of the model requires that the water saturation at the beginning of the steam plateau is at a minimum value. This minimum value becomes zero whenever the irreducible water saturation immediately behind the steam plateau is zero.

Applying a proper energy balance over a differential element of volume yields the following partial differential equation:

$$\begin{aligned}
 & - \frac{u_g \rho_g}{\rho_l C_l} \frac{\partial}{\partial x} \left\{ f_s [C_w (T' - T_e) + L_v] + (1 - f_s) C_g (T' - T_e) \right\} \\
 & - \frac{2U}{r \rho_l C_l} (T' - T_e) = \frac{\partial}{\partial t} (T' - T_e) \quad (2)
 \end{aligned}$$

where:

$$\rho_l C_l = (1 - \phi) \rho_f C_f + \phi (S_w \rho_w C_w + S_o \rho_o C_o) \quad (3)$$

It is assumed that all the components of the fluid/solid system at a given point in space are at the same temperature. The derivation of the energy balance equation (Eq.2) for a differential element in the steam plateau is described in Appendix A. The appropriate initial and boundary condition is:

$$T' = T_i \quad @x = 0, \quad t > 0 \quad (4)$$

Equation of State:

Assuming steam and non-condensable gases to be ideal solutions at equilibrium, Raoult's Law and Dalton's Law may be combined to calculate

vapor fraction of each component in the vapor and liquid phases. Raoult's and Dalton's Laws may be expressed as follows:

$$P_s = x_s P_v \quad (\text{Raoult's Law}) \quad (5)$$

$$P_s = y_s P \quad (\text{Dalton's Law}) \quad (6)$$

Since the only liquid phase considered is water, x_s becomes one. Therefore the partial pressure of steam is equivalent to the vapor pressure of steam and Equations 5 and 6 yield:

$$y_s = \frac{P_v}{P} \quad (7)$$

This conclusion also indicates that the partial pressure of steam in the gas phase is considered to be equal to the saturation pressure of steam corresponding to liquid water temperature.

Since steam and non-condensable gases behave like ideal solutions, the mass fraction of steam in the gas phase is related to the molar fraction of steam in the gas phase as follows:

$$f_s = \frac{M_w}{M_g} y_s \quad (\text{from } f_s = \frac{m_s}{m_g} = \frac{n_s M_s}{n_g M_g} = \frac{M_w}{M_g} y_s) \quad (8)$$

Combining Equations 7 and 8 gives:

$$f_s = \frac{M_w}{M_g} \frac{P_v}{P} \quad (9)$$

The Clasius-Clapeyron equation expresses the dependence of the vapor pressure on temperature:

$$\frac{1}{P_v} \frac{dp_v}{dT'} = \frac{M L'_v}{R(T')^2} \quad (10)$$

If dp_v/dT' is assumed constant through the steam plateau (this is a reasonably valid assumption since the temperature distribution is nearly flat through the steam plateau), Equation 10 can be written in a way to give the vapor pressure, p_v , as a function of temperature, T , only:

$$p_v = \frac{R}{M \frac{L'_v}{w}} \left(\frac{dp_v}{dT'} \right) (T')^2 \quad (11)$$

Substituting Equation 11 into Equation 9 yields:

$$f_s = \frac{R}{M \frac{L'_p}{g} \frac{L'_v}{p}} \left(\frac{dp_v}{dT'} \right) (T')^2 \quad (12)$$

In this last equation, the unit of temperature is $^{\circ}R$. If it is converted to $^{\circ}F$, Equation 12 becomes:

$$f_s = \frac{R}{pM \frac{L'_p}{g} \frac{L'_v}{p}} \left(\frac{dp_v}{dT'} \right) (T_a + T')^2 = \alpha (T_a + T')^2 \quad (13)$$

where:

T_a = Conversion to absolute Temperature $460^{\circ}F$,

$$\alpha = \frac{R}{pM \frac{L'_p}{g} \frac{L'_v}{p}} \frac{dp_v}{dT'}, \text{ a constant for the conditions assumed} \quad (14)$$

Let:

$$T = T' - T_e \quad (15)$$

Therefore Eq. 13 becomes:

$$f_s = \alpha (T'_a + T)^2 \quad (16)$$

where

$$T'_a = T_a + T_e \quad (17)$$

Combining Equations 2, 15, and 16 gives the governing partial differential equation:

$$\begin{aligned}
 & - \frac{u_g \rho_g}{\rho_l c_l} \left\{ c_g + \alpha (C_w - C_g) (T'_a)^2 + \alpha (T'_a)^2 \frac{L_v}{(T_i - T_e)} + 4\alpha \left[(C_w - C_g) + \frac{L_v}{(T_i - T_e)} \right] T'_a T \right. \\
 & \left. + 3\alpha \left[\frac{L_v}{(T_i - T_e)} + (C_w - C_g) \right] T^2 \right\} \frac{\partial T}{\partial x} = \frac{\partial T}{\partial t} + \frac{2U}{r \rho_l c_l} T
 \end{aligned} \tag{18}$$

Let:

$$T_D = \frac{T}{T_i - T_e} \tag{19}$$

Equation 18 then becomes:

$$\begin{aligned}
 & - \frac{u_g \rho_g}{\rho_l c_l} \left\{ c_g + \alpha (C_w - C_g) (T'_a)^2 + \alpha (T'_a)^2 \frac{L_v}{(T_i - T_e)} + 4\alpha \left[(C_w - C_g) + \frac{L_v}{(T_i - T_e)} \right] T'_a (T_i - T_e) T_D \right. \\
 & \left. + 3\alpha \left[(C_w - C_g) + \frac{L_v}{(T_i - T_e)} \right] (T_i - T_e)^2 T_D^2 \right\} \frac{\partial T_D}{\partial x} = \frac{\partial T_D}{\partial t} + \frac{2U}{r \rho_l c_l} T_D
 \end{aligned} \tag{20}$$

This is the energy balance equation for the steam plateau. If a moving coordinate system is desired, such that the steam plateau is always defined with its start at the zero on the x-coordinate, the following change of variable is used:

$$x' = x - v_{sp} t \tag{21}$$

Using this coordinate change, the partial differential equation becomes:

$$\begin{aligned}
& \left(\frac{u_g \rho_g}{\rho_1 C_1} \left\{ C_g + \alpha(C_w - C_g)(T'_a)^2 + \alpha(T'_a)^2 \frac{L_v}{(T_i - T_e)} + 4\alpha \left[(C_w - C_g) \right. \right. \right. \\
& \left. \left. \left. + \frac{L_v}{(T_i - T_e)} \right] T'_a (T_i - T_e) T_D + 3\alpha \left[(C_w - C_g) + \frac{L_v}{(T_i - T_e)} \right] (T_i - T_e)^2 T_D^2 \right\} \right. \\
& \left. - v_{sp} \right) \frac{\partial T_D}{\partial x'} + \frac{\partial T_D}{\partial t} = - \frac{2U}{r \rho_1 C_1} T_D \quad (22)
\end{aligned}$$

The following terms can be defined, all of which are constants for any specified combustion run conditions:

$$\beta = \frac{u_g \rho_g}{\rho_1 C_1} \left[C_g + \alpha(C_w - C_g)(T'_a)^2 + \alpha(T'_a)^2 \frac{L_v}{(T_i - T_e)} \right] - v_{sp} \quad (23)$$

$$\gamma = \frac{u_g \rho_g}{\rho_1 C_1} \left\{ 4\alpha \left[(C_w - C_g) + \frac{L_v}{(T_i - T_e)} \right] T'_a (T_i - T_e) \right\} \quad (24)$$

$$\epsilon = \frac{u_g \rho_g}{\rho_1 C_1} \left\{ 3\alpha \left[\frac{L_v}{(T_i - T_e)} + (C_w - C_g) \right] (T_i - T_e)^2 \right\} \quad (25)$$

$$\theta = \frac{2U}{r \rho_1 C_1} \quad (26)$$

Using the constant parameters defined in Eqs. 23-26, and substituting them in Eq. 22,

$$(\beta + \gamma T_D + \epsilon T_D^2) \frac{\partial T_D}{\partial x'} + \frac{\partial T_D}{\partial t} = -\theta T_D \quad (27)$$

The initial condition becomes:

$$T_D = 1 \quad @t = 0, x' = 0 \quad (28)$$

Equation 27 with initial condition Eq. 28, describes the nonisothermal flow of steam and non-condensable gases through porous media.

4.3 Solution to the Governing Equation Using the Method of Characteristics

Equation 27 is the first-order non-linear hyperbolic type of partial differential equation and it describes heat transfer in the steam plateau in the absence of heat conduction.

Because the temperature in the system is a function of the two independent variables, distance and time, $T_D(x',t)$, the total differential of T_D may be written:

$$dT_D = \left(\frac{\partial T_D}{\partial x'} \right)_t dx' + \left(\frac{\partial T_D}{\partial t} \right)_{x'} dt \quad (29)$$

Dividing by dt and rearranging gives:

$$\frac{dT_D}{dt} = - \frac{dx'}{dt} \left(\frac{\partial T_D}{\partial x'} \right)_t + \left(\frac{\partial T_D}{\partial t} \right)_{x'} \quad (30)$$

Equations 27 and 30 can be compared term by term. Such a comparison indicates that the characteristic line lying entirely in the solution or integral surface in the x' - t plane is given by:

$$\frac{dx'}{dt} = \beta + \gamma T_D + \epsilon T_D^2 \quad (31)$$

and that the temperature of a fictitious particle following this characteristic line must satisfy:

$$\frac{dT_D}{dt} = - \theta T_D \quad (32)$$

Thus, a fictitious particle injected into the core at $x'=0$ moving into the steam plateau with temperature T_i , will decay in temperature according to Equation 32 and will move with a velocity given by Equation 31.

Equations 31 and 32 are commonly called the equations of the characteristics⁴⁵. Actually, these equations are a pair of independent, first-order, ordinary differential equations which can be integrated to give;

$$x' - (\beta + \gamma T_D + \epsilon T_D^2)t = c_1 \quad (33)$$

and

$$T_D = c_2 e^{-\theta t} \quad (34)$$

The constants c_1 and c_2 are arbitrary, so that Equations 33 and 34 are a two-parameter family. Equation 33 gives the projections of the characteristics on the plane of the independent variable, and the lines are often called the base characteristics or merely the characteristics. Along each base characteristic, the ratio $T_D / \exp(-\theta t)$ is constant; hence, in general c_2 is a function of c_1 . That is

$$\frac{T_D}{\exp(-\theta t)} = g \left(x' - (\beta + \gamma T_D + \epsilon T_D^2)t \right) \quad (35)$$

where g is an arbitrary function of one variable. Equation 35 is thus the general solution of Equation 27. From the initial condition, Equation 28, it follows that c_2 is equal to 1.0, thus Equation 34 becomes,

$$T_D = \exp(-\theta t) \quad (36)$$

Substituting Equation 36 into Equation 33, and applying the initial condition, Equation 28, we get,

$$x' = \beta t + \frac{\gamma}{\theta} \left[1 - \exp(\theta t) \right] + \frac{\epsilon}{2\theta} \left[1 - \exp(-2\theta t) \right] \quad (37)$$

Equation 36 and 37 give the temperature decay and location, both as functions of time, of a fictitious particle moving into the steam plateau with temperature T_i at $x' = 0$.

Behavior of this solution and the propagation profiles are shown on Fig. 3. The solution simply behaves as a sharp front which moves down the core.

Equation 31 can be rearranged to give dt :

$$dt = \frac{dx'}{\beta + \gamma T_D + \epsilon T_D^2} \quad (38)$$

If Equations 32 and 38 are combined, we get,

$$\frac{dT_D}{dx'} = \frac{-\theta T_D}{\beta + \gamma T_D + \epsilon T_D^2} \quad (39)$$

Noting the definitions of θ, β, γ , and ϵ from Equations 23-26, we see that Equation 39 can be approximated by the following expression,

$$\frac{dT_D}{dx'} \approx \frac{-U}{u_g \rho_g} \quad (40)$$

This indicates that the rate of decline of temperature with distance primarily depends on the factor $U/(u_g \rho_g)$. Thus, either a high U , or a low $(u_g \rho_g)$ can cause T_D to fall to essentially zero by the end of the core. Physically, this occurs if all the injected heat is lost to the surrounding media before it can reach the outlet end of the core. Figures 4 and 5 show the effects of $(u_g \rho_g)$ and U on the solution.

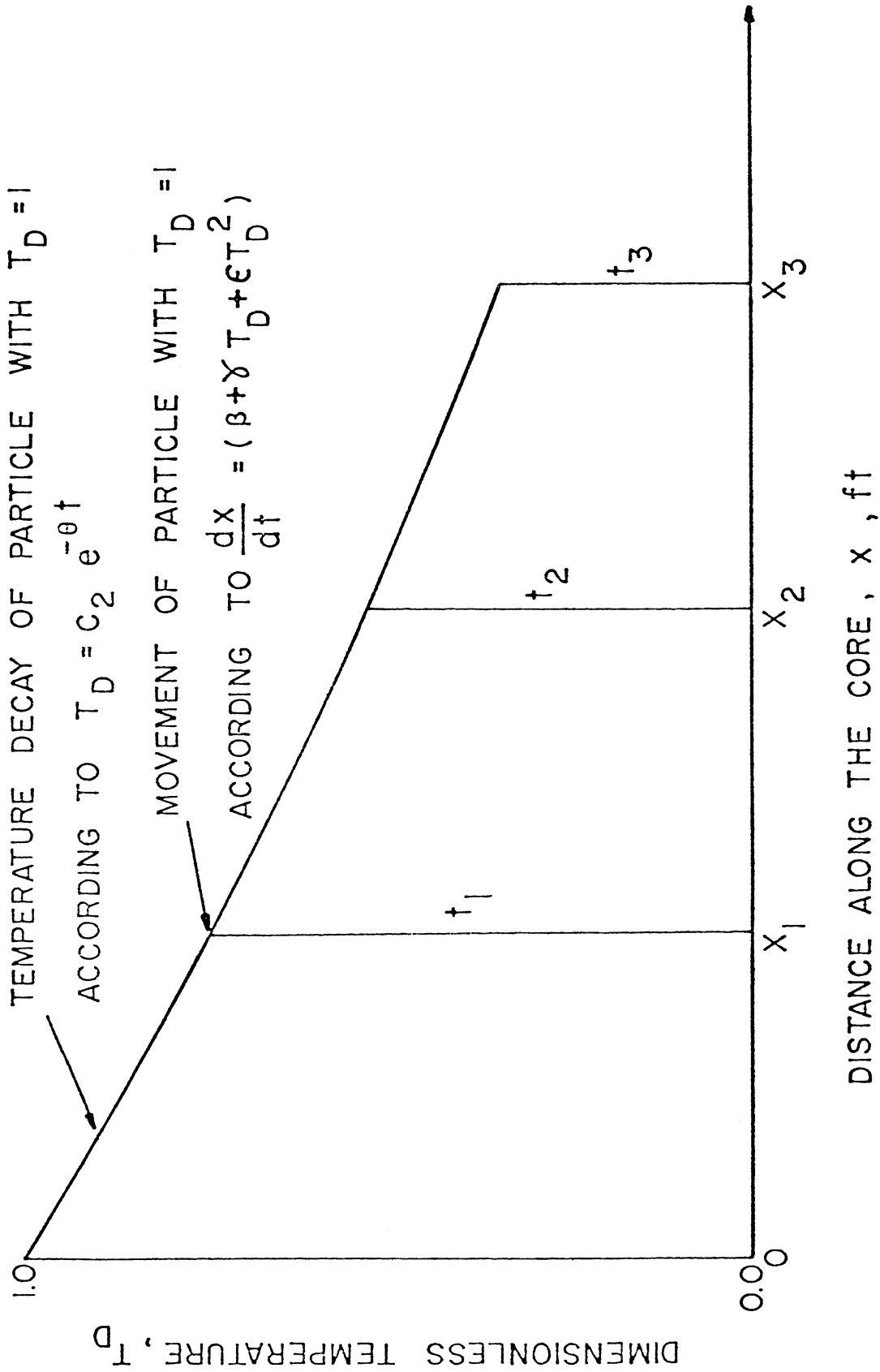


FIG. 3: BEHAVIOR OF THE STEAM PLATEAU MODEL AND PROPAGATION PROFILES FOR CONSTANT MASS INJECTION RATE, CONSTANT INJECTION TEMPERATURE, AND CONSTANT THERMAL PROPERTIES

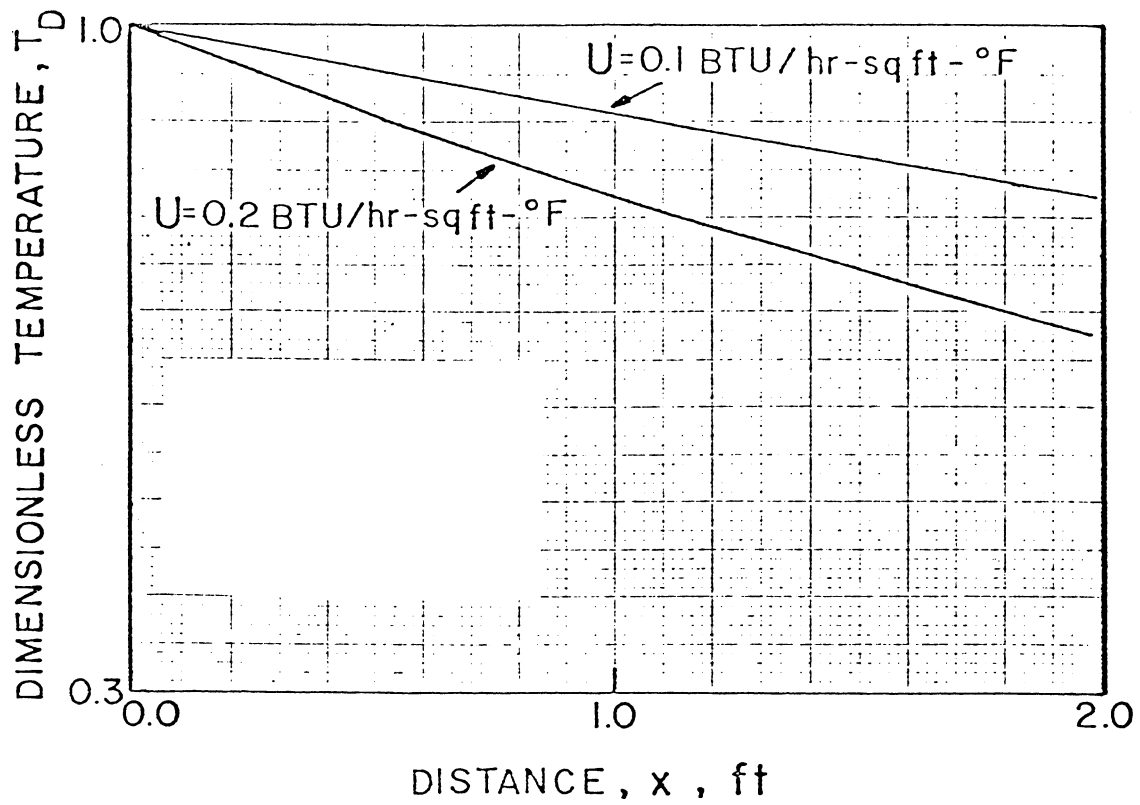


FIG. 4: THE EFFECT OF OVERALL HEAT TRANSFER COEFFICIENT ON THE SOLUTION

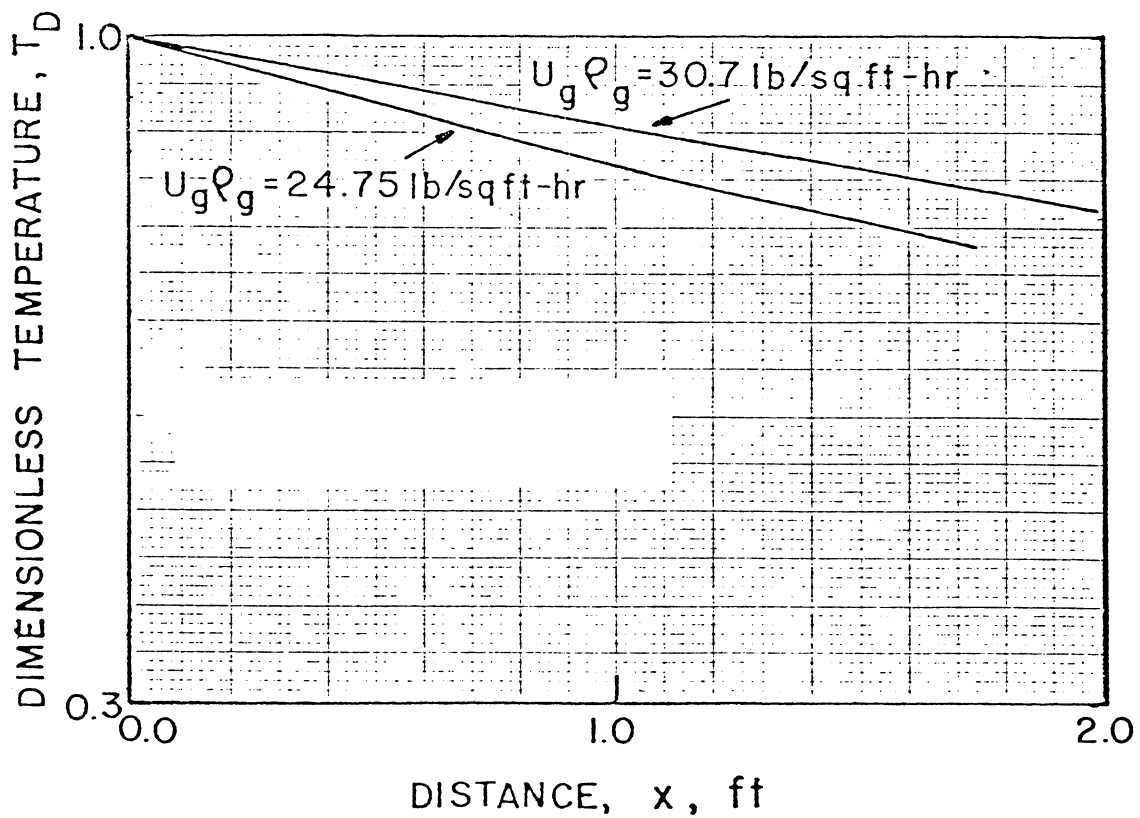


FIG. 5: THE EFFECT OF MASS FLUX INTO THE STEAM PLATEAU ON THE SOLUTION

The mathematical procedure for finding a solution for a zero heat loss case is described in Appendix B.

4.4 Application of the Steam Plateau Model to The Laboratory Runs

Fig. 6 shows an example of the calculated temperature distributions in the steam plateau at various times for Run 78-2. For the calculation, the following constants were used:

$$\begin{aligned}\rho_l C_l &= 34 \text{ Btu/ft}^3\text{-}^\circ\text{F} \\ u_g &= 4.34 \text{ scf/hr} \\ A &= 0.0456 \text{ ft}^2 \\ v_{sp} &= 0.30 \text{ ft/hr} \\ U &= 0.133 \text{ Btu/hr-ft}^2\text{-}^\circ\text{F} \\ C_w &= 1.00 \text{ Btu/lb-}^\circ\text{F} \\ C_g &= 0.243 \text{ Btu/lb-}^\circ\text{F} \\ M_g &= 27 \text{ lb/lb mole} \\ \rho_g &= 0.071 \text{ lb/ft}^3 \\ L_v &= 945.5 \text{ Btu/lb} \\ \alpha &= 0.350 \cdot 10^{-6} (\text{}^\circ\text{F})^{-2} \\ T_i &= 250^\circ\text{F} \\ T_e &= 160^\circ\text{F} \\ t_{ign} &= 0.9 \text{ hrs} \\ p &= 100 \text{ psig}\end{aligned}$$

The term, t_{ign} , is the time spent to ignite the pack. The times shown on the temperature traverses in Fig. 6 also include t_{ign} . Therefore to determine the real time in which the steam plateau has moved, t_{ign} is

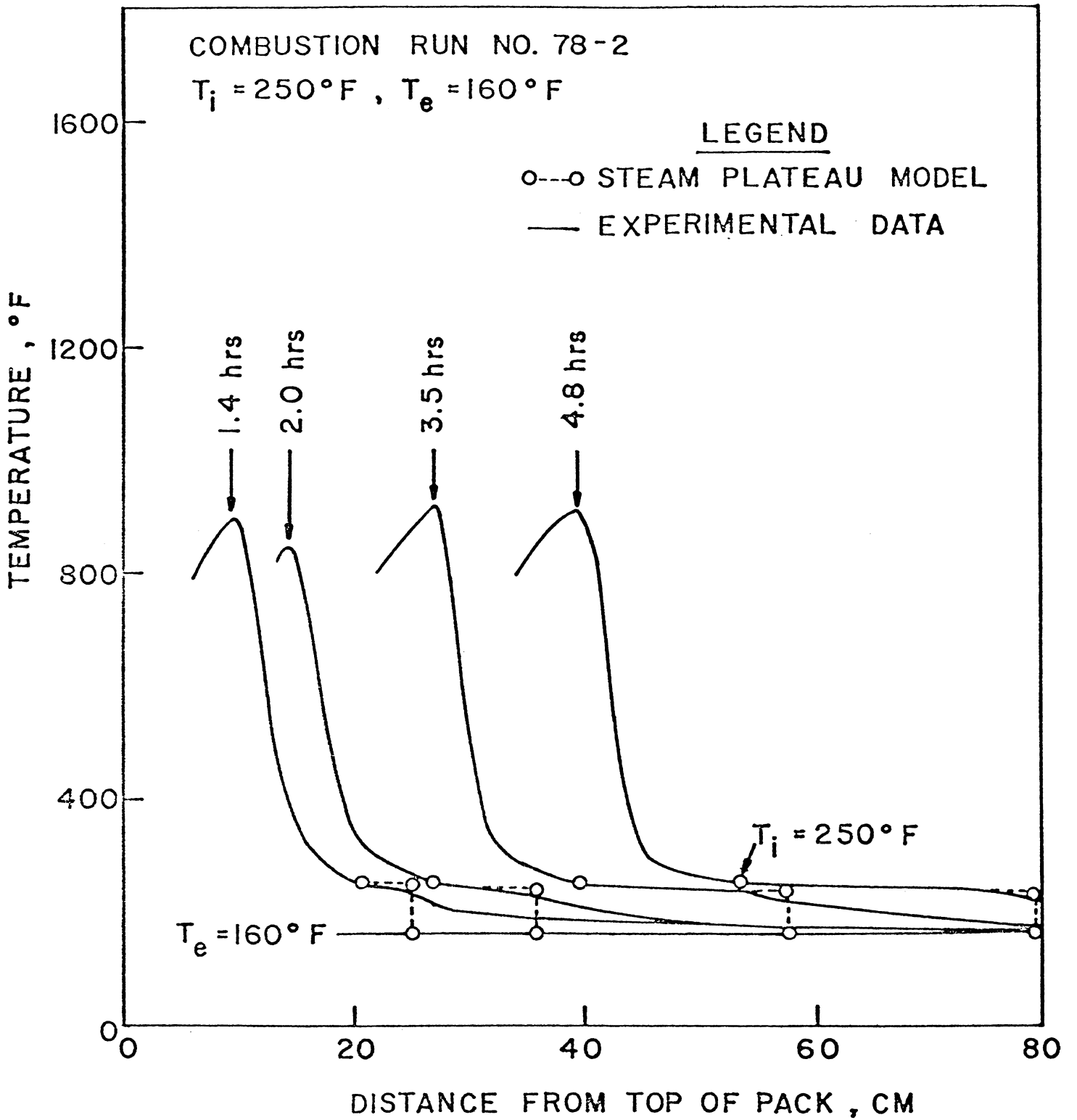


FIG. 6: COMPARISON OF THE CALCULATED AND EXPERIMENTAL RESULTS FOR RUN 78-2

subtracted from the time shown on each temperature traverse. It is found that convective heat transport from the burning front into the steam plateau does not start at the beginning of a combustion tube run, but rather at a later time, which turns out to be identical with the ignition time at which the burning front starts moving. This ignition time depends on the power of the igniter, heat loss, and air flux. One possible way of obtaining an approximate value for t_{ign} follows.

If the straight line representing the burning front locations in Fig. 16 is extrapolated to the zero distance from top of the pack, the time where the extrapolated line crosses the abscissa gives an estimate for t_{ign} . Actually, 0.9 hrs for t_{ign} was obtained from Fig. 16 by using this procedure.

During t less than t_{ign} heat transport into the steam plateau is purely conductive. According to the theory presented in this study, the steam plateau would remain cold ($T_D=0$) until t equals t_{ign} since heat conduction by the fluid/solid mixture was neglected. In reality, heat is also transported by conduction. The effect of conduction is important at the start of the combustion run. This can be observed by examining Fig. 7. This figure shows the growth of the steam plateau for Run 78-2. In this figure, there are three temperature traverses shown. The temperature scale is expanded in order to concentrate on the steam plateau regions of the traverses for clarity. The traverse at $t=0.87$ hrs represents the temperature distribution ahead of the burning front immediately before the burning front starts moving. There is no steam plateau formed as yet. Heat is transferred by conduction, due to heat introduced by the igniter, and by convection due to gas flow. The traverse at $t=1.40$ hrs represents

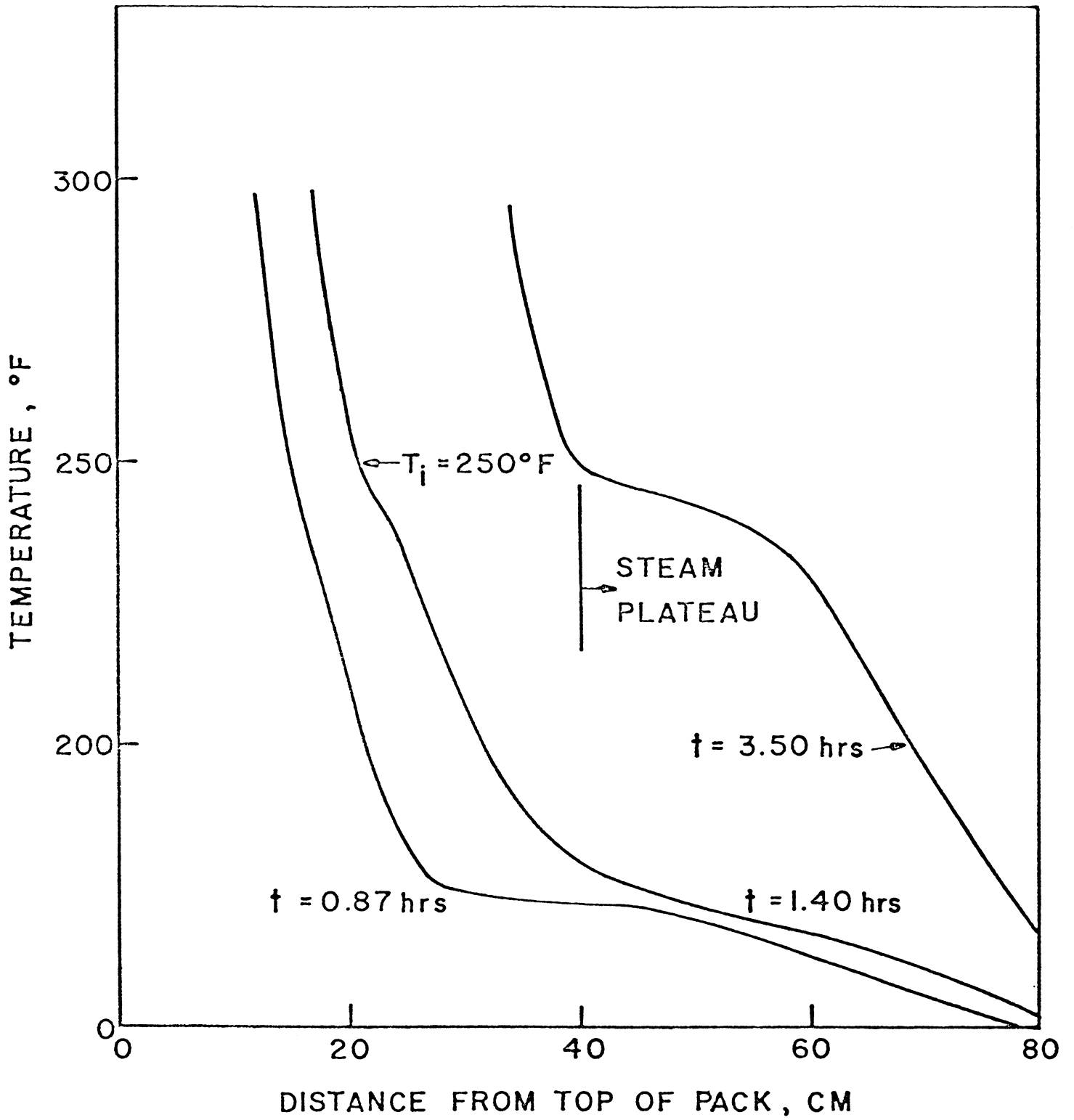


FIG. 7: GROWTH OF THE STEAM PLATEAU DURING RUN 78-2

the temperature distribution after the burning front has started moving. It can be seen that the steam plateau has already started to form. Therefore the latent heat has become the dominant heat transfer mode in that region. The temperature profile is curved at approximately 250°F indicating the temperature at the beginning of the steam plateau, T_i . The break on this particular profile occurs between 240° and 260°F . As an average of that temperature region 250°F is chosen to represent T .

The temperature at the start of the steam plateau can also be approximately based on the stoichiometric equations and the material balance considerations on the operation of the combustion tube. Using these concepts, the amount of the water vapor in the gas phase can be approximated which in turn defines the steam plateau temperature. The water vapor in the gas phase consists of; (1) water formed due to combustion at the burning front, and (2) water vaporized in the region between the burning front and steam plateau. The amount of water formed due to combustion can be determined by standard combustion calculations. The amount of water vaporized can also be determined by combining and using the combustion calculations, material balance considerations and phase equilibrium relationships. A summary of calculations of the amount of water formed and water vaporized is described in Appendix C. In summary, these calculations indicate that the volume of water vaporized is equivalent to a water saturation of 0.15 which agrees closely with the probable irreducible water saturation of this porous medium.

The third temperature traverse in Fig. 7 shows the fully developed steam plateau ahead of the burning front. Latent heat is now the dominant factor. It flattens the temperature profile in the steam plateau and it

also supplies heat to compensate for the heat loss to the surroundings. The flat portion of the temperature profile is the condensing steam region. The sharp temperature decrease at the front indicates that all steam in the flowing fluid stream has been condensed. This point may be considered the leading edge of the steam plateau.

The overall heat transfer coefficient may be determined either by (1) evaluating the size of each heat transfer coefficient, or (2) by trial and error until a match is achieved with the experimental data. The computed result based on evaluating the size of each heat transfer coefficient indicated an overall heat transfer coefficient of $0.133 \text{ Btu/hr-sqft-}^{\circ}\text{F}$. For the trial and error method of determining U, one of the longtime traverses (for example the 3.50 hr one shown in Fig. 7) was used and Eqs. 36 and 37 were used until a match was obtained. It indicated $0.116 \text{ Btu/hr-sqft-}^{\circ}\text{F}$ for U. The computed result is in good agreement with the result from the trial and error method.

A closer examination of Fig. 6 and detailed investigation of the overall heat transfer coefficient and its effect on the steam plateau model indicated that the model represents the long-time temperature profiles accurately while it does not match the early-time behavior equally well. This suggested that the early-time behavior appears to be controlled by an overall heat transfer coefficient which is larger than that controlling the long-time behavior. This was also pointed out for Arihara's⁶ cold/hot water injection experiments by Atkinson.⁵ This result indicates that the effective overall heat transfer coefficient is probably unsteady in nature. This should be expected since the effective heat transfer coefficient is actually the result of a combination of conduction and convection as discussed by Atkinson.⁵

Fig. 8 shows the comparison of experimental and computed results of only one temperature traverse for Run 78-2. As may be seen, the agreement

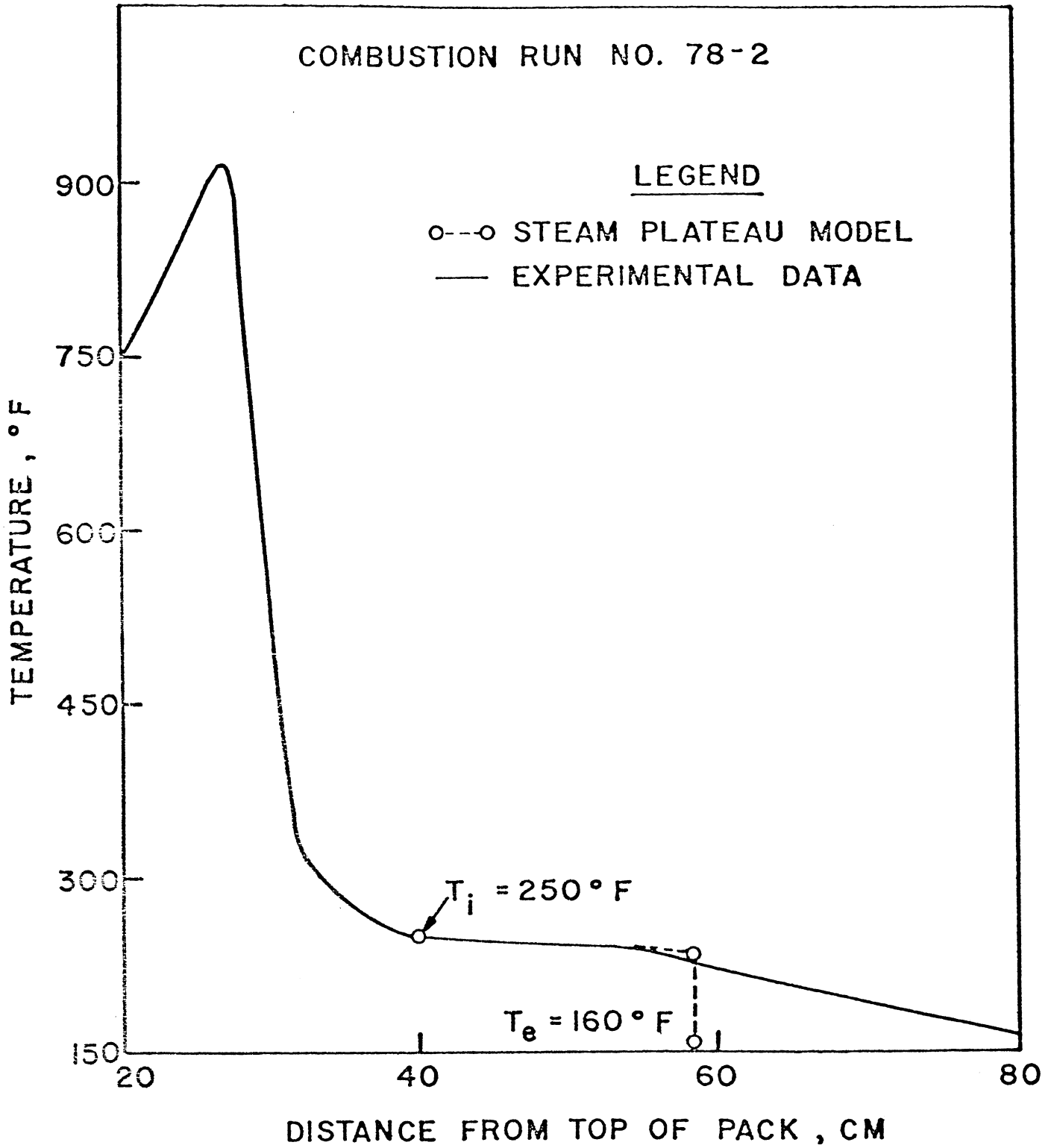


FIG.8: COMPARISON OF THE CALCULATED AND EXPERIMENTAL RESULTS FOR ONE TRAVERSE OF RUN 78-2

is reasonably close to the experimental results. As also it is noticed, the analytical solution indicates a larger size for the steam plateau. This is essentially due to the fact that the steam plateau with a sharp front moves as an idealized step function temperature profile. A schematic temperature profile is shown in Fig. 9. The movement of a steam plateau with a sharp front is mainly a result of neglecting heat transport by conduction. This result is also similar to the comparisons indicated by Atkinson on Arihara's injection data.

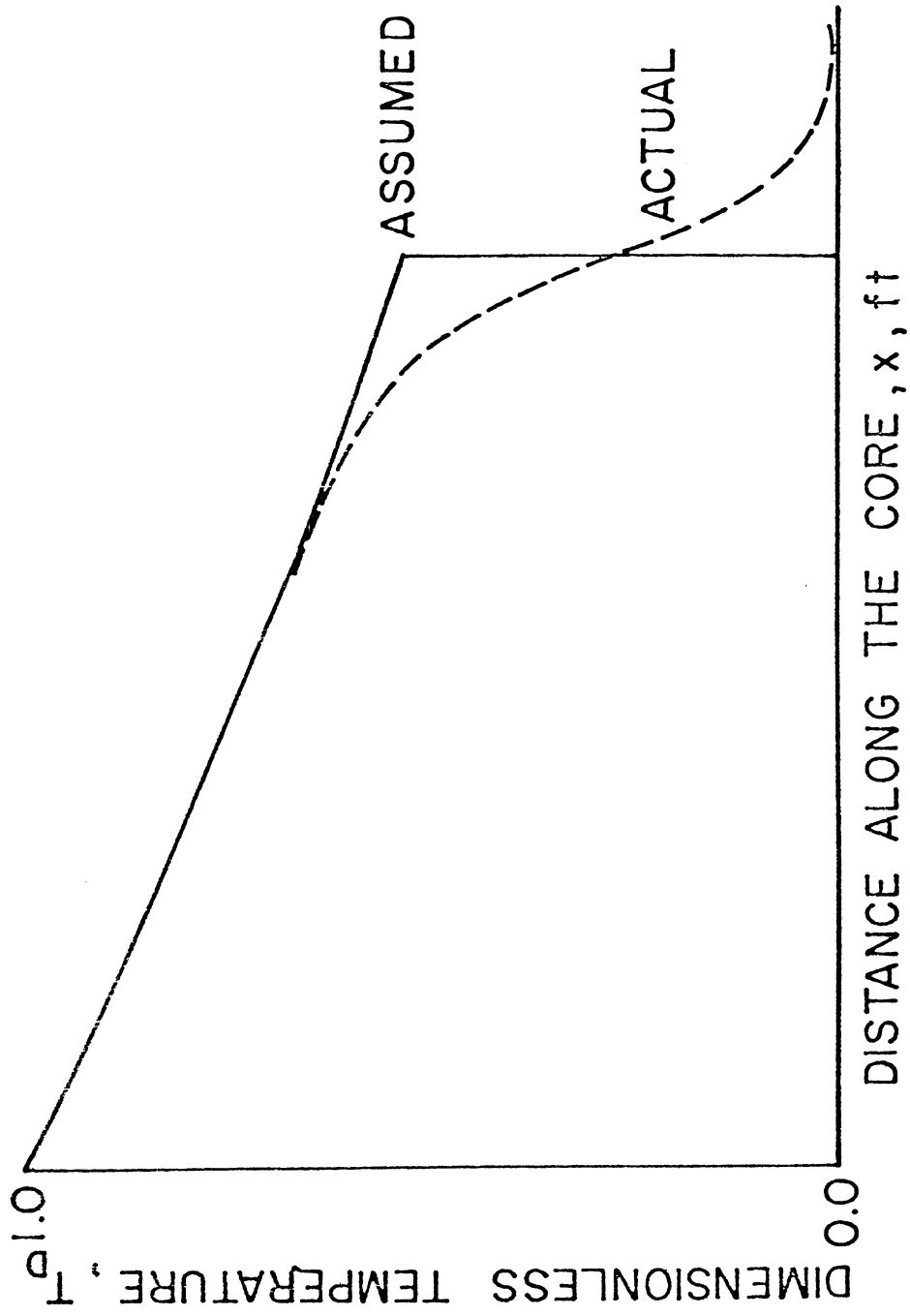


FIG. 9: SCHEMATIC TEMPERATURE PROFILE

5. EXPERIMENTAL EQUIPMENT

A schematic diagram of the combustion tube apparatus is illustrated in Fig. 10 and Table 1. The combustion tube and assembly were enclosed in an angle iron frame. Components mounted in this frame include the combustion tube, pressure shell, pressure gages, control valves and other complementary equipment. These main parts were available from previous studies.

The combustion tube is a 39.19" long by 2.968" diameter, type 321 stainless steel tube with a 0.016" wall thickness and has flanges at both ends silver soldered to the tube as shown in Fig. 11. Liner and pressure shell detail is presented in the same figure. The top flanges are secured against a ten-gage copper wire gasket, while the bottom flanges connected with a Teflon gasket and with two stainless steel wire screens of different mesh fitted exactly in the groove. One of the screens is of 200 mesh to prevent the sand from coming out through the production line, and the other is of 10 mesh to support the upper one.

The combustion tube is inserted in a pressure shell. Insulation is obtained by filling the annular space between the combustion tube and the pressure shell with Santocel.

The igniter is a 240 volt, strap-on resistance type heater that is clamped around the combustion tube just above the packed sand face. The voltage to the igniter is controlled by a 110 volt transformer.

For Run 78-1, an electrical heating tape was wrapped around the pressure shell to preheat the combustion tube to simulate reservoir temperature.

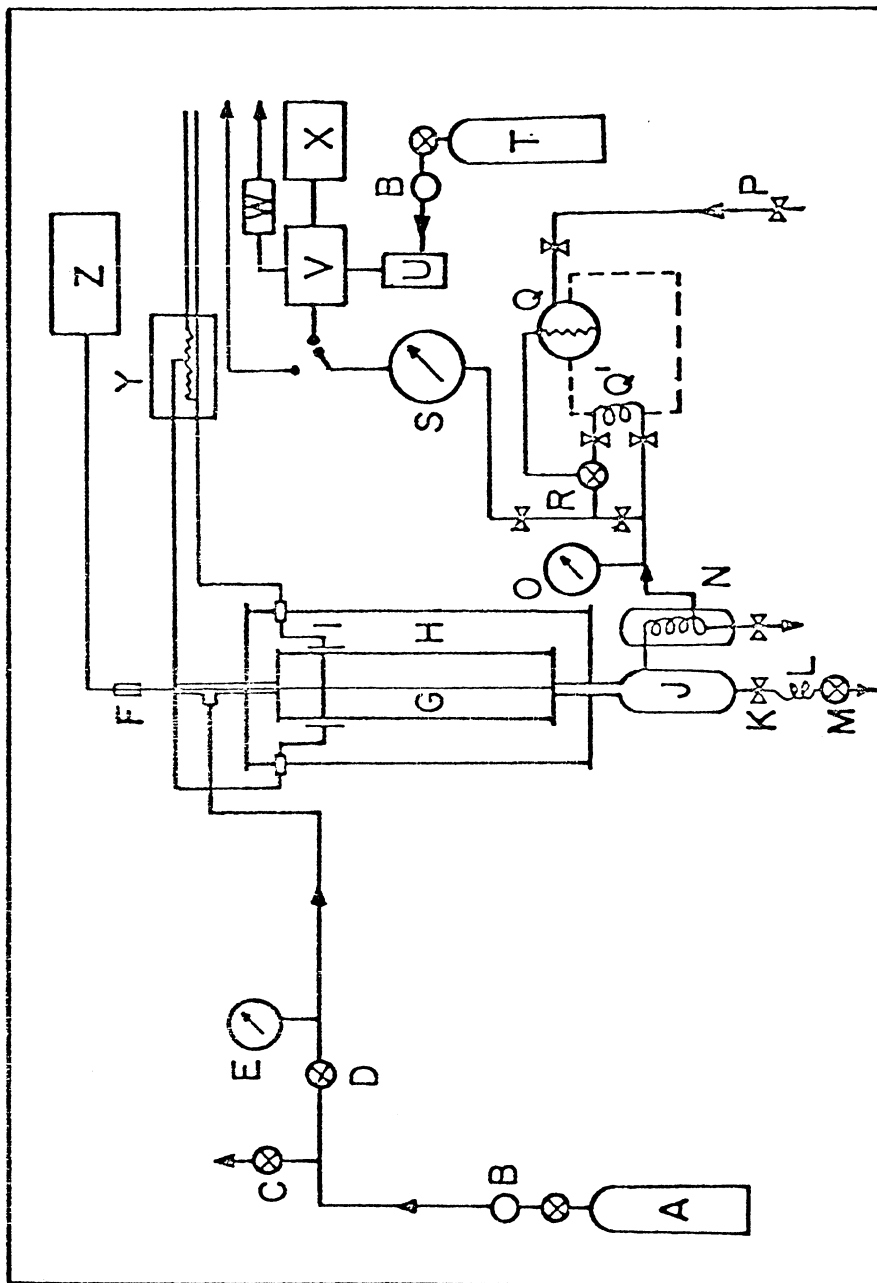


FIG. 10: SCHEMATIC DIAGRAM OF THE COMBUSTION TUBE APPARATUS

TABLE I. PARTS OF THE COMBUSTION TUBE APPARATUS

SHOWN ON FIGURE 10

A. Air Supply	N. Condenser
B. Regulator	O. Exit Gas Pressure Gage
C. Air Release Valve	P. Laboratory Air Supply
D. Inlet Air Control Valve	Q. Differential Pressure Cell
E. Inlet Air Pressure Gage	Q'. Capillary Tubing
F. Axial Thermocouple and Extension Wire	R. Flow Rate Control Valve
G. Combustion Tube	S. Wet Test Meter
H. Annulus	T. Helium
I. Igniter	U. Driarite
J. Separator	V. Gas Chromatograph
K. Gate Valve	W. Purge Meter
L. Coiled Copper Tube	X. Recorder
M. Produced Oil Control Valve	Y. Transformer
	Z. Temperature Recorder

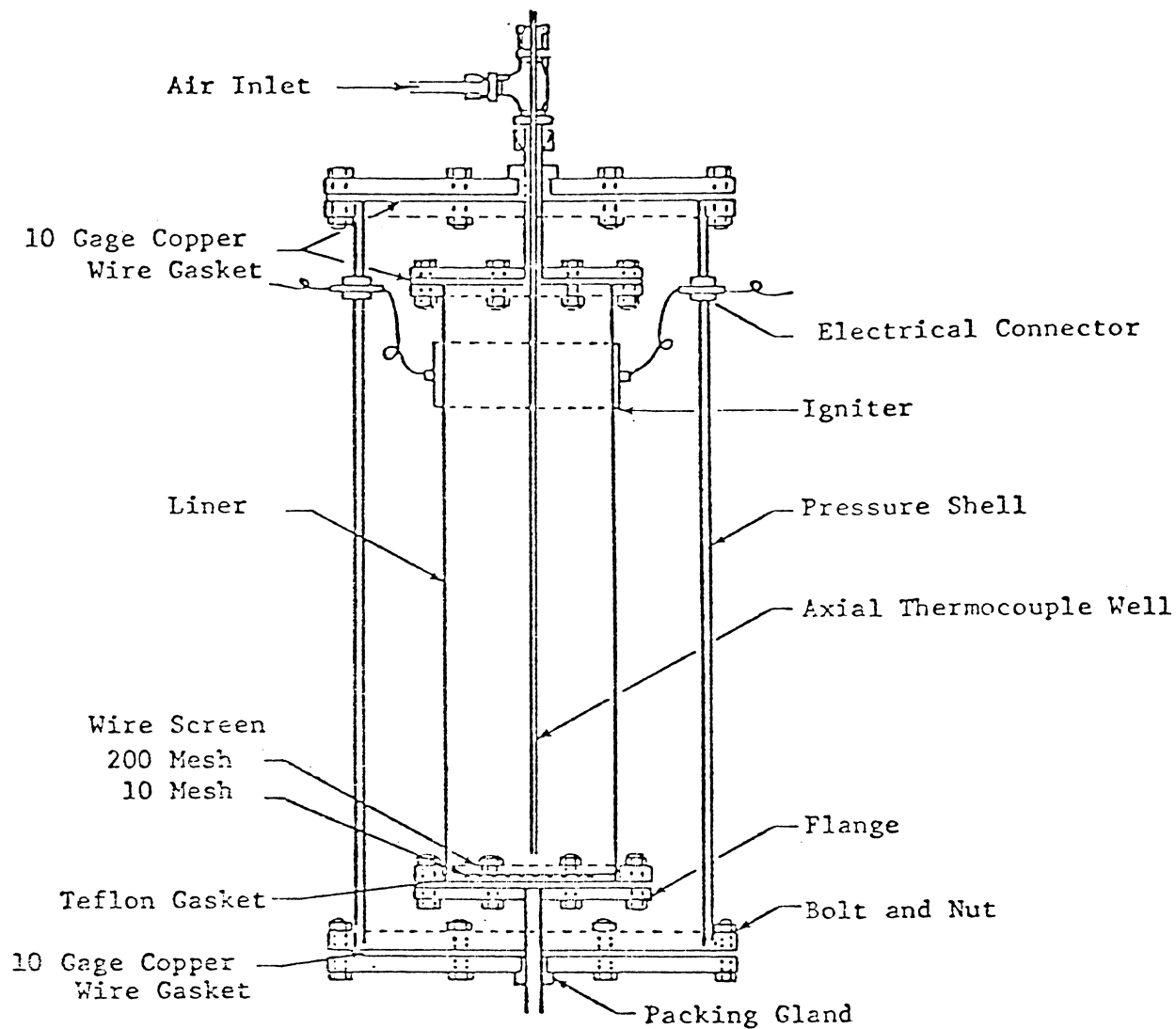


FIG. 11: COMBUSTION TUBE ASSEMBLY

In order to have a more uniform temperature distribution, three separate heating tapes were wrapped for Runs 78-2 thru 78-6.

Temperature measurement in the combustion tube was performed by probing the entire length of the combustion tube with a 1/25" diameter chromel alumel thermocouple which was inserted in a 0.72" thermocouple well positioned in the center of the tube. The measured temperatures were recorded every half hour.

Air supply for combustion was obtained from a 2000 psi cylinder of compressed air equipped with a two-stage pressure regulator.

All exit gas and liquid passed through a separator constructed by connecting two caps with a coupling between. A two-valve exit system was used for draining the liquid from the separator. The top valve was a gate valve while the lower valve was a needle valve.

Pressure gages were connected so that inlet and exit pressure could be observed.

Combustion gases were metered through a wet test meter and analyzed for composition by means of a gas chromatograph. The output from the chromatograph was plotted on a Texas Instruments recorder.

A manually operated exit gas-glow control was replaced with an automatic flow control system in order to have the experiment operate with a burning front and steam plateau moving at constant velocity and temperature. This control system was based on the pressure drop across a capillary tube which was monitored by a delta-pressure cell with a 3- to 15-psi output pressure signal. This was necessary because the manual valve required the constant attention of one man throughout the entire tube run. Heating tape wrapped around the outside of the pressure shell

to increase the ambient tube temperature also reduced the possibility of fluid blocking from viscous oil and high oil saturations.

5.1 Experimental Procedure

The combustion tube was prepared for a run by first mixing the sand, clay, oil, and water to yield the desired fluid saturation distributions. This mixture was then tamped into the combustion tube with care to avoid moving the axial thermowell.

In order to yield a fast, uniform ignition approximately three cubic centimeters of linseed oil was dropped on the sand face before bolting the top flange assembly on the combustion tube. The tube was then set in a horizontal position, and tested for leaks by applying 100 psig air pressure. After this test, the combustion tube was positioned into the pressure shell, and Santocel insulation was poured into the annular space. The top flange was secured on the pressure shell, the tube was connected to inlet air pipe, separator, and wet test meter, and every connection was tested for leaks with a soap solution, while 125 psig air pressure was applied to the system.

After leak control, the external tape heater was turned on to bring the initial temperature of the sand pack to the desired elevated temperature. The flow rate control system was calibrated. Also, the gas analyzer was calibrated and brought to thermal equilibrium.

At the start of the run, inlet pressure was set at injection pressure and the flow control system was regulated to allow a flow rate of 113 lit/hr (4 cu ft/hr).

The combustion tube pressure, shell pressure, volume of gas metered out of the system and any special observances were recorded every 15 minutes

throughout the entire run. The separator was checked for the first sign of liquid production. Produced oil and water was collected in glass jars of known weight, and weighed as additional production was received.

Shortly after ignition had been achieved, the entire length of the combustion tube was traversed with the axially probing thermocouple. This enabled an accurate determination of the combustion front position and temperature distribution. Subsequent traverses were taken every half hour. Gas analyses were taken every 10 to 15 minutes.

All of the data-taking operations were performed throughout the run until the burning front reached the bottom flange. The run was then terminated.

The equipment was dismantled and the analyses of the data were begun. These included analyses of liquid samples and a complete materials balance of all the material originally packed into and produced from the combustion tube.

5.2 Experimental Method and Results

The experimental method consisted of three major parts: (1) preparation of the oil sand test pack, (2) the combustion run, and (3) analysis of products and results.

5.2.1 Preparation of Pack: A mixture of known weight of sand, clay, water, and oil, prepared such as to yield the desired porosity and fluid saturation distributions, was tamped into the combustion tube. Samples were taken at the top, middle and bottom of the pack. These samples were then used to check the calculated oil and water saturations.

Table 2 presents the initial pack conditions for the six runs in which the saturations, clay content and porosity were determined based on the weights of the materials put into the unconsolidated pack.

5.2.2 Combustion Characteristics: After packing and all those necessary check-ups mentioned above, air flow through the pack was established. The axial thermocouple was positioned at the upper sand face (air inlet side) and the igniter was turned "on." Temperature at the sand face was recorded until a sharp rise in the heating curve signaled ignition of the sand face.

Produced gas rate and produced gas composition all as functions of time and temperatures as a function of distance from top of the pack were measured periodically. Figure 12 shows the produced gas rate as a function of run time for Run 78-4. Produced gas composition versus run time for Run 78-3 is shown in Figure 13. Temperatures along tube axis for Run 78-2 is shown in Fig. 14. The temperature traverses graphed on Fig. 14 were selected to provide representative information, the additional curves were omitted for clarity of presentation.

Figure 15 shows cumulative oil and water production for Run 78-2. The cumulative liquid production data shown on this figure were determined from BS and W measurements on portions of the produced liquids. Results are presented as weight percentages of the total produced.

The burning front and steam plateau locations for Run 78-2 as function of time are presented in Figure 16. The burning front and steam plateau locations were determined from temperature traverses, and the locations are expressed in centimeters from the top of the pack (air inlet side). The location of the burning front was taken to be the peak temperature,

TABEL II. INITIAL PACK CONDITIONS FOR TUBE RUNS

TUBE RUN NUMBER

	78-1	78-2	78-3	78-4	78-5	78-6
Type of Oil	Lombardi Zone- San Ardo					
Type of Sand	Ottowa Sand 20-30 Mesh	Ottowa Sand 20-30 Mesh	Ottowa Sand 20-30 Mesh	Ottowa Sant 80 Mesh	Ottowa Sand 80 Mesh	Ottowa Sand 80 Mesh
Type of Clay	Fire Clay	Fire Clay	Fire Clay	Fire Clay	Fire Clay	Fire Clay
Clay Content, Wt. %	1.0	1.2	5.8	8.5	8.9	4.8
Porosity, % Bulk Volume	40.5	40.0	47.8	46.4		39.0
Oil Saturation, % Pore Volume	30.1	43.7	24.1	39.2	29	48.0
Water Saturation, % Pore Volume	21.7	20.3	12.7	0.0	0.0	22.0
Gas Saturation, % Pore Volume	48.2	36.0	63.2	60.8	71.0	30.0
Initial Temp., °F	165	160	145	210	80	145

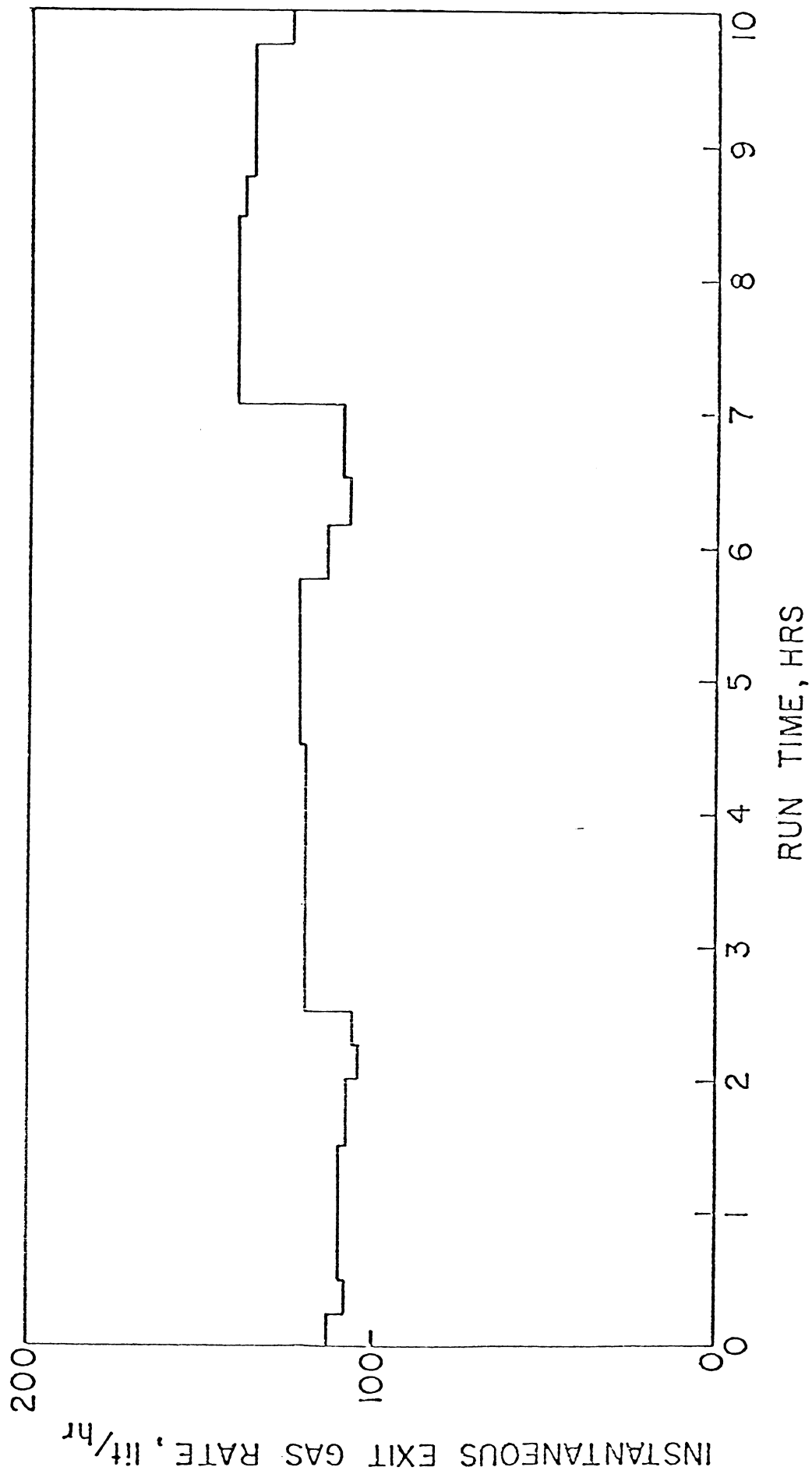


FIG. 12: PRODUCED GAS RATE VS RUN TIME FOR RUN 78-4

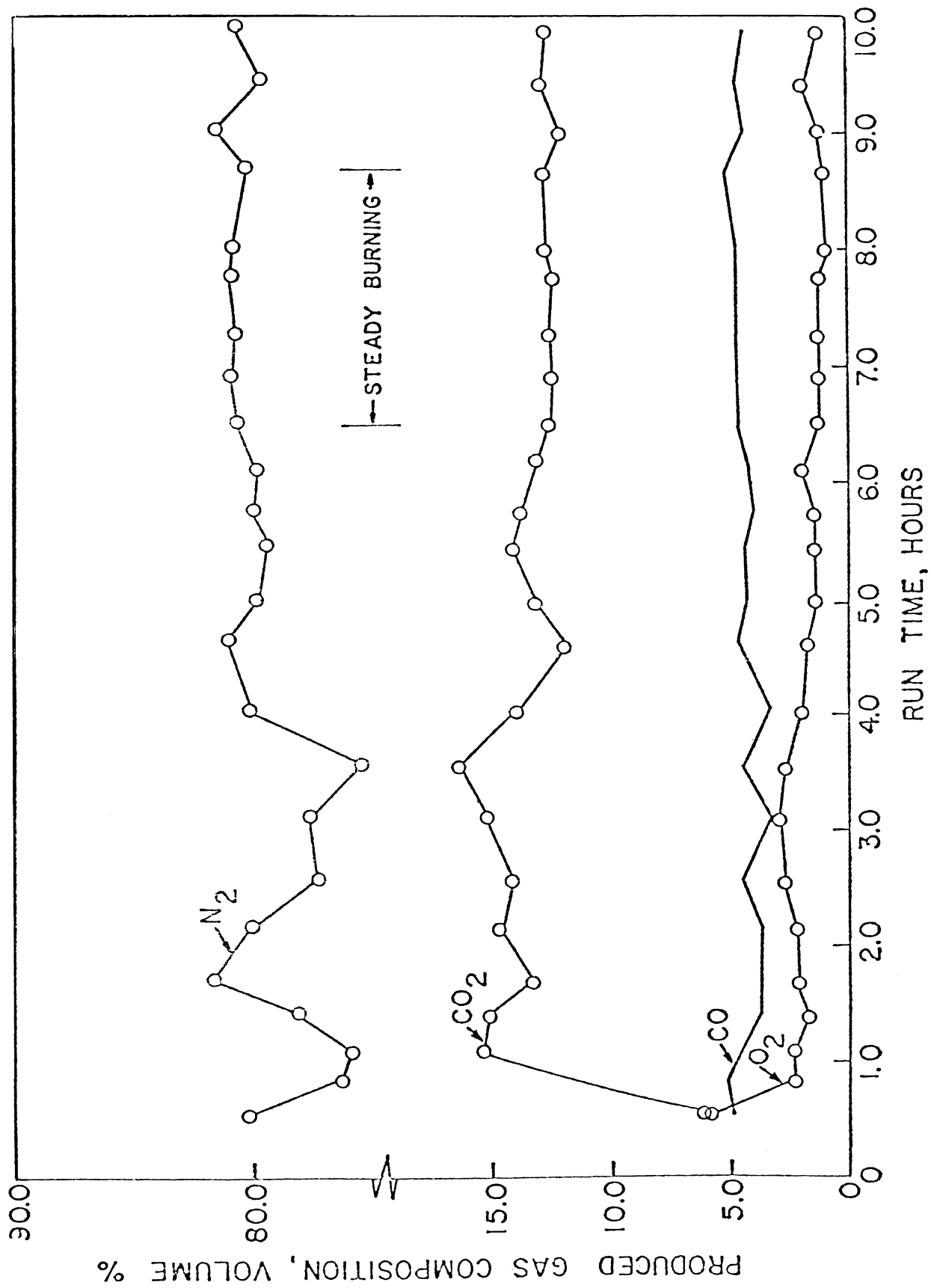


FIG. 13: PRODUCED GAS COMPOSITION VS RUN TIME FOR RUN 78-3

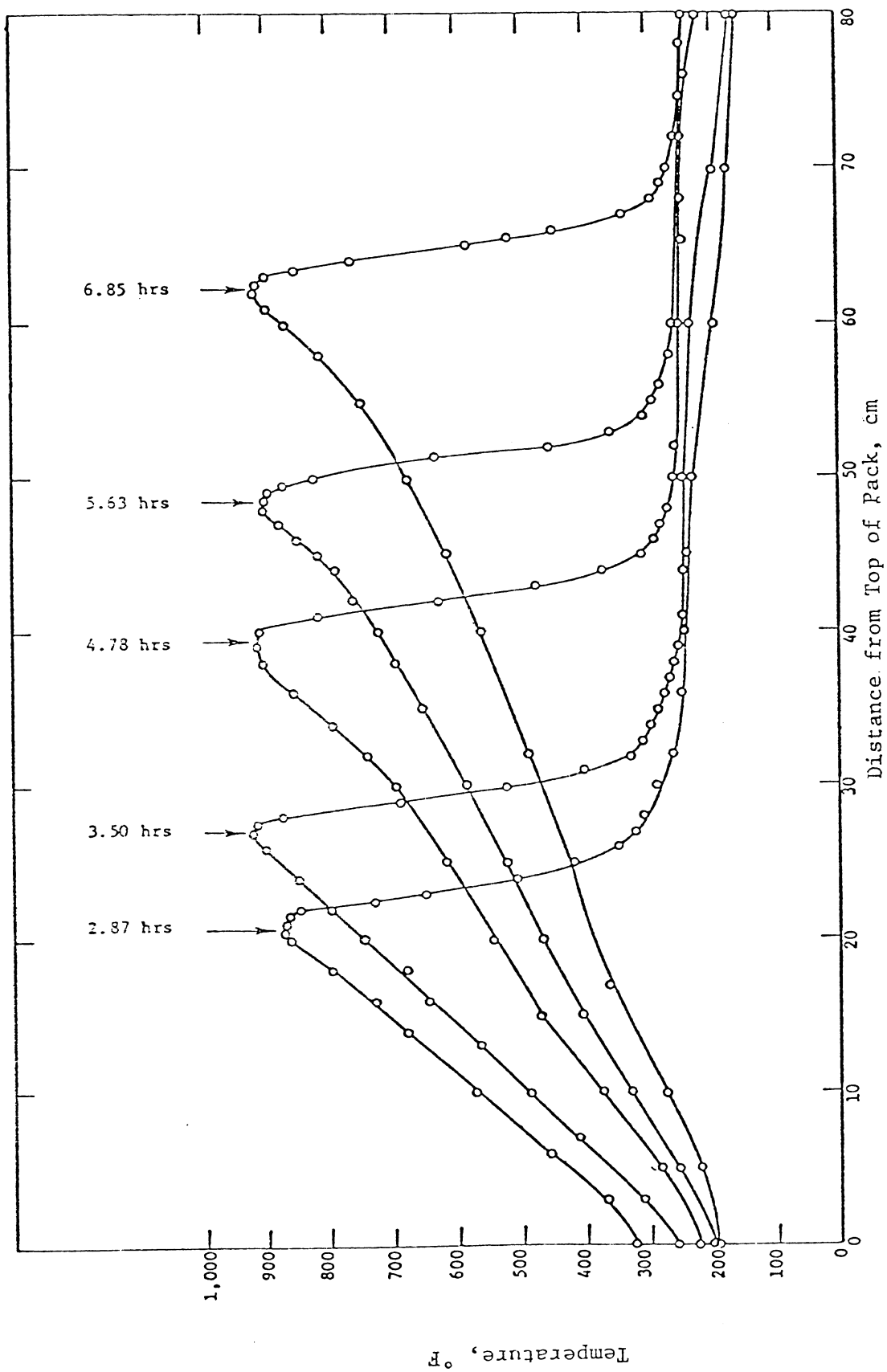


FIG. 14: TEMPERATURE PROFILES FOR RUN 78-2

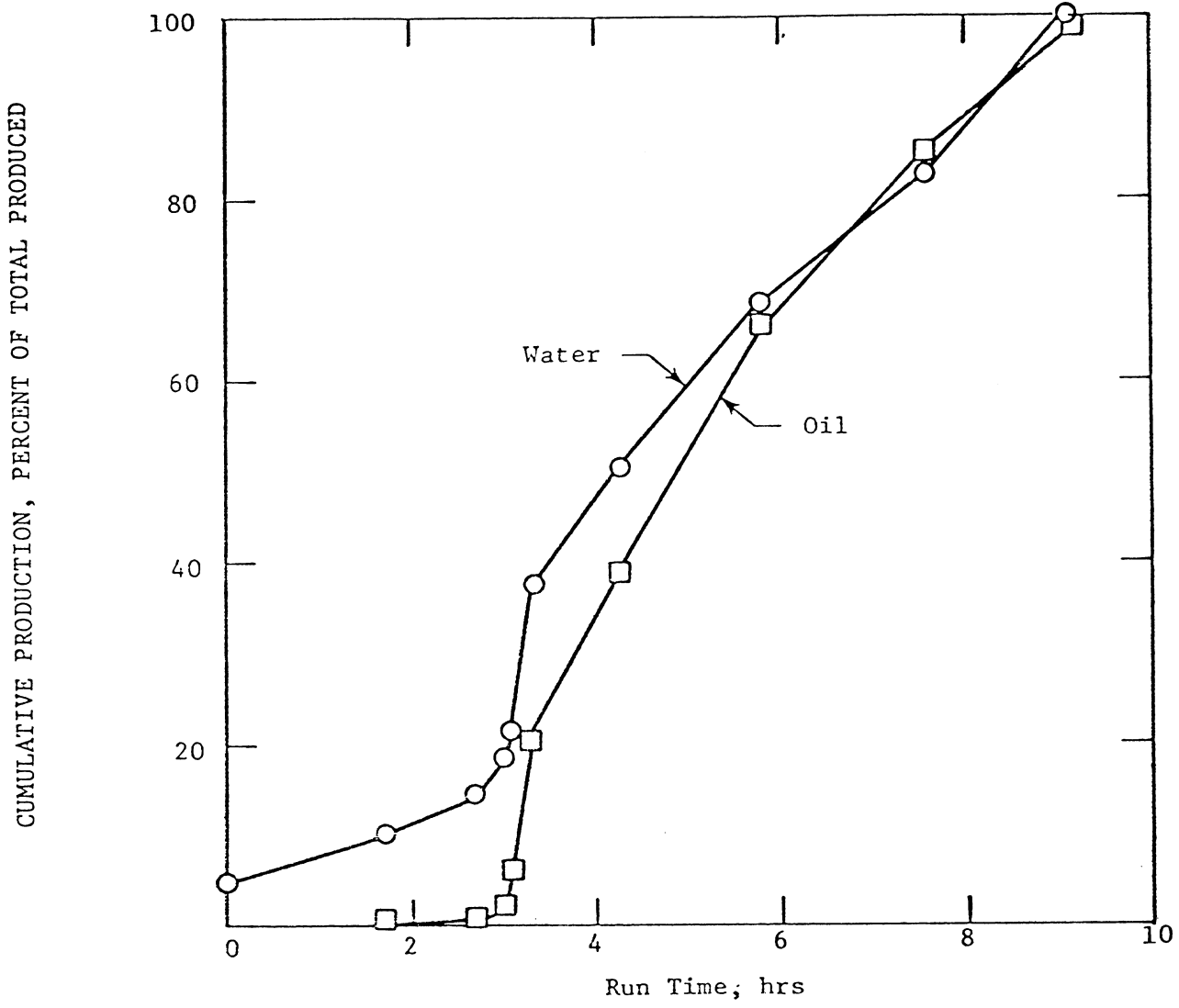


FIG. 15: CUMULATIVE LIQUID PRODUCTION FOR RUN 78-2

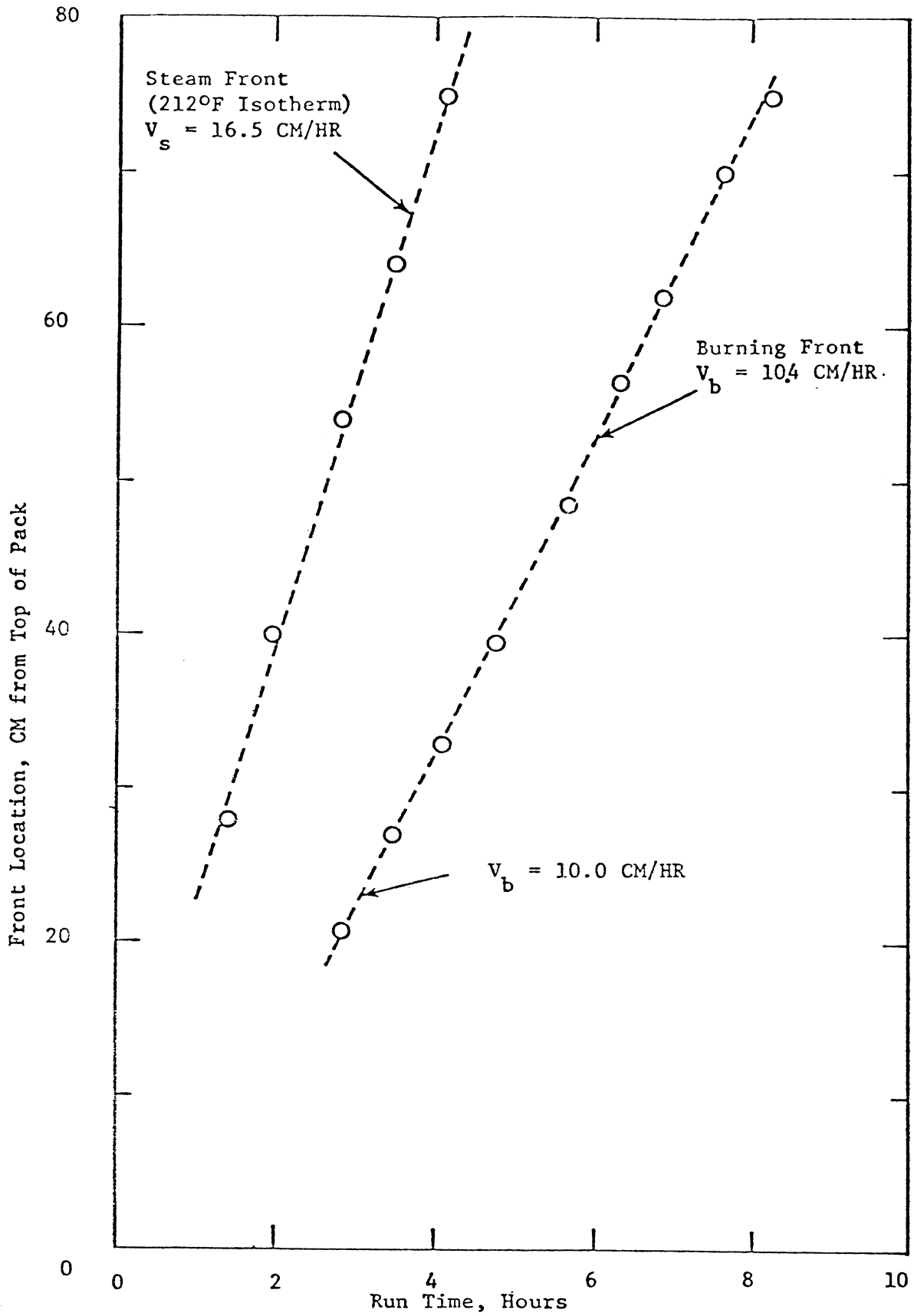


FIG. 16: THE BURNING FRONT AND STEAM PLATEAU LOCATIONS FOR RUN 78-2

while the 212°F isotherm was taken to be the location of the leading edge of the steam plateau. Other temperature than 212°F could be used, but the results would be similar. This isotherm is representative of the growth of the steam plateau and therefore of its velocity under the conditions employed for the runs.

Complete details on all these runs have been given in reports Numbers TR-7³⁹ and TR-10⁴⁰.

5.2.3 Analysis of Products and Results: There were three main purposes of the experimental phase of this study:

1. It is expected to promote a better understanding of the problems and mechanisms involved in laboratory investigations and field applications of the in-situ combustion process.
2. It will provide data to test our analytical formulation of the steam plateau.
3. Better understanding of in-situ combustion will also help to check the accuracy of the correlation work for in-situ combustion field applications. In the course of this study, six combustion tube runs were performed.

Also results of other combustion tube experiments 27, 28 were used to accomplish the main purposes mentioned above.

The tube runs were designed in such a manner that a variety of conditions could be observed experimentally. Conditions that varied were; amount of clay in sand, water saturation, oil saturation, injection pressure, air flux, and the initial tube temperature. Under this variety of operating conditions, the basic fundamentals of the combustion process, mainly of the steam plateau, and the factors that affect it have been

studied. A summary of combustion-tube results of each tube run is shown in Table 3.

As can be seen from Tables 2 and 3, the amount of clay in the sand basically changes the combustion characteristics of the matrix. Due to the oil absorption capability of clay, increasing clay content increased combustion efficiency. An increase in heat availability caused by the absorption of oxygenated hydrocarbons on the clay components in the matrix was also observed in Differential Thermal Analysis thermograms made by Hardy²⁹. However, change of clay content did not have any particular effect on the steam plateau.

Although the primary purpose of the heating tape was to simulate elevated formation temperatures and to reduce fluid blocking, a number of important effects were observed as a result of varying initial conditions. With a higher initial temperature, the steam-plateau velocity increased. Generally lower steam plateau velocities were observed for lower initial pack temperatures and the difference between burning front velocity and steam plateau velocity became minimum (see Runs 78-3, 78-5, and 78-6 in Table 2). This is partly due to the heat loss and partly due to the overall energy balance. The lower initial pack temperature causes higher heat loss and therefore the velocity of the steam plateau is smaller than it is for higher initial pack temperature runs. A lower initial temperature also requires more heat to be deposited in the steam plateau region in order to achieve steam plateau temperature, thus the total steam plateau movement must be smaller. This can be seen from the coefficients in Equations 36 and 37. The important coefficients, β , γ and ϵ , become smaller due to a lower initial pack temperature (see Equations 23-25) and thus the

TABLE III

SUMMARY OF COMBUSTION TUBE RESULTS

	TUBE RUN NUMBER					
	78-1	78-2	78-3	78-4	78-5	78-6
Injected Air Flux, lit/hr	115	123	156	120	167	165
Injection Pressure, psig	100	100	100	100	100	200
Burning Front Velocity, cm/hr	11.8	10.2	10.8	7.2- 12.3	13.0	15.4
Steam Plateau Velocity, cm/hr	16.9	16.5	11.3	---	13.5	15.7
Produced Gas Analysis, Vol. %						
Carbon Dioxide	10.8	10.6	12.5	14.7	14.5	12.9
Carbon Monoxide	1.5	6.1	4.7	3.5	5.2	5.2
Oxygen	4.4	3.7	1.1	1.9	1.4	2.3
Nitrogen	82.3	78.7	80.7	78.8	78.9	78.4
Atomic H/C Ratio of Fuel	1.9	0.86	1.29	0.66	0.67	0.68
Fuel Concentration, lb/ft ³ Bulk Vol.	1.07	1.53	1.44	2.22	1.87	1.39
Air-fuel Ratio, scf/lb	232	117.5	199.3	168.5	162.5	164.0
Air-sand Ratio, mmscf/ac-ft	10.7	11.7	10.7	16.3	12.8	9.9

growth rate of the steam plateau decreases.

Another important effect of elevated formation temperature was observed during Run 78-4. As Fig. 17 shows, there was no apparent steam plateau. Elevated temperature for this run was 210^oF and it contained no initial water saturation. Since water saturation was zero, the only water available to form a steam plateau was the water formed due to combustion of fuel. The partial pressure of that amount of water vapor in the gas phase was not enough to form a steam plateau at a higher temperature than elevated temperature. This result obviously supports the theory which states that the temperature in the steam plateau is set by the partial pressure of water vapor in the gas phase and water vapor in the gas phase consists of (1) water formed due to combustion at the burning front, (2) water vaporized in the region between the burning front and steam plateau. Most of this water is normally the vaporized water, which did not exist in Run 78-4.

Air injection pressure is another of the major factors affecting the steam plateau. Equation 11 indicates that increasing air injection pressure should raise the partial pressure of steam and therefore the steam plateau temperature. Figure 18 shows two temperature traverses Runs 78-2 and 78-6. Conditions were similar for the two runs, except that Run 78-6 was made with air injection pressure of 200 psig while run 78-2 was made with 100 psig. Notice that Run 78-6 has a steam plateau temperature of 300^oF which is higher than steam plateau temperature of 250^oF for Run 78-2. This result is also consistent with the steam plateau theory.

The effect of air flux was also investigated. To do this, the combustion tube results of Reference 27 were used. Figure 19 shows two temperature traverses for Runs 10 and 12 of Reference 27. Conditions

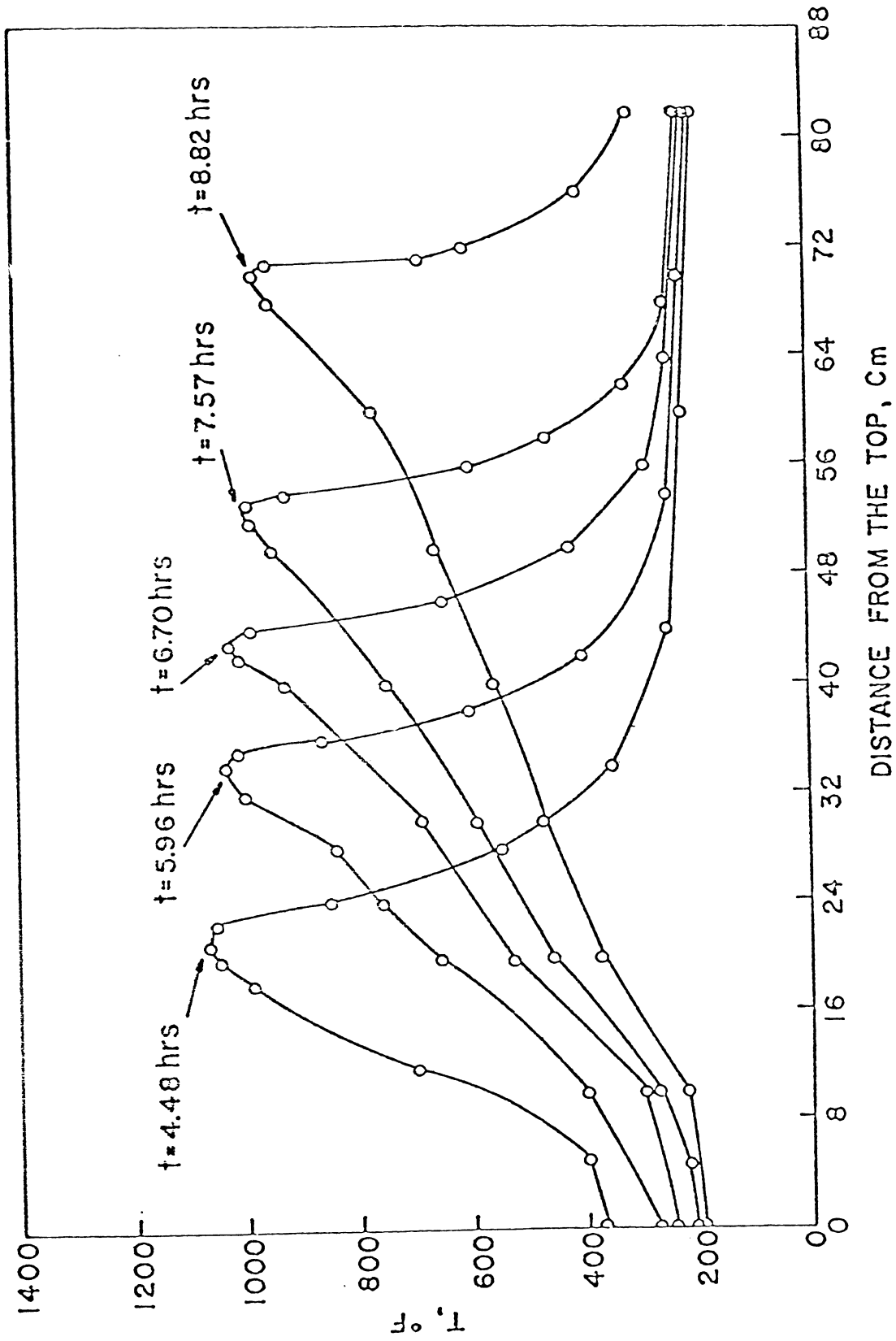


FIG. 17: TEMPERATURE PROFILES FOR RUN 78-4

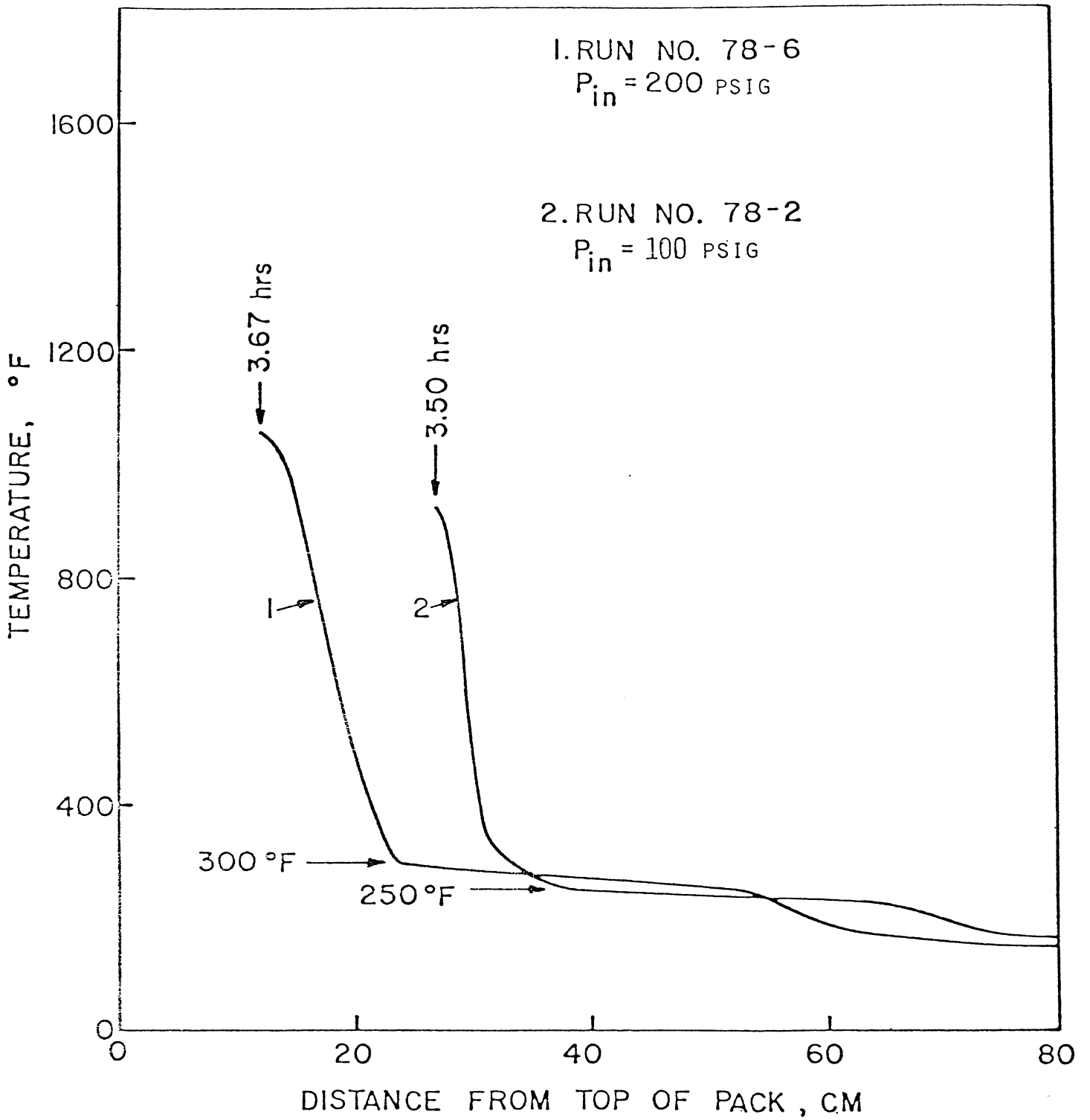


Fig. 18: EFFECT OF AIR INJECTION PRESSURE ON THE STEAM PLATEAU TEMPERATURE

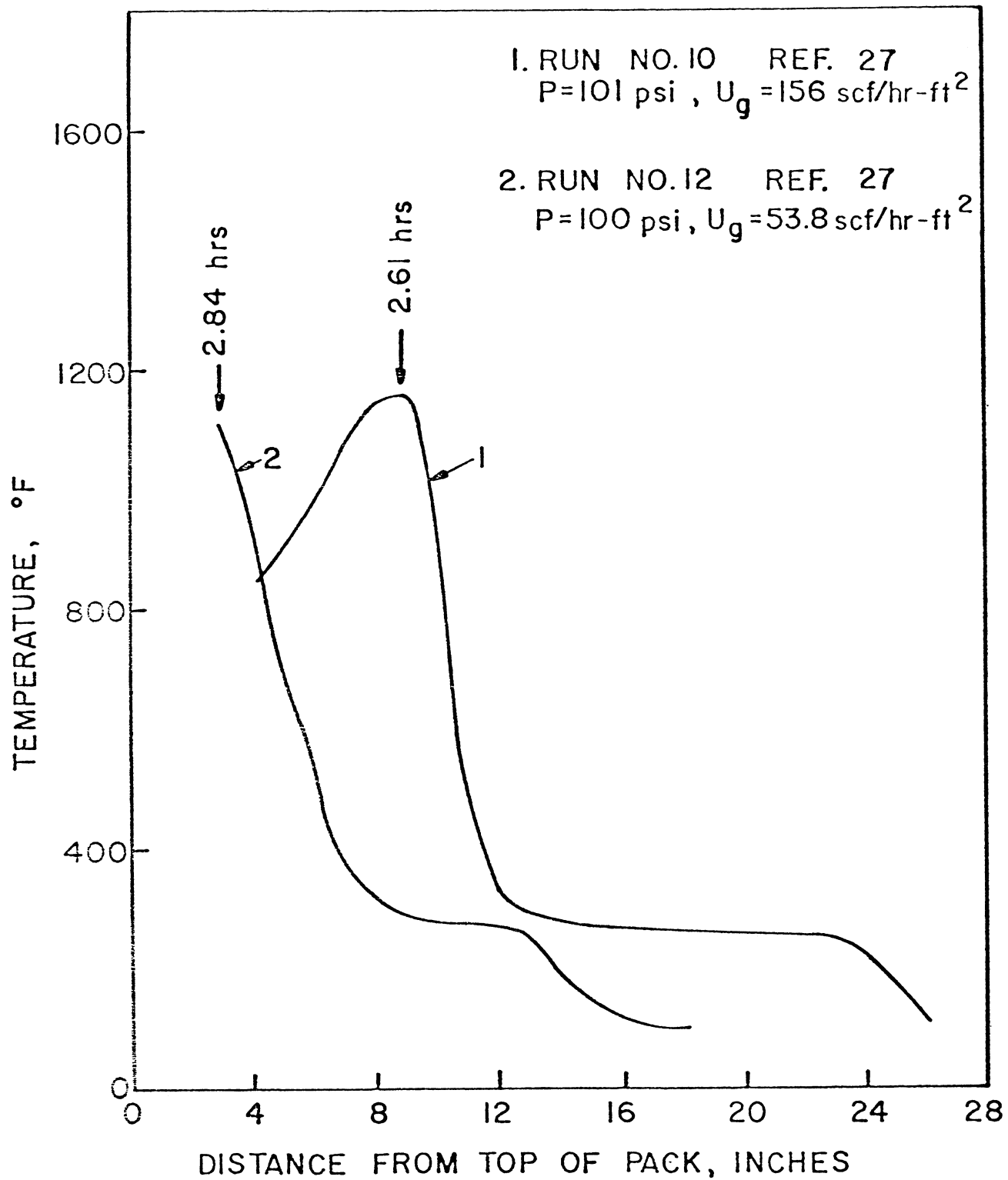


FIG. 19: EFFECT OF AIR FLUX ON THE STEAM PLATEAU GROWTH

were similar except that the air flux for Run 10 was nearly three times higher than the air flux for Run 12. As should be expected, the steam plateau grows faster with a higher air flux than with smaller air flux. The theory also predicts the same result (see Figure 5).

All of the factors except the clay content of the matrix, as mentioned, directly affect the behavior of the steam plateau. Particularly it can be concluded that the steam plateau temperature is controlled by the air injection pressure and initial water saturation; and the rate of growth of the steam plateau may be controlled by the air flux rate and by the level of the elevated formation temperature.

The results of combustion runs were also studied in order to check the effect of the variables involved in the correlation equations for dry in-situ combustion field cases (to be discussed in the Section 6). From three variables, oil saturation, thickness and oil viscosity, only the effect of oil saturation was properly investigated in the combustion runs. Runs with different oil saturations showed different oil recovery histories. Generally, runs with higher oil saturation had faster oil recovery responses. In terms of the correlation equations, Equations 44 and 47 discussed later, this means that higher oil recovery would be possible for a field with higher oil saturation. This is of course consistent with the correlation equations; they lead to the same conclusion.

6. RECOVERY CORRELATIONS FOR IN-SITU COMBUSTION PROCESSES

For any enhanced recovery project, its relative success depends on the additional oil recovered, the value of that oil, and the additional cost associated with recovery of the oil. If the value of the additional oil exceeds the additional cost involved, the project is economically successful. Although this concept is simple in principle, there are subtle problems in determining or predicting these terms. A detailed discussion of economics of fire flooding can be found in the literature³¹.

6.1 Parameters Affecting Combustion Performance

Crude oil properties and reservoir properties are also very important economic parameters, for they are the parameters which determine what will be the volume of additional oil recovered and volume of air injected in any in-situ combustion. Therefore these economic parameters and important crude oil and reservoir properties will be discussed in the following paragraphs.

Incremental oil recovery is the additional oil recovered beyond that which would have been recovered by continuing the process in use at the time in-situ combustion was initiated. Fire flooding can be initiated at any time in the life of the field as long as there is enough oil present to make it an economically attractive project. To compare incremental oil recovery from several fields, it will be necessary to normalize the results in a reasonable fashion.

Total recovery also depends on the vertical and areal sweep efficiency in the reservoir. Vertical sweep efficiency can be affected by the permeability variation of the formation, and also by gravity segregation, which, in turn, is affected by formation thickness, permeability and injection rate. Gravity segregation can either help or harm recovery, depending on the geometry of the flow system.

Areal sweep efficiencies also depend on the pattern geometry. Attempts have been made in field tests to improve the areal coverage by curtailing production from selected wells, with little success. It appears that the direction of movement of the air is affected only slightly by such measures. Both vertical and areal sweep efficiencies can be severely reduced by factors such as cross bedding, incipient fractures, and permeability anisotropy.

Besides incremental oil recovered, the required volume of air injection is also an important factor in the success of a combustion project. Air injection is a major cost in fire flooding operations. The cost depends primarily on the volume of air injected and to a somewhat lesser extent on the injection pressure. A general way to treat this is either to relate it to the oil produced through the air-oil ratio, or to correlate air injection against oil recovery. These numbers can then later be related to costs specific to a given field operation.

It is usually desirable to have air rates as high as possible consistent with the injectivity of the air, the ability of the producing wells to handle the oil, and the maximum pressure the reservoir can handle without fracturing.

When water is injected with the air, generally it is assumed that less air is required to produce a given amount of oil, depending on the water-air ratio used, but the injectivity will drop due to relative permeability effects.

To predict rates of injection and recovery, all these interactions must be accounted for.

Oil saturation and fuel content are both important to the process. Movable oil ($S_o - S_{or}$), total oil content (ϕS_o), and fuel content all are important to the process. For dry combustion, Peottman²⁰ has suggested a minimum value of ϕS_o equals 0.10, and Geffen²¹ has suggested ϕS_o greater than 0.05 for wet combustion. Both these suggested values are rule of thumb numbers based on their experience. Fuel content generally has to be above 0.5 - 0.75 lb fuel/ft³ sand for the combustion front to be sustained by air injection alone³². Fuel content depends on many parameters; among them: initial oil saturation, oil properties, combustion temperature, pressure, and formation characteristics.

Peottman²⁰ suggested that the net formation thickness should be at about 10 ft or more to minimize heat losses. Also it is known that a very thick formation needs a high air injection rate to achieve good sweep efficiencies. But this would lead to high project costs or even economic failure if this high injection rate could not be afforded. Further, there is a number of combustion projects in sands less than 10 ft thickness (see Table 4B in Section 6.1), so the formation thickness question is not yet completely resolved.

The porosity of the formation should be sufficient in magnitude to provide an oil volume large enough to burn and to recover economic quantities of oil. Actually it is a question of the ϕS_o term mentioned above.

In regard to oil viscosity, usually fire flooding is applied to heavy oil reservoirs of less than 30° API oil, which implies high viscosity. An upper bound on the viscosity of oil in a successful fireflood has been

suggested. Chu²⁴ has suggested 1,000 cp as an upper limit on the ground that steam flooding is preferable for very viscous oils. As a lower bound, he chose 150 cp. No reason was given to substantiate this range of viscosities, further there are a number of field cases which have operated outside this viscosity range.

6.2 In-Situ Combustion Correlation Efforts

Since December 1976, results of in-situ combustion processes have been gathered from various sources: published papers, unpublished reports from companies performing the tests, ERDA reports, and personal interviews. Many companies were contacted. The personal interviews were particularly helpful, for through these discussions we were able to get detailed information that was not otherwise available and were also able to get personal impressions about various field projects that are often suppressed in company reports or published papers. At present, we have detailed information on 40 field tests. From the literature^{22,23,24} it appears that about 100 field tests have been run. We were not able to get detailed information on all these for the following reasons:

1. Many of the tests were failures. Most of these should have been expected to be failures for the reservoir properties were simply not suitable for combustion. They were run for such a short time that little data exists. Further, there is a natural reluctance to talk about such tests.
2. Some tests were run so long ago that the data no longer exists.
3. A few companies (a small minority) were not willing to release the data on their field tests since they had not been published in the open literature.

4. There are a few results in foreign language journals²³ that we have not yet had time to translate.
5. An additional 5 to 10 field tests have not been included in our list for they are in reservoirs where several secondary producing mechanisms are occurring simultaneously and it is difficult to separate out the recovery due to each mechanism.

The detailed information on these 40 field tests has been coded into punched cards for easy access. The data has also been tabulated. The information is in Tables 4A, 4B, and 4C. Table 4A shows the general characteristics of these field tests; Table 4B shows the rock and fluid properties, i.e., data available in the fields prior to the start of in-situ combustion; Table 4C shows the important operating characteristics of the combustion tests in these fields.

A study of the data in Table 4A shows that there is a broad variety of operating modes associated with these tests. Some are for dry combustion, others used water, either injected with the air or after the air was injected. Some are for pilot tests, where only part of the field is under combustion recovery, while others are using combustion recovery in the entire field. Some use steam stimulation at the producing wells as well as air into the injection wells.

A comment is in order concerning those fields in which only pilot testing has occurred. It is possible to find some pilot tests where over 100% of the original oil in the pilot has been recovered during the tests. Clearly, in this case, there has been recovery from outside the pilot area. Unfortunately, no a priori method is available at present for assessing the extent of that additional area, so a somewhat different means will need to

TABLE 4A: IN-SITU COMBUSTION TEST GENERAL CHARACTERISTICS

No.	Field	State	Company	Formation	Start Date	Pilot(P) Fieldwide(F)	Dry(D) Wet(W)	Test Pattern Type	Acres
1.	S. Belridge	Ca	Mobil	Unc. Sand	3/56	P	D	5-Spot	2.75
2.	S. Belridge 12	Ca	Mobil	Unc. Sand	6/64	F	D*	--	164
3.	Moco	Ca	Mobil	Unc. Sand	1/60	F	D	Irreg	150
4.	W. Casablanca	Tx	Mobil	Con. Sand	2/67	F	D	Irreg	250
5.	Cox Penn S.	Ok	Mobil	Sand	1/62	F	D	Irreg	11
6.	N. Government	Tx	Mobil	Sand	9/62	F	D	Line	728
7.	Fosterston NW	Canada	Mobil OC	Semi Con. Sand	2/70	F	D	Irreg	257
8.	Trix Liz	Tx	Sun	Con Sand	9/68	F	D	Line	250
9.	May Libby	La	Sun	Con Sand	8/66	P'	W	5-Spot	40
10.	Bartlesville	Kan	Sun	Semi Con Sand	4/65	F	W	5-Spot	20
11.	Glen Hummel	Tx	Sun	Semi Con Sand	1/68	F	D	Line	544
12.	Gloriana	Tx	Sun	Semi Con Sand	5/69	F	D	Line	534
13.	Heidelberg	Miss	Gulf	Con Sand	12/71	F	D	Irreg	400
14.	Tar Sands	Ky	Gulf	Semi Con Sand	9/59	P	D	5-Spot	0.26
15.	S.E. Kansas	Kans	Sinclair	Sand	mid/56	F	D	Irreg	60
16.	D. Childers	Ok	Sinclair	Bart Sand	11/60	P	D	5-Spot	2.22
17.	Belleuve	La	Cities SC	Nacatoch Sand	3/71	P	D,W	9-Spot	29.4
18.	Bodreau-B	La	Cities SC	Nacatoch Sand	9/76	P	D	9-Spot	20
19.	Belleuve	La	Getty	Unc. Sand	9/63	P,F	D,W	Line	2.8
20.	M. Sunset	Ca	CWOD	Unc. Sand	1/72	P,F	D	5-Spot	1.4
21.	Pontotac	Ok	Magnolia	Sand	--	P	D	7-Spot	30
22.	Fry	Il	Marathon	Sand	10/61	P,F	D	Irreg	160
23.	West Newport	Ca	G.E.K.S.	Unc. Sand	3/56	P,F	D	--	23
24.	Shannon	Wyo	PanAm	Friable Sand	7/58	P	D	Irreg	5
25.	B. Glinda	Ca	Union	Sand	3/72	F	D	Irreg	31
26.	S.E.P.	Ok	Sohio	Unc. Sand	1/69	F	D	Line	325
27.	C. Parish	La	Kirby	Sand	2/69	P	W	5-Spot	2.75
28.	N. Tisdale	Wyo	Contin	Sand	5/59	P,F	D	Line	12.3
29.	Parker P.	Il	Worthington	Penn Sand	9/53	P	W	5-Spot	0.28
30.	Carlyle P.	Kans	Layton	Bart. Sand	2/63	P	W	7-Spot	4.2
31.	Niitsu	Japan	Teikoku	Sand	11/57	P	D	Irreg	0.04
32.	E.T. Juana	Venez	Shell	Sand	66	P	W	7-Spot	11.4
33.	Miga	Venez	Mene Grande	Con. Sand	4/64	F	D	Irreg	--
34.	Field A	--	--	--	--	P	D	5-Spot	4
35.	Field B	--	--	--	--	P	D	--	3.2
36.	Field C	--	--	--	--	P	W	5-Spot	4
37.	Field D	--	--	--	--	F	D**	Irreg	-
38.	Field E	--	--	--	--	F	D**	Line	811
39.	Field F	--	--	--	--	F	D**	Line	2116
40.	Sloss	Nebr	Amoco	Con. Sand	5/63	P,F	W	5-Spot	960

* Steamflood was also applied simultaneously.

** Waterflood was also applied simultaneously.

TABLE 4B: IN-SITU COMBUSTION TEST ROCK AND FLUID PROPERTIES

Field	Thickness, ft.	Depth, ft.	θ %	k md	Reservoir T, OF	P, psi	Oil μ @ res. T, cp	Oil, °API	@ Start		Oil Content Bbl/ac-ft	θ So, %
									So, %	Sw, %		
S. Belridge	30	700	36	8000	87	220	2700	12.9	60	37	1645	0.22
S. Belridge-12	93	1080	34	3000	93	180	>1600	13	67	26	1727	0.23
Moco	129	2400	36	1575	110	850	110	14.5	75	25	1980	0.27
W. Casablanca	12.5	1030	34	600	100	30	>150	20.4	45	30	1152	0.15
Cox Penn. S.	50	1500	24	1000	85	75	90-900	21	59	23	--	0.14
N. Government	18	2320	32	800	120	330	10	22	36	41	800	0.12
Fosterton NW	27.7	3100	28.8	958	125	240	13.5	23.6	45.5	54.5	1010	0.13
Trix Liz	9+	3650	28	500	138	200	26	24	56	35	1155	0.16
May Libby	8.3	3400	31.2	1069	135	<1000	3.0	40	37	30	739	0.12
Bartlesville	17	830	21.2	88.1	77	50	750	20.1	70.5	21.1	1159	0.15
Glen Hummel	8.11	2432	36	1000	115	800	74	21.9	65	30	1766	0.23
Gloriana	4.4	1600	35	1000	112	300	174	20.8	52.8	41.5	1419	0.18
Heidelberg	40	11200	16.4	39	221	1500	4	20	79	15	961	0.13
Tar Sands	20.4	100	22	2000	56	--	150000	10.6	64	12	1092	0.14
S.E. Kansas	8.8	830	20.3	85	78	--	70	23	77	23	1089	0.16
D. Childers	45.5	600	20.6	118	--	--	6	33	36.6	30	584	0.08
Bellevue	60	390	34.9	695	75	40	676	19	63.3	26.7	1640	0.22
Bodreau-B.	42	450	33.9	700	75	33	676	19	69.6	27.4	1909	0.24
Bellevue	74	360	38	500	75	--	500	19.5	51	--	--	0.19
M. Sunset	90	1600	33.5	1400	120	20	4430	11.5	60	--	1559	0.20
Pontotac	17	195	27.2	7680	66	80	5000	18.4	64	35	1350	0.17
Fry	50	875	19.8	354	65	20	40	28.5	68	20	1040	0.13
West Newport	120	1000	37	1070	105	85	700	15.2	69	--	1925	0.25
Shannon	33	950	23.3	250	68	--	76	25	60	40	--	0.14
B. Olinda	150	3550	29	300	135	--	20	22	50	--	1155	0.15
S.E.P.V	100	4300	39	1500	110	--	7500	10	57	15	1470	0.22
C. Parish	16	1031	35.2	606	80	--	280	21.1	52	32	1700	0.18
N. Tisdale	50	929	24.5	1034	73	290	175	21	61.4	35.4	1230	0.15
Parker P.	35.5	275	20.8	175	60	--	50	26.3	42	32	675	0.09
Carlyle P.	35	860	25.3	2050	74	230	700	19.5	68	27	1350	0.17
Niitsu	32.8	610	32.2	750	75	--	178	18.2	25.4	74.6	--	0.08
E.T. Juana	128	1560	41	5000	104	--	6000	12.5	73	--	--	0.30
Miça	20	4050	22.6	5000	146	--	355	13	75	22	--	0.17
Field A	13	735	20	136	--	293	18.5	31.1	42	53	640	0.08
Field B	200	950	39.4	855	81	--	>83.2	13.4	64	--	--	0.25
Field C	25	2175	25.4	193	80	470	8.61	34	26	74	504	0.07
Field D	35.2	2950	26	1265	110	550	70.3	18.6	66.2	33.8	1221.6	0.17
Field E	32	2950	27.3	1265	110	202	70.3	18.6	70.9	29.1	1359	0.19
Field F	18.7	2900	25.1	905	110	250	80	18.6	60.7	39.3	1155	0.15
Sloss	14.3	6200	19.3	191	200	2274	0.8	38.8	30	70	427	0.06

TABLE 4C: IN-SITU COMBUSTION TEST RESULTS

Field	Fuel		Consumed		Air Requirement		O ₂ Utilization %	Average AOR, MCF/B	Previous Recovery % OOIIP	Combustion Recovery, % OOIIP
	lb	cu ft sand	lb	100 lb	SCF	lbMCF ac-ft				
S. Belridge	2.02	--	--	--	--	27	100	20	2.61	52.1
S. Belridge-12	--	--	--	265	--	16.8	100	5.6	9.1	13.2
Moco	2	--	--	--	--	18	100	3.1	0.4	11.3
W. Casablanca	--	--	1.5	218	347	15.1	91	12.1	28	7.3
Cox Penn S.	--	--	--	--	--	--	--	8.0	--	--
N. Government	--	--	1.44	212	--	--	95.5	15.5	39.5	>5
Fosterton NW.	1.75	--	2.40	--	367	16.0	90	12.5	23.2	2.4
Trix Liz	0.96	--	--	136	250	10.9	98	8.14	14	7.7
May Libby	0.8	--	--	--	10.5	10.5	92.1	14.3	47	35
Bartlesville	--	--	--	210	310	--	97	27	--	6.5
Glen Hummel	--	--	--	137	253	--	98.5	2.9	10.4	13.5
Gloriana	--	--	--	153	256	--	86.9	5	11.4	10.0
Heidelberg	--	--	--	--	--	--	--	2.64	6.7	2.0
Tar Sands	--	--	--	--	--	--	--	42	--	54
S.E. Kansas	2.5	--	--	--	20	20	80	20	5.3	11.4
D-Childers	1.9	--	--	--	--	17.5	80	28.5	--	50
Bellevue	2.0	--	--	--	17	17	--	21.5	21.5	10.7
Bodcau-B.	2.0	--	--	--	--	--	--	20.1	--	2.8
Bellevue	0.68	--	--	--	--	--	--	16	5	45
M. Sunset	2.15	--	--	--	390	--	100	10.5	23.3	45
Pontotac	1.92	--	1.59	--	420	18.2	70	31	7.1	39.4
Fry	0.90	--	--	--	--	--	90	17.5	--	--
West Newport	2.08	--	2	--	--	--	13	13	<15	22
Shannon	--	--	--	--	--	10.4	Poor	6.4	2	34
B. Olinda	1.25	--	--	--	255	--	100	--	27.8	7.6
S.E.P.V.	--	--	--	--	--	--	--	6	3.3	0.31
C. Parish	2.15	--	--	289	415	18.1	90	14.1	0.1	27
N. Tisdale	1.8	--	--	230	366	--	72	14	5	1.36
Parker P.	0.32	--	--	--	--	--	--	--	--	80
Carlyle P.	--	--	--	--	--	--	--	32	3.5	9.23
Nitsu	1.62	--	--	--	--	--	99	13.4	40	--
E.T. Juana	--	--	--	--	--	--	--	0.94	--	--
Miga	1.4	--	--	--	--	--	100	11	3.3	12
Field A	1.07	--	--	229	--	--	78	--	--	--
Field B	--	--	--	--	--	--	--	--	--	5
Field C	--	--	--	--	367	16.0	47.5	89	--	--
Field D	--	--	--	--	--	--	85	7.9	6.3	7.7
Field E	--	--	--	--	--	--	85	3.8	4.8	7.5
Field F	--	--	--	--	--	--	86	2.6	3.6	8.1
Sloss	--	--	--	--	--	--	90+	21	--	13.5

be developed for correlating the pilot results than for correlating the fieldwide results. Case history analysis of pilot projects will be discussed in a separate section later in the text.

Also, it appears that those fields which use water along with air should have a different injection-recovery history than those which are using dry combustion alone. Further, these differences would be expected to depend strongly on the amount of water injected with the air. Thus, it seems prudent to concentrate first on those fields using only dry combustion as a recovery mechanism.

6.3 Correlation Technique

The ultimate purpose of correlating these field data is to be able to predict recovery versus time and volume injected, and to predict the economic viability of any given field. It must be kept in mind that any economic evaluation can not be simply a yes/no evaluation, for with the broad variation in reservoir properties possible for combustion, there is a continuous spectrum of economic possibilities.

It must be further recognized that an economic evaluation is actually made up of several evaluations of reservoir mechanisms. First, the recovery must be predicted as a function of the volume injected. This is the most important first step, but it is only the first step. Second, both recovery and volume injected with time must be related, for all cost parameters are intimately associated with the time of operation. Both of these predictions depend on reservoir parameters but they must be handled separately. For example, the recovery versus injection prediction will depend primarily on the volume of oil in place, amount of fuel burned, combustion efficiency and terms of that type, while the volume versus time prediction will depend

primarily on Darcy's law terms such as permeability, viscosity, and pressure drop. The last step is then fairly easy: relating these injection volumes, production volumes, and time correlations to costs and income.

The correlation work reported here is on the first step, i.e., recovery versus volume injected. This is the more difficult correlation to develop. Our approach is to use basic engineering analysis of combustion, combining heat balance and material balance considerations as a means of including those correlating parameters which should be most important. Only after this approach has been exhausted will other parameters be included by purely statistical means.

6.4 Case History Analysis of Fieldwide Dry In-Situ Combustion Tests

As mentioned earlier, first only those cases which are fieldwide and where only dry combustion was used as a recovery mechanism will be studied. There were a total of 12 fields where these criteria held. All the data on cumulative incremental oil versus air injection for these fields are graphed in Fig. 20. Here cumulative incremental oil is only that recovery caused by the combustion process itself. A recovery rate prediction was made for the recovery process that was being used at the time combustion was begun, and this rate was subtracted from the total recovery rate. The curves in Fig. 20 differ by a factor of over 4 to 1. Fig. 20 can also be used to determine the air injected-oil produced ratios of those 12 fields. As far as the air injected oil produced ratios are concerned, Fig. 20 indicates that Moco and Glen Hummel projects represent the most successful field projects among the ones on the figure.

In Figure 21, both coordinates were normalized for field size. The abscissa is the cumulative air injected divided by the oil in place at

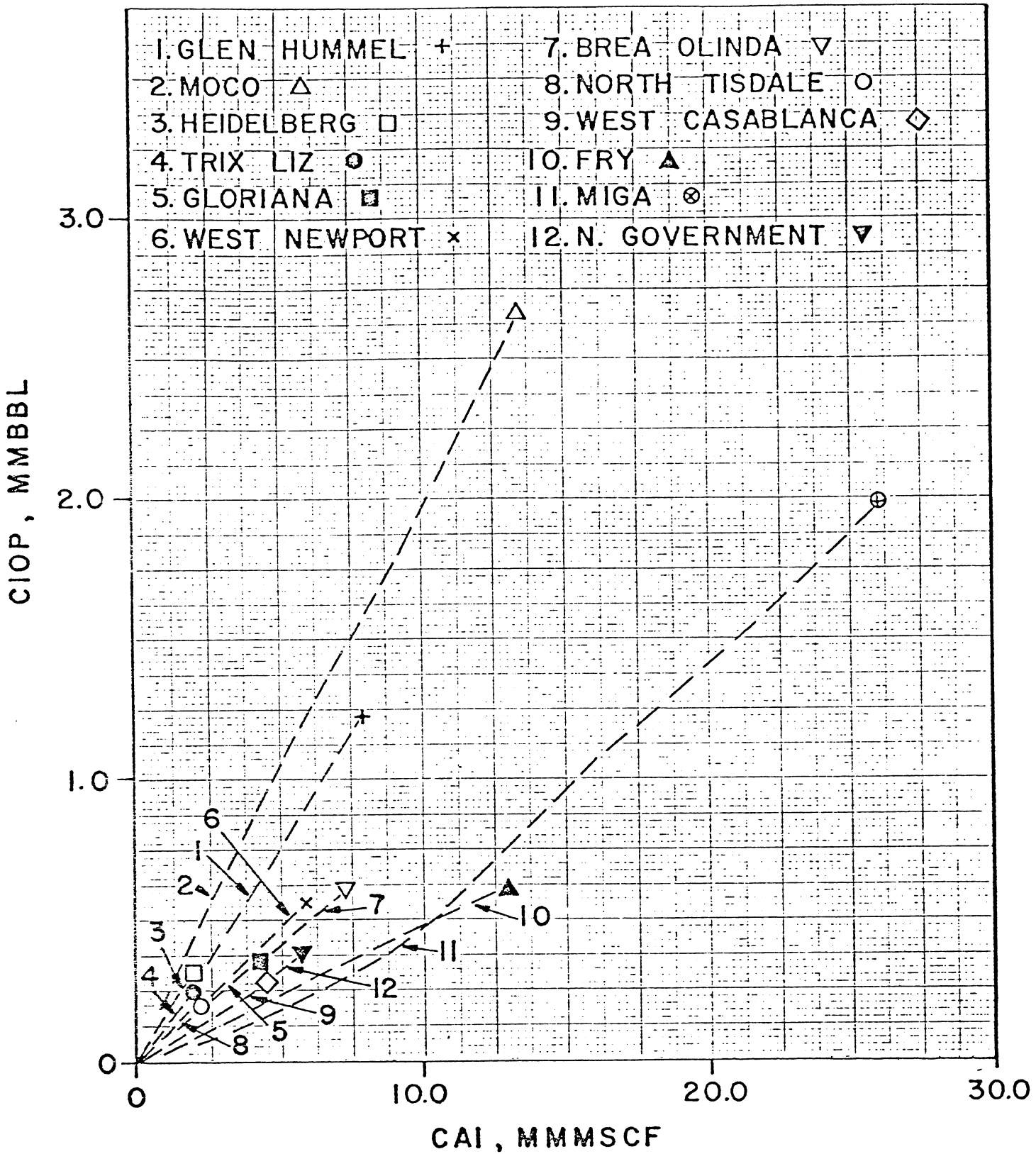


FIG. 20: CUMULATIVE INCREMENTAL OIL PRODUCTION VS CUMULATIVE AIR INJECTION FOR FIELDWIDE COMBUSTION TESTS

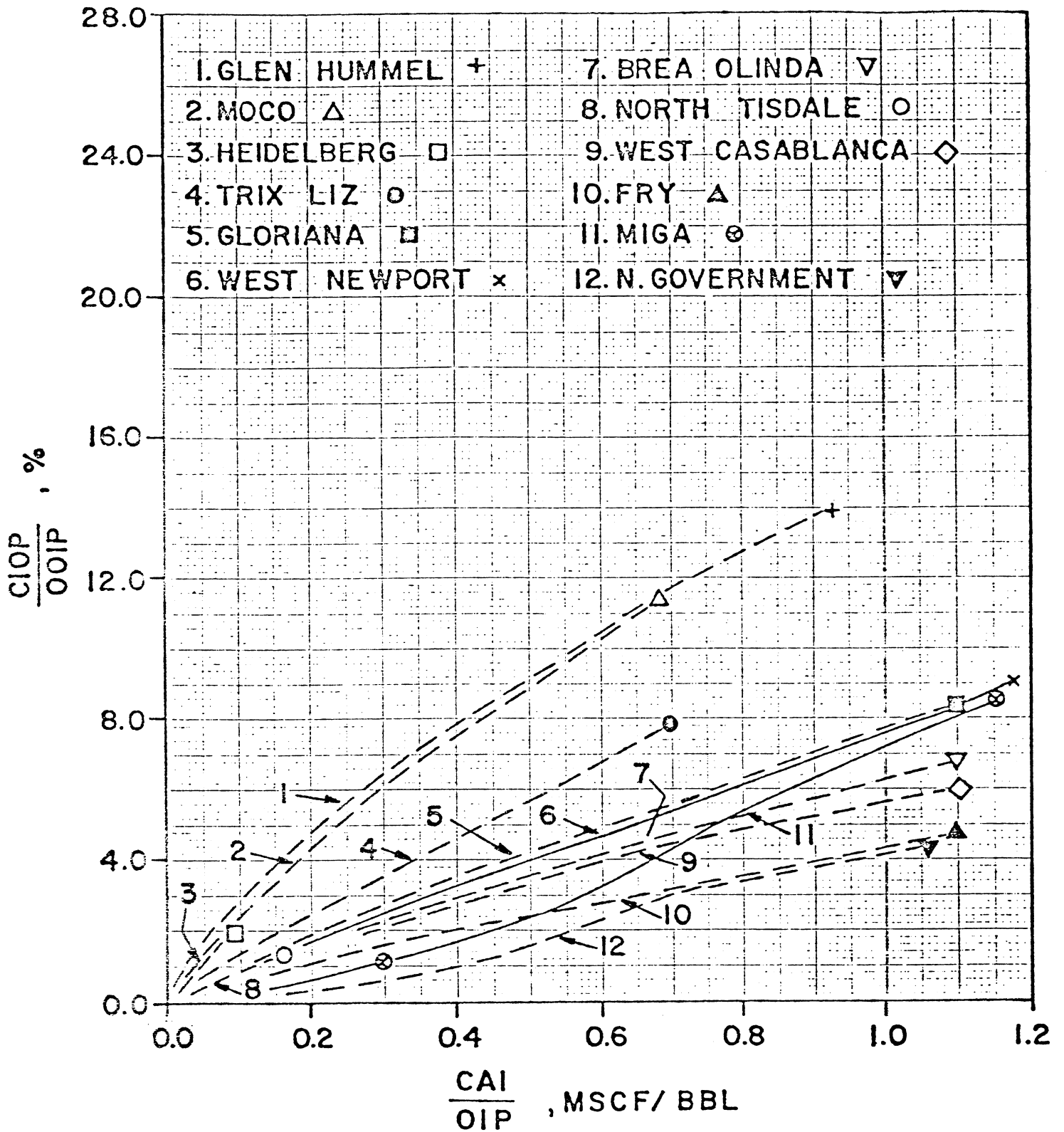


FIG. 21: DIMENSIONLESS CUMULATIVE INCREMENTAL OIL VS AIR INJECTION FOR FIELDWIDE COMBUSTION TESTS

the start of combustion, and the ordinate is the combustion recovery divided by the original oil in place, e.g., fractional recovery. Notice in Figure 21 that the recovery in these fields still differs by a factor of over 3 to 1; but also notice that the recovery versus volume injection curves appear to have similar shapes, so that simple multiplying factors may be useful in correlating these data.

The next step was to consider that air injection was really a measure of the amount of heat added to the reservoir, for in all combustion operations a given volume of air supplies nearly a fixed amount of heat from combustion. Further, it is recognized that a large percentage of the heat added to the reservoir is deposited in the rock behind the front, thus the rock volume is an important parameter. The rock volume can be calculated as follows:

$$\text{Rock Volume} = \frac{\text{OIP}}{\phi S_o} (1-\phi) \quad (41)$$

It is also recognized that not all fields had 100% oxygen utilization ($O_2 Ut$), thus the effective air injected was less than the actual volume injected. Using all these terms together we can change the abscissa to a dimensionless air injected-rock volume function as follows:

$$\text{Abscissa} = \text{CAI} \left[\frac{\phi S_o}{\text{OIP}} \right] \left[\frac{O_2 Ut.}{1-\phi} \right] \quad (42)$$

It is known that some of the oil in place is burned and therefore not available for recovery. Therefore this fact was taken into account by adding the fuel burned to the ordinate. The ordinate thus became:

$$\text{Ordinate} = \frac{\text{CIOP+FB}}{\text{OOIP}} \quad (43)$$

The results are shown in Fig. 22, using these parameters. Note the improvement in the correlation as a result of these changes in the correlating parameters. The maximum difference near the end of the data is only $\pm 40\%$, or a factor of 2/1. Remember also that these correlating parameters were not developed using any arbitrary statistical model. They are based entirely on the process variables that one would expect to be important based on heat and material balance considerations.

The next step was to improve the correlation shown in Fig. 22. To accomplish this, multiple linear regression analysis was used to include some parameters which were expected to be important, but which were not adequately included in Fig. 22; e.g., depth, thickness, oil viscosity, and oil saturations. Multiple linear regression analysis was used basically for two purposes:

1. to show the effect of the parameters on the correlation, and
2. to develop a correlation equation for combustion recovery in terms of those variables.

The results of the analysis showed that the formation depth did not have any consistent effect on recovery, and this variable was dropped from the correlation. An equation was sought by multiple linear regression analysis to relate the ordinate as the dependent variable with the independent variables S_o , μ_o , and h .

The first results of this correlation effort were reported by Satman *et al.*²⁶. In this correlation the recovery function, the ordinate in Fig. 22, was correlated against the abscissa as a linear function of oil saturation, S_o , thickness, h , and oil viscosity, μ_o . The result was:

$$\frac{y}{36.53} = (2.00 S_o - 0.0010 h - 0.0082 \mu_o) x \quad (44)$$

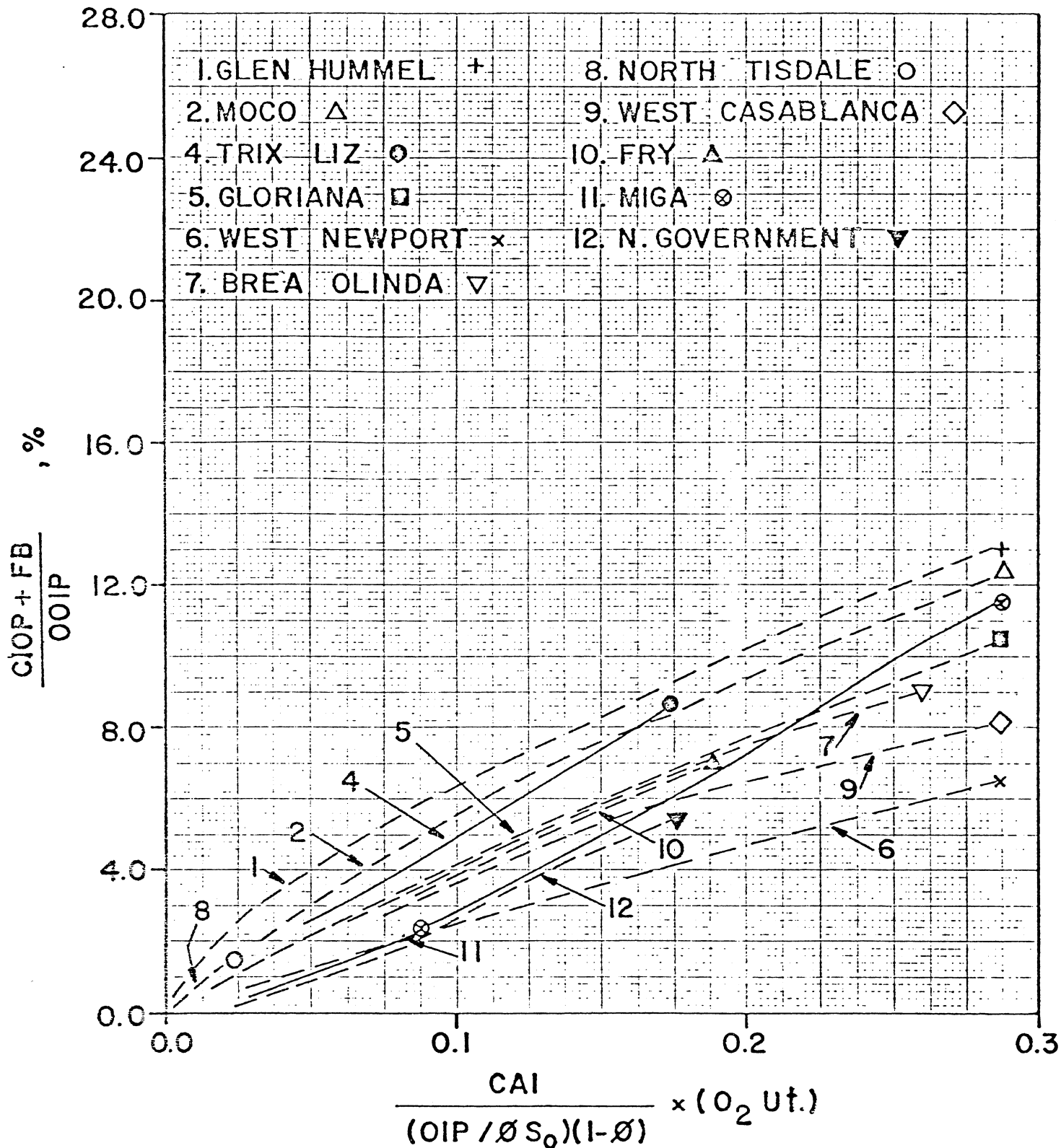


FIG. 22: EFFECTS OF FUEL BURNED, ROCK VOLUME, AND OXYGEN UTILIZATION ON CUMULATIVE INCREMENTAL OIL VS AIR INJECTION FOR FIELDWIDE COMBUSTION TESTS

where

$$y (\%) = \frac{CIOP+FB}{OOIP} 100 \quad (45)$$

and

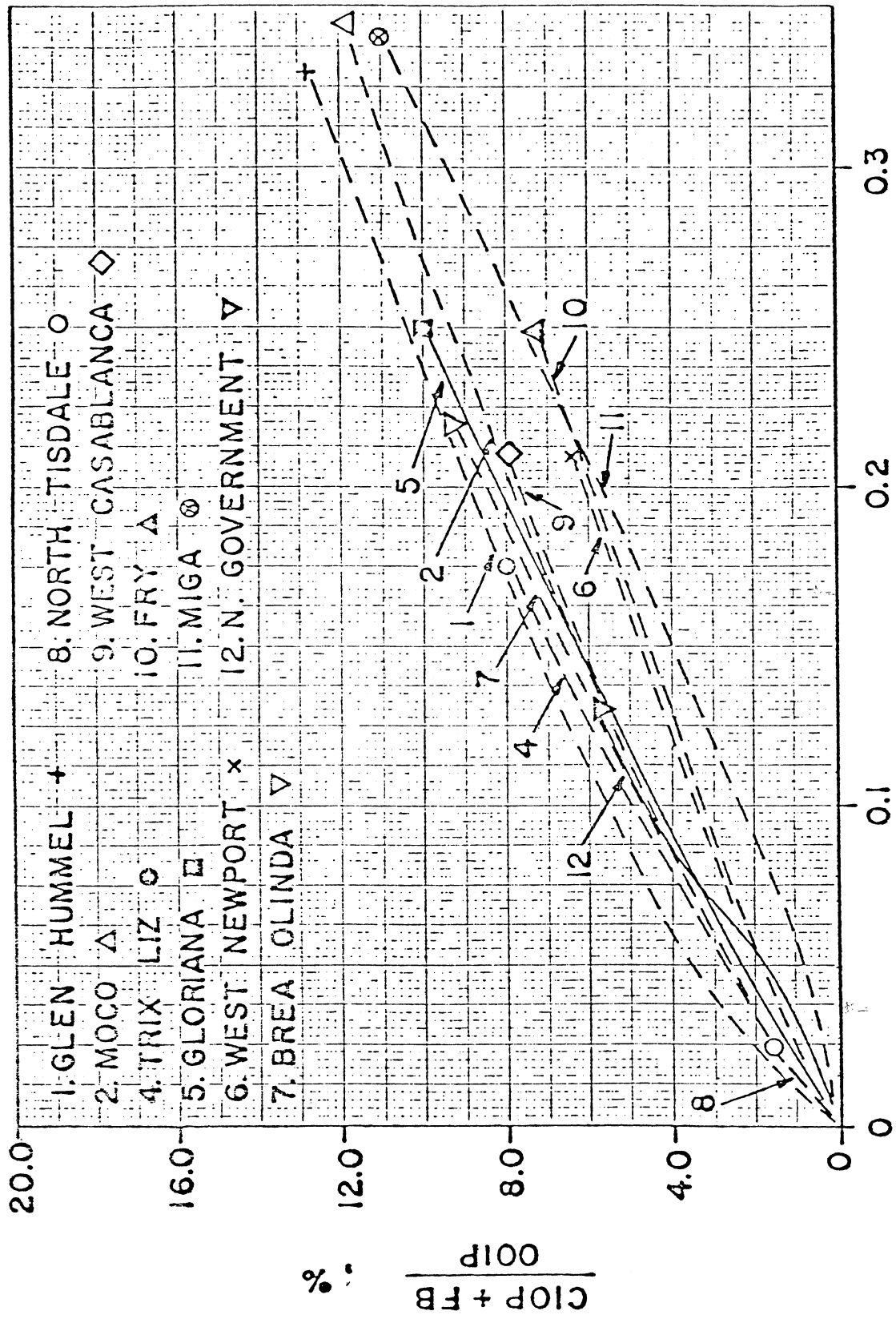
$$x \left[\frac{MSCF}{bbl} \right] = \frac{CAI (O_2 \text{ Ut.})}{(OIP/\phi S_o)(1-\phi)} \quad (46)$$

Figure 23 shows the actual values of the recovery function (y) versus the values on the right hand side of Equation 44 for each of the fields analyzed in the correlation. There is considerable improvement in the resulting correlation. The scatter was reduced to a maximum difference of $\pm 15\%$ in the latter portion of the field results where the abscissa is 0.26.

A more definitive way to assess the validity of the correlation is to calculate the standard deviation of the error. This was calculated at 0.20 on the abscissa since there are more data available at this air injection level. The standard deviation was calculated to be 17% and the maximum error was 21% at this point.

Equation 44 was also analyzed by calculating the multiple correlation coefficient. It is over 0.99 for the later life of the field tests, and is around 0.94 for the early life. This also shows the greater accuracy apparent later in the life of the floods.

A smooth curve can be drawn through the data of Fig. 23. This is the general recovery correlation curve. It is shown in Fig. 24. Thus it is a simple procedure to predict fire flood recovery as a function of air injected, providing all the necessary parameters are known: S_o , h , μ_o , ϕ , oxygen utilization ($O_2 \text{ Ut.}$), and fuel content. The last two normally must



$$(2.00 S_0 - 0.001h - 0.00082 \mu_0) \frac{CA \times (O_2 \text{ U}^\dagger)}{(OIP / \delta S_0) (1 - \delta)}$$

FIG. 23: EFFECT OF MULTIPLE LINEAR REGRESSION ANALYSIS ON DATA ON
FIG. 22

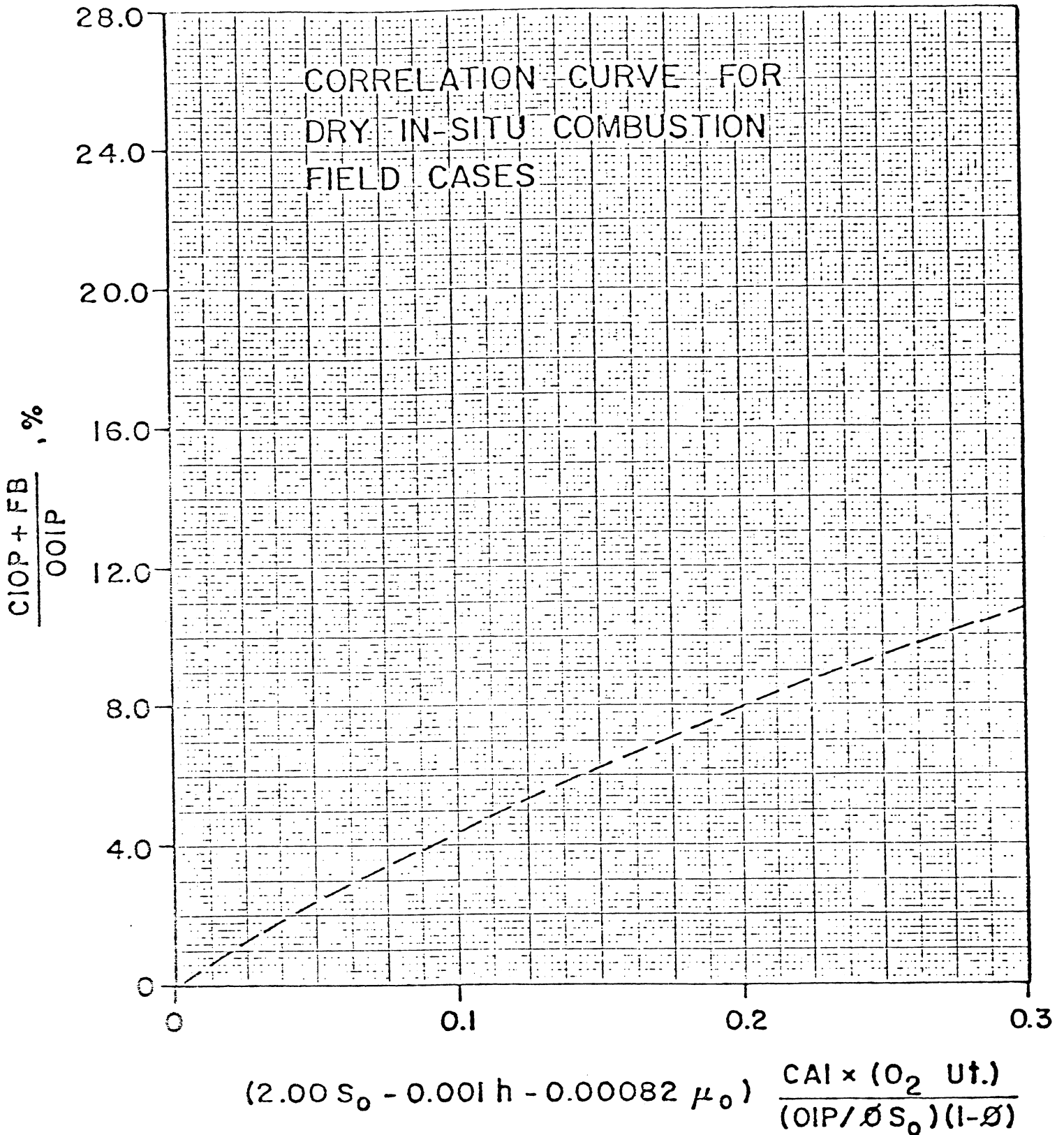


FIG. 24: FIRST CORRELATION CURVE

be obtained from laboratory burn data. The first four are parameters that must always be assessed prior to predicting any recovery process.

The reader is cautioned on the use of this correlation. If any parameters are outside the range of data used to develop this correlation, the results could be in error. The ranges of oil saturation, oil viscosity, and reservoir thickness used were as follows:

$$S_o = 0.36 \text{ to } 0.79$$

$$h = 4.4 \text{ to } 150 \text{ ft}$$

$$\mu_o = 10 \text{ to } 700 \text{ cp}$$

In particular, we emphasize the effect of viscosity. The relationship is linear with viscosity, with a negative coefficient. Thus we predict a lower recovery for a higher viscosity reservoir. Although this is qualitatively correct, if one used the correlation to predict recovery for an oil of several thousand centipoises, the prediction will be unrealistically low.

Because of this effect of oil viscosity on the recovery predicted from the correlation, it appeared that the viscosity ought to be handled in some other fashion, than it is in Equation 44. Oil viscosity was carefully investigated as an independent variable by multiple regression analysis. The reciprocal of viscosity was tried and also the logarithm of viscosity, but these ideas did not improve the correlation. Then we considered that the effect of viscosity should be according some power less than one. The reason for this is that combustion is primarily a method of getting heat to the reservoir, and the viscosity of a crude is not linear with temperature³⁴. For example, a 10,000 cp oil may have a viscosity of 20 cp at steam plateau temperature, while a 1,000 cp oil may have a viscosity of 10 cp at the same temperature. Thus a viscosity ratio of 10/1 at initial conditions

may only be effectively 2/1 at actual reservoir displacement conditions.

These concepts led to study of the reciprocal of viscosity at a power less than one as a correlating factor. The results showed that a power of 0.25 fit the data best. Also in the development of the second correlation, the oil in place at the start of the combustion process rather than original oil in place was used to normalize the ordinate in the correlation. This seemed logical, since a few fields exhibited considerable recovery prior to the onset of combustion.

The resulting correlation equation with $(1/\mu_o)^{0.25}$ as an independent variable was:

$$\frac{y}{47.00} = 0.427S_o - 0.00135h + 2.196 \frac{1}{\mu_o} 0.25 X \quad (47)$$

where

$$y(\%) = \frac{CIOP+FB}{OIP} \times 100 \quad (48)$$

and

$$X \left[\frac{MSCF}{bb1} \right] = \frac{CAI \times (0.2 \text{ Ut.})}{(OIP/\phi S_o)(1-\phi)} \quad (49)$$

Figure 25 shows the actual values of the recovery function (y) versus the values on the right hand side of Eq. 47 for each of the 12 fields. The scatter is $\pm 14\%$ in the latter portion of the field results where the abscissa is 0.20. As was done for the first correlation, a smooth curve was drawn through the data of Fig. 25. This curve can be used as a general recovery correlation curve and is shown in Fig. 26.

The standard deviation was calculated for this second correlation at the same abscissa value (0.20); it was 9%. Thus it is clear that this correlation fits the field results considerably better than does the first correlation.

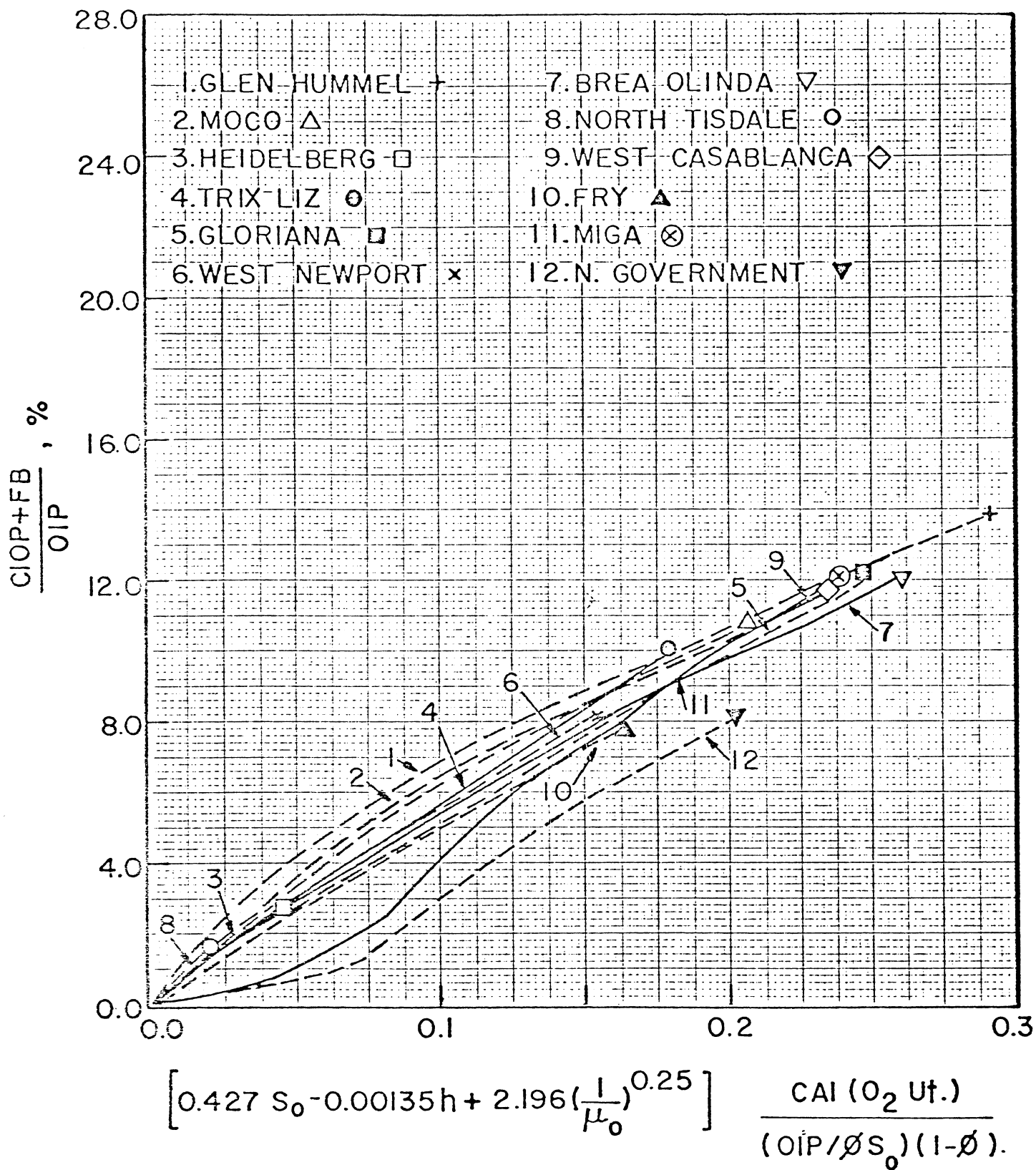


FIG. 25: DATA FOR THE SECOND CORRELATION

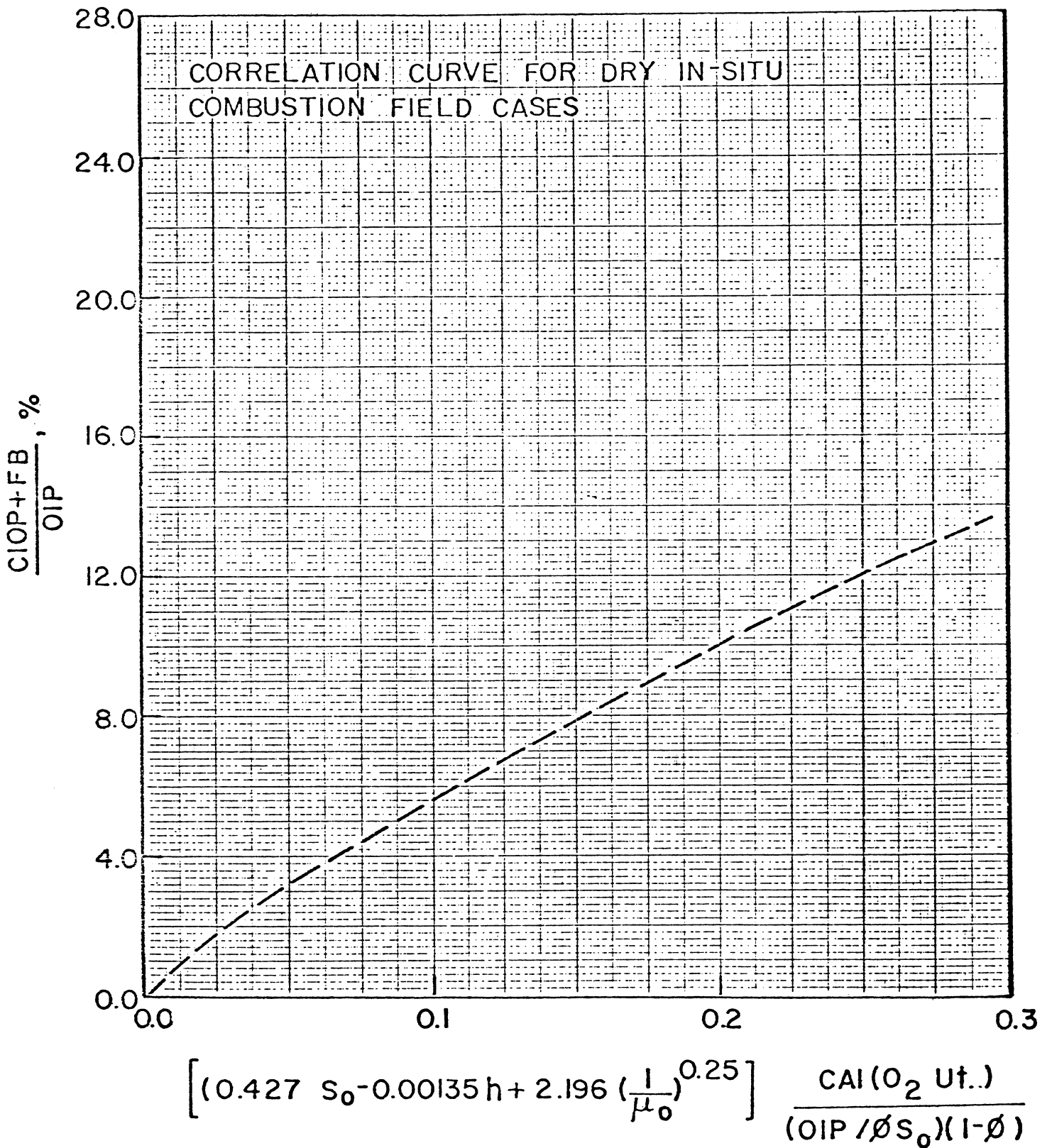


FIG. 26: SECOND CORRELATION CURVE

Note that only one field (North Government) deviates significantly from the correlation data in Fig. 25. H.J. Ramey⁴⁴ stated that there is some doubt about the oil saturation in this field. There is some evidence that it is smaller than the value we used in this correlation. If this were true, the correlation would be even better than the above results indicate.

The use of the second correlation is also restricted. If any parameters are outside of the range of data used to develop this correlation, the results could be in error. The ranges of S_o , μ_o , and h used were the same as given for the first correlation. However, the effect of the viscosity is different for the second correlation. If one used the correlation to predict recovery for an oil of smaller than ten centipoises, the prediction could well be unrealistically high.

There are two basic differences between the two correlation equations, Eqs. 44 and 47: (1) The dependent variable, y , represents the incremental oil recovery per original oil in place for Eq. 44, and the incremental oil recovery per oil in place at the start of the combustion process for Eq. 47, (2) Equation 44 has μ_o as one of the three independent variables while Eq. 47 used $(1/\mu_o)^{0.25}$. Because of these two differences in the correlations, the user should prefer to use one or the other of them depending on the values of the parameters used in the correlations:

- (1) Whenever the oil viscosity is 10 cp or smaller the first correlation, Eq. 44 and Fig. 24 should be used;
- (2) Whenever the oil viscosity is 700 cp or higher, the second correlation, Eq. 47 and Fig. 26, should be applied;
- (3) Whenever there has been considerable recovery prior to the onset of in-situ combustion, the second correlation should be preferable to the

first one. In general, it appears that for most applications, the second correlation will be the one to use.

6.5 Case History Analysis of Pilot Dry Combustion Tests

The prediction of field in-situ combustion performance involves many factors. It is necessary to have reliable information on the displacement efficiency, reservoir heterogeneity, and reservoir rock and fluid properties. Thus, pilot tests are conceived as a means of studying oil recovery performance on an in-place sample of the reservoir itself. This recovery performance could then be scaled up to yield the performance to be expected from full-scale in-situ operations.

Technically and economically, a pilot is a desirable tool for estimating field performance. However, it has the following limitations:

1. Injected air may be lost outside the pilot area due to reservoir heterogeneities and low oxygen utilization.

2. It is possible to recover some oil from outside the pilot area particularly in the case of heavy crude oil reservoirs. Or the reverse may also occur: oil migration losses from a single pilot pattern may yield an estimated recovery lower than that to be expected.

3. With a small pilot, the probability of locating it in a non-representative portion of the reservoir is increased. The effects of a damaged well will be very significant to the recovery performance.

The correlation technique used for field wide dry in-situ combustion tests was also used for pilot tests. There were 8 pilots where dry combustion was used as a recovery mechanism. The data on combustion recovery versus air injection for these pilots are first graphed in Fig. 27. This

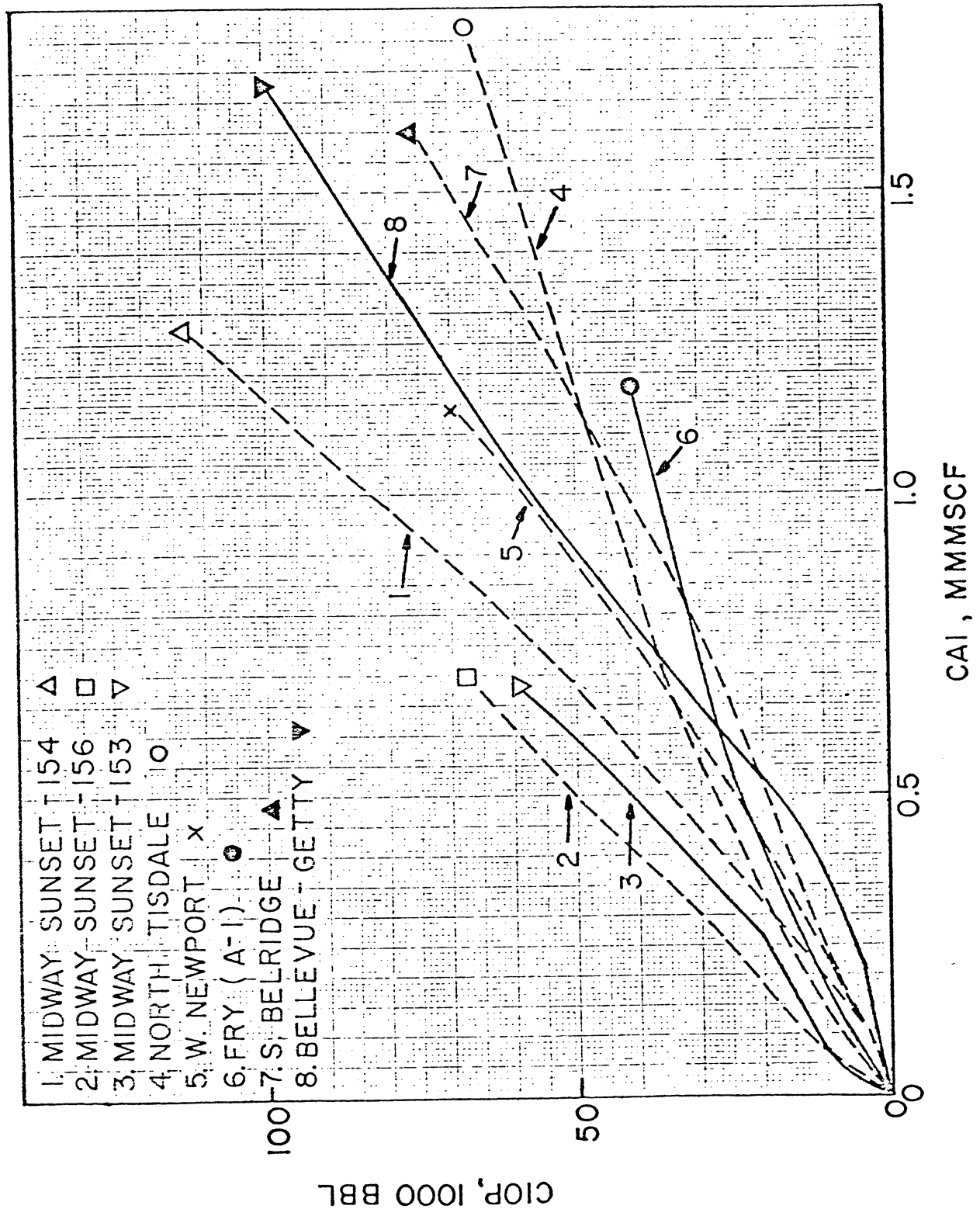


FIG. 27: CUMULATIVE INCREMENTAL OIL PRODUCTION VS CUMULATIVE AIR INJECTION FOR PILOT DRY COMBUSTION TESTS

figure can be used to determine the air injected-oil produced ratios. As far as these ratios are concerned, Fig. 27 indicates that the Midway Sunset pilots are the most successful ones among eight pilots. The curves in Fig. 27 differ by a factor of approximately 2.5 to 1.

The next step was to consider the rock volume, fuel burned, and oxygen utilization for all pilots. These are the same parameters used in the fieldwide correlations. The results are shown in Fig. 28, using these parameters. There was no clear improvement in the correlation as a result of these changes in the correlating parameters.

As a next step, the second correlation developed for fieldwide dry combustion processes (Eq. 47) was used to improve Fig. 28. Since it is expected that the dry pilot projects should show recovery histories similar to fieldwide projects, this correlation was considered. All the pilots had high oil viscosities, therefore the second correlation with Eq. 47 and Fig. 26 was applied. Using this correlation would also allow us to check the validity of the correlation equation. Figure 29 shows the actual value of recovery function (y) versus the values on the right hand side of Eq. 47 for each of the eight pilots. Although there was considerable improvement in the result for five of the pilots, the three Midway Sunset pilots did not fit in with the rest. This indicated that there were some other factors involved in pilot tests which affect the performance. A closer examination of the case histories of pilots, however, helped to diagnose these factors.

The three Midway Sunset pilots had the highest recoveries among the pilots. In this field, cyclic steam stimulation recovered 12% of the original oil in place by the time the first pilot began air injection. Also during air injection, steam cycling was continued at the production

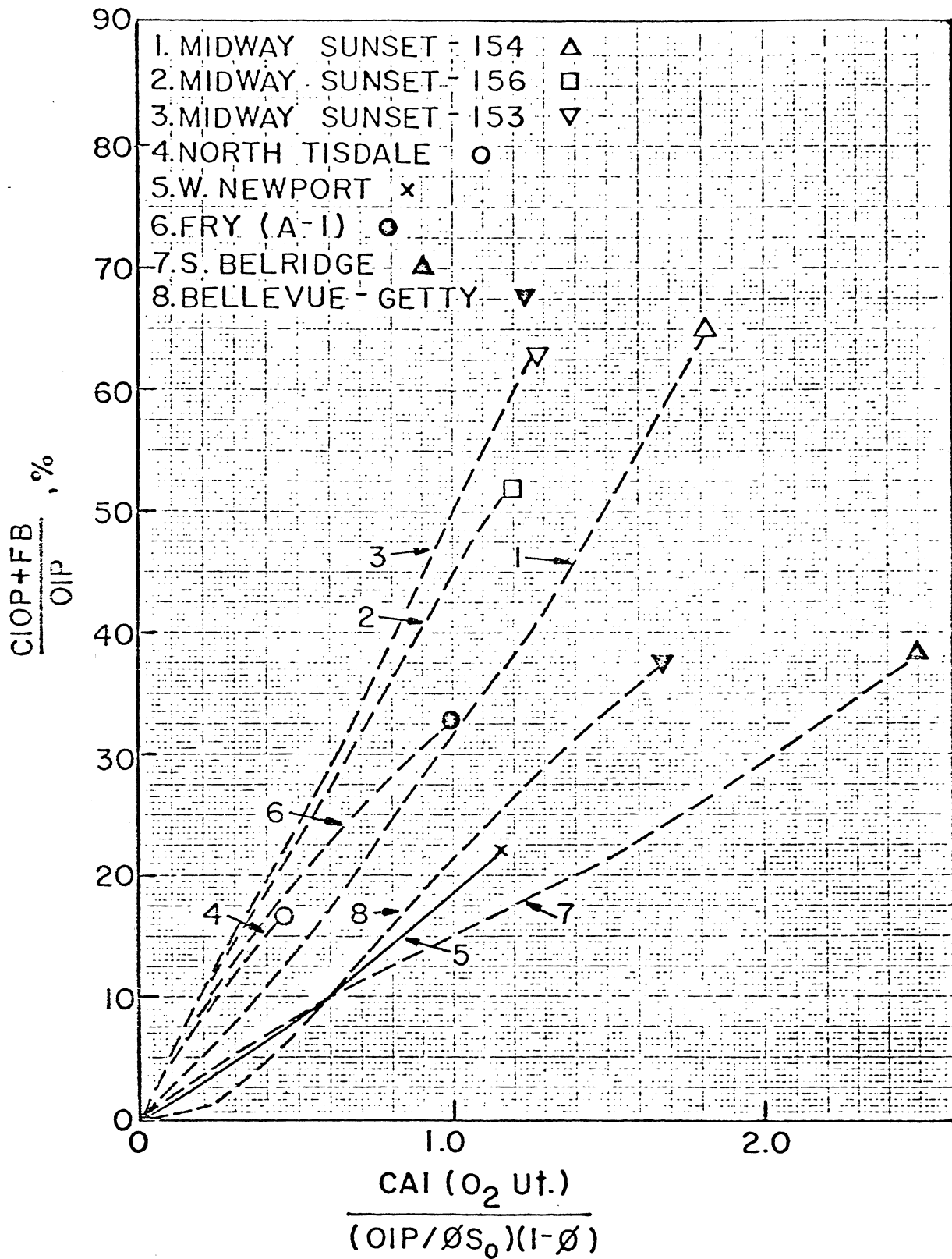


FIG. 28: EFFECTS OF FUEL BURNED, ROCK VOLUME, AND OXYGEN UTILIZATION FOR PILOT DRY COMBUSTION TESTS

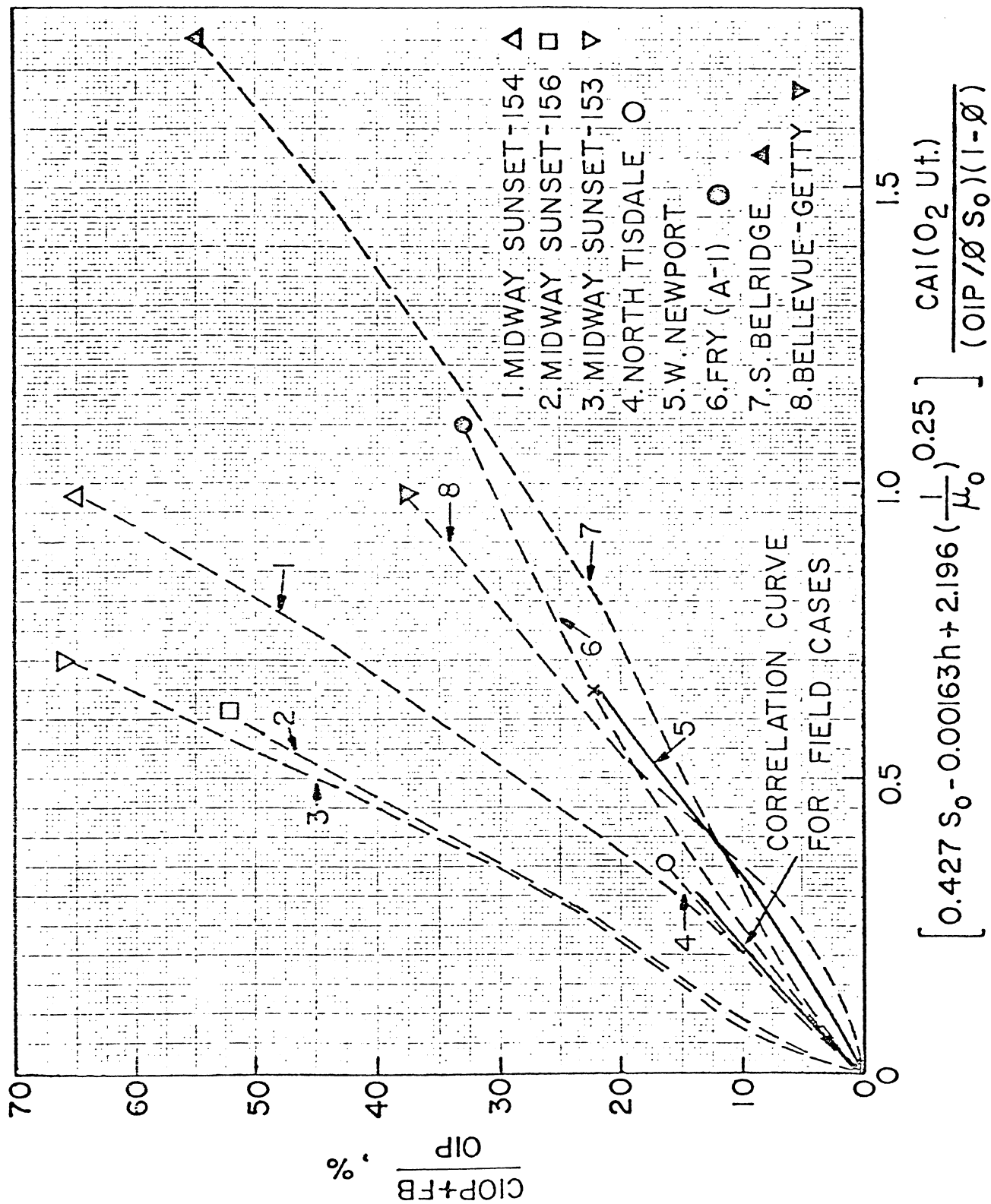


FIG. 29: APPLICATION OF THE SECOND CORRELATION TO PILOT DRY COMBUSTION TESTS

wells of the three pilots. Engineering calculations also indicated that the pilots produced off-pattern oil. Based on these facts, one can conclude that there are three probable reasons why the Midway Sunset pilots showed higher recovery than did the others: (1) the predicted primary and the effects of the previous steam cycling recovery were neglected, i.e. all the recovery during the process was attributed to combustion, (2) cyclic steam stimulation increased oil recovery, (3) pilots produced off-pattern oil. Unfortunately there is not enough data and no method available to take the effects of these three factors into consideration.

For convenience and comparison the correlation curve for field cases was also graphed in Fig. 29. It is interesting to see that the five remaining pilot tests show similar trends with the fieldwide correlation curve. This result supports the correlation and it is also expected. In the case of these five pilots, their recovery was generally lower than the recovery predicted by the correlation curve for field cases. This indicates that air injection loss and/or oil migration losses are important factors affecting the recovery mechanism of a pilot project. One other observation that can be made in Fig. 29 is that the recovery histories for fieldwide projects are fairly small as compared to the recovery histories for pilots.

Excluding the Midway Sunset pilots, the improvement in Fig. 29 is considerable. The scatter is $\pm 18\%$ in the latter portion of the pilot results. This leads to the conclusion that the correlation parameters used for fieldwide projects appear to be reasonable to use as correlating parameters for dry pilot projects.

6.6 Case History Analysis of Wet Combustion Tests

This study also attempted to develop a recovery correlation for wet combustion processes, but as could be seen in Table 4A, there are only three fieldwide combustion tests available. The number of projects were too small for any correlation work; however, a case history study of these projects indicated that the wet combustion is an operable process. It requires extra engineering attention due to water injection^{35,36}. More general conclusions about the wet combustion process are not possible at this time.

6.7 Application of Correlations

After developing the correlations for fieldwide dry in-situ combustion cases, their validity was tested to the extent possible. Unfortunately there is not another dry in-situ combustion field project published or available to test the correlations. However, this study attempted to use some other types of combustion projects which were not included in the correlation work. Two of these fields, a Bartlesville sand in Kansas and the Sloss field in Nebraska, had wet combustion. The third field, the South Belridge field in California, had combustion and cyclic steam processes simultaneously. The injection and recovery data of these three fields were used to study the correlation,

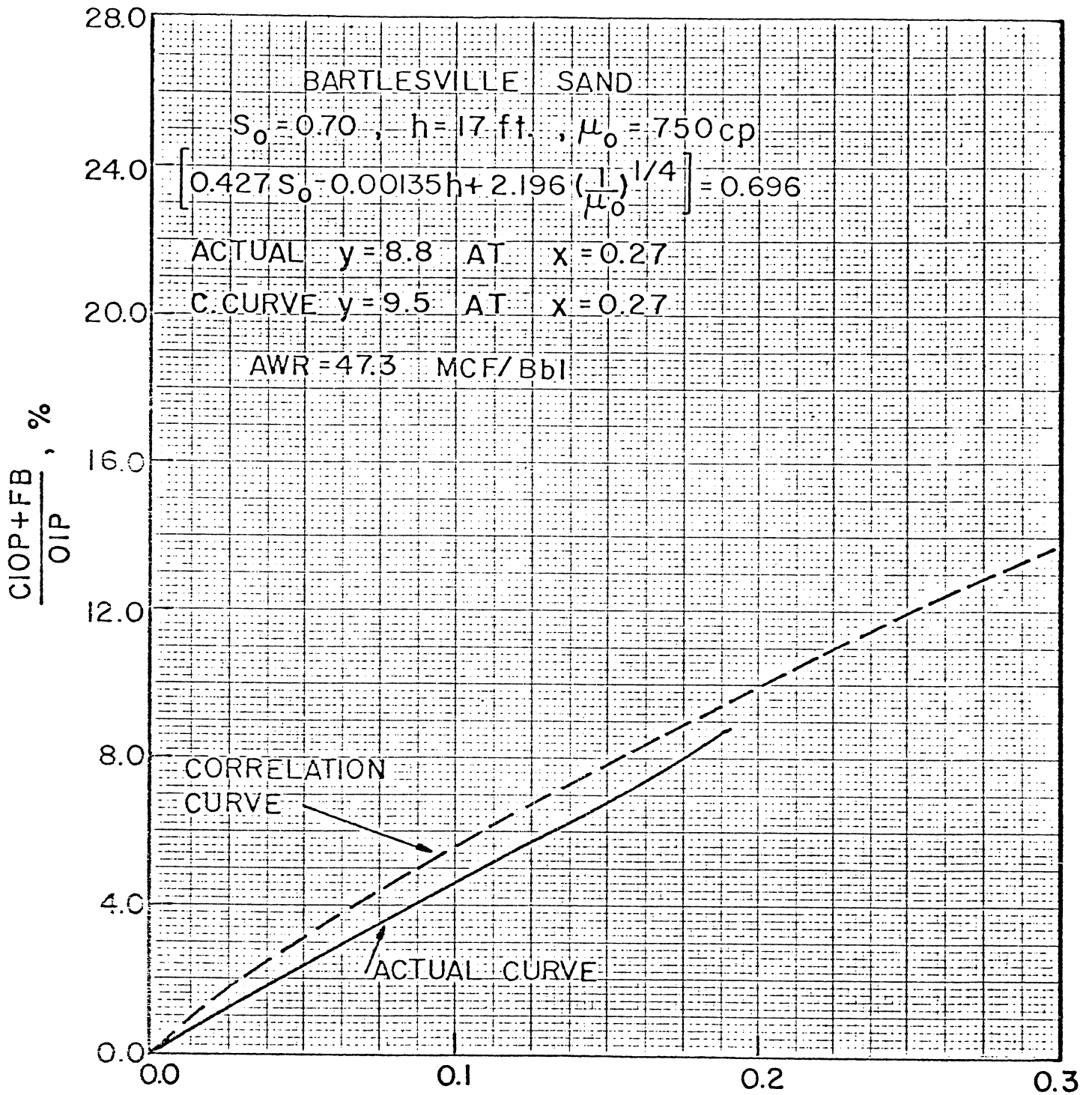
Generally speaking, either wet combustion or the simultaneous application of dry combustion with cyclic steaming would be expected to recover more oil than dry combustion could recover by itself. During wet combustion, the injected water moves heat further ahead of the combustion front, and thus aids all the oil recovery mechanisms; therefore a higher

recovery is anticipated. Simultaneous application of dry combustion with cyclic steaming also increases oil recovery because both of these processes introduce heat into the reservoir, and thus more oil is expected to be recovered.

In the following sections, the applications of the second correlation to these three fields will be discussed. The correlation will be used as a predictive device to calculate the relative amount of recovery from each recovery mechanism.

6.7.1 Bartlesville Sand Reservoir, Kansas

An in-situ combustion field test was conducted in a shallow Bartlesville sand reservoir, the Iola Fire Flood Unit in the Southwest Moran Field, Allen County, Kansas³⁶. The project consisted of two patterns. The oil recovery was 51,212 barrels compared with 88,238 barrels displaced from the burned zone. The air injected-water injected ratio was calculated to 47 Mscf/bbl which is quite small for a wet combustion. The wet combustion is defined as the injection of both air and water, either simultaneously or alternately at air/water ratios of less than about 3,000 scf per barrel of water (3,000 scf/bbl)³⁵. Since 47 Mscf/bbl is a high number compared to 3 Mscf/bbl, the water injection in the Bartlesville sand would not be expected to significantly effect the oil recovery. The actual oil production-air injection data is shown in Fig. 30. Since oil viscosity is 750 cp, the second correlation is applied and also shown in the same figure. As can be seen, the correlation curve predicts a higher oil recovery than the actual one. Comparison of Figs. 29 and 30 indicates that the actual oil production-air injection data for the Bartlesville sand follows the general trend seen by the pilots shown in Fig. 29; pilots



$$\left[0.427 S_0 - 0.00135 h + 2.196 \left(\frac{1}{\mu_0} \right)^{0.25} \right] \frac{CAI(O_2 \text{ Ut.})}{(OIP/\phi S_0)(1-\phi)}$$

FIG. 30: APPLICATION OF THE SECOND CORRELATION TO BARTLESVILLE SAND

recover less oil than predicted by the correlation for fieldwide projects. This supports the theory that air losses and oil migration are important factors for pilot projects.

6.7.2 The Sloss Field, Nebraska

The second field was used to test the validity of the correlations was the Sloss Field in Nebraska³⁷. This field with about 38 million barrels of original oil in place is one of the larger fields in Nebraska. About 11% of OOIP, 4.2 million barrels, was recovered during pressure depletion operations. By the start of the combination of forward combustion and waterflooding (COFCAW) most of the reservoir had been waterflooded. Table 4B indicates that this field is one of the leanest reservoirs ($S_o = 0.30 \pm 0.10$) where the thermal recovery was tested. During the air injection period, 13.7 billion scf of air and 10.8 million bbl of water were injected into the pattern wells. In addition, 1.6 million bbl of water were injected into peripheral wells. This resulted in an air/water injection ratio of one of the lowest found in the literature, 1.2 Mscf/bbl. Cumulative incremental oil production over that predicted from waterflooding was about 527,000 bbl.

Uncertainty about the value of S_o makes the application of correlations to the Sloss field very complicated. The oil saturation given is between 0.20 and 0.40. Due to that much difference in oil saturation, determining the amount of oil in place at the start of the combustion process may be in error. Also the oil viscosity, 0.8 cp, is outside the range of data used to develop the recovery correlations. Because of these differences, none of the correlations could be properly used to predict oil recovery. However, in the following paragraphs, some possible values of S_o will be assumed and the applications of correlations to the Sloss field will be discussed.

When S_o and μ_o are treated as 0.30 and 0.8 cp, the second correlation predicts approximately 16% oil recovery as compared to 12.1% of actual recovery at $x = 0.16$. This means a difference of 35% between prediction and actual data. However, when μ_o is treated as though it were the lowest value used to develop the correlation which is 10 cp, the correlation curve indicates 10.8% oil recovery based on OIP. This value is smaller than 12.1% actual oil recovery, and the difference might have been attributed to the wet combustion.

When S_o and μ_o are treated as 0.20 and 0.8 cp, the second correlation predicts approximately 16% oil recovery as compared to 18.3% of actual recovery at $x = 0.16$. In this case, the predicted value is smaller than the actual recovery, and also the difference can be attributed to the wet combustion.

These variable results cannot lead us to any strong conclusion about the validity of the correlation. However, it appears that the water injected in the Sloss Field had little effect beyond what we would have predicted using the correlation. This result is somewhat surprising, for it is counter to the view generally held concerning the effect of water injection in an in-situ combustion project.

6.7.3 The South Belridge Field, California

Another field was the South Belridge Field, Kern County, California³⁸. In this field, in-situ combustion and cyclic steam processes were used simultaneously. In-situ combustion, drilling of new wells and use of cyclic steam resulted in the production of 3.8 million bbl of oil or 13.2% of the original oil in place which was about two times the expected ultimate primary recovery. Cyclic steam usage during the in-situ combustion

process was 2.5 million bbl. Application of two enhanced recovery processes simultaneously made the interpretation of the results very difficult.

An attempt was made to test the correlations. Although we are not positive that the correlation will give a correct combustion recovery prediction, but it can be used in an attempt to interpret the field results. The purpose here is to predict what would have been expected from combustion recovery by itself. To do this, the primary recovery was predicted and subtracted from the total oil recovery. Since the viscosity of oil was 1600 cp, the second correlation was used to predict the oil recovery caused by in-situ combustion only. This resulted in a cumulative incremental oil production of 2.0 million bbl as shown in Fig. 31. The primary recovery was predicted to be 1.2 million bbl; thus the cyclic steam recovery was approximated to be 0.6 million bbl. This results in an oil/steam ratio of 0.24, which though possibly a bit high, is a reasonable value. Thus, again the correlation appears reasonable. The results are shown in Fig. 32. In summary, a study of the South Belridge Field indicates that net of the total of 3.8 million bbl recovery, approximately 53% was due to in-situ combustion, approximately 32% was due to primary recovery and approximately 16% was due to cyclic steaming.

These applications admittedly do not prove the accuracy of the correlations. One does not like to make sweeping conclusions based on these results. These three field results help support the correlation work, but also are not conclusive. It is recommended that these correlations be tried by others who have in-situ combustion recovery results so that the correlation can be tested further.

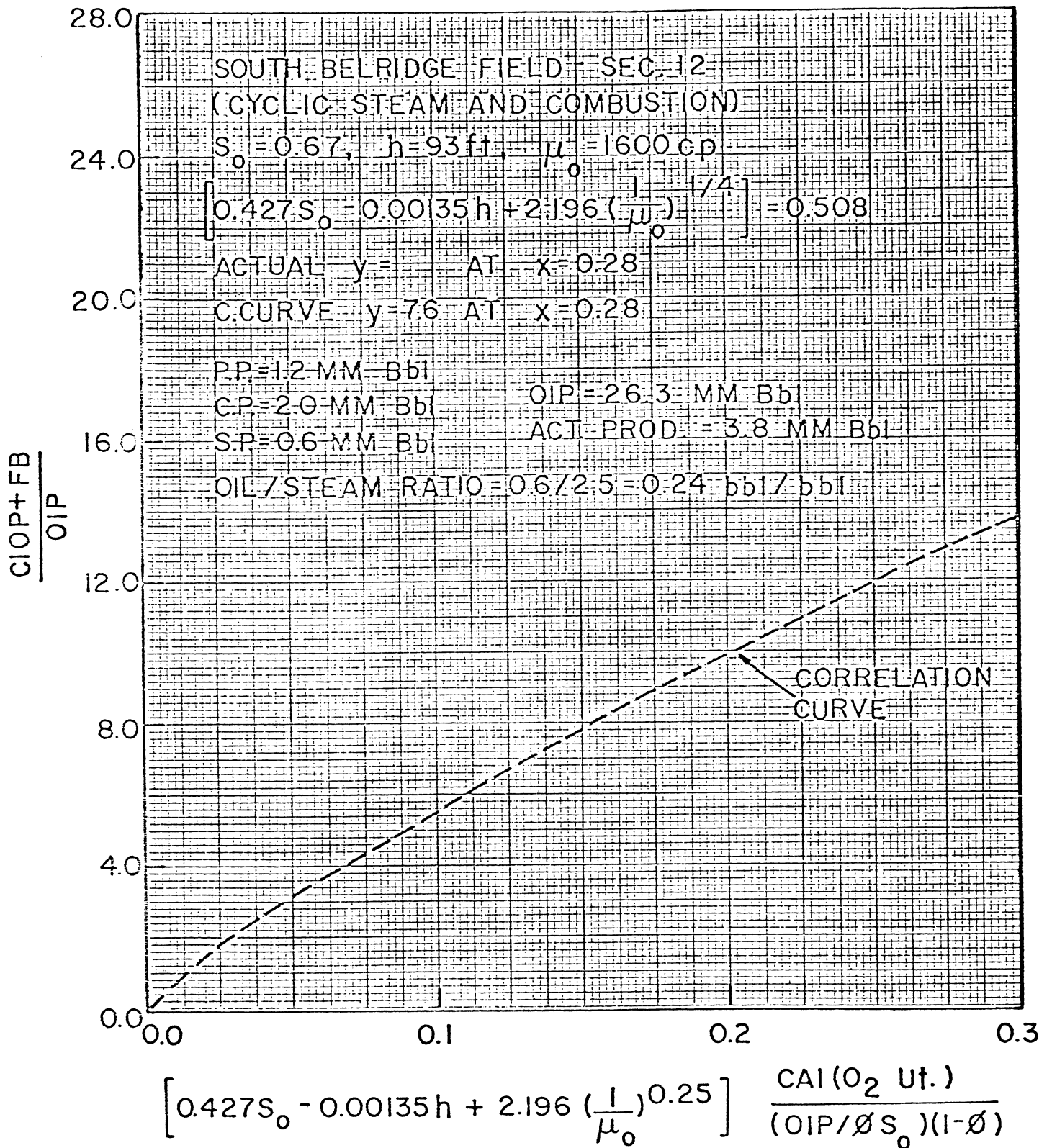


FIG. 31: APPLICATION OF THE SECOND CORRELATION TO THE SOUTH BELRIDGE FIELD

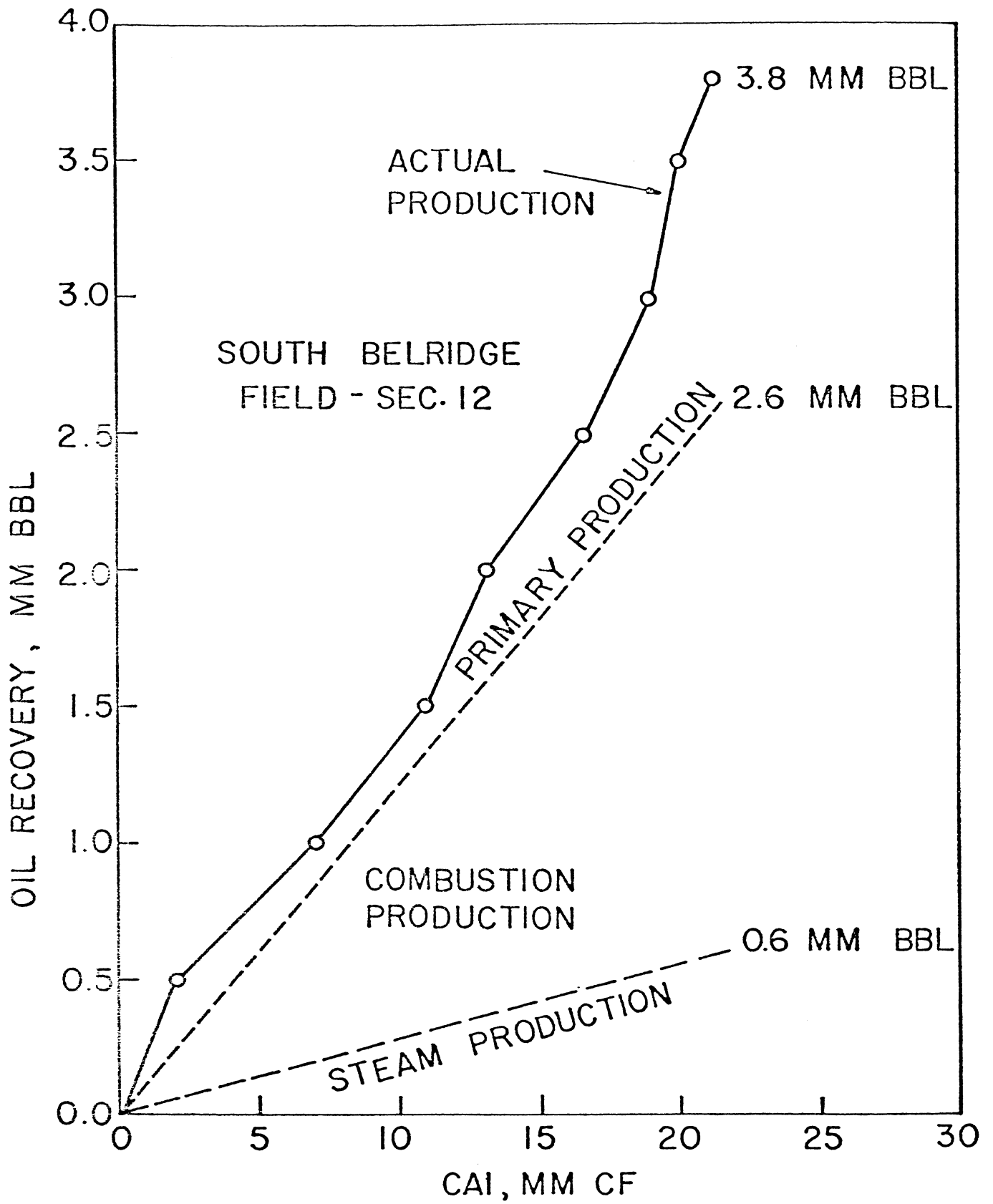


FIG. 32: RESULTS OF THE APPLICATION OF THE SECOND CORRELATION TO THE SOUTH BELRIDGE FIELD

7. CONCLUSIONS

This study has focused on the two important parts of in-situ combustion process:

1) The temperature distribution in the steam plateau portion of the combustion tube experiments has been investigated and a mathematical model has been developed to describe the non-isothermal fluid flow behavior in this region.

2) A case history analysis has been made on the field applications of the combustion process as an enhanced recovery technique and recovery correlations for dry in-situ combustion processes have been developed. Although these two parts seem different, they are interrelated. Combustion process variables investigated in the first part have a significant effect on the oil recovery process. In fact the correlation equations developed in the second part are based on the variables such as fuel burned, oxygen utilization, air injected, and oil saturation which are all studied in the first part.

The results of the analysis of the steam plateau portion of the combustion tube runs indicates that the analytical formulation for the steam plateau can be solved by the method of characteristics and the study of this solution resulted in the following conclusions:

1) The temperature distribution in the steam plateau is principally controlled by phase equilibrium.

2) The steam plateau temperature is set primarily by the air injection pressure and secondarily by the initial water saturation. The rate

of growth of the steam plateau is controlled by the air flux, the initial formation temperature and/or heat loss.

3) Condensation of water and convection of steam and non-condensable gases are important heat transfer modes to describe the temperature distribution in the steam plateau.

4) The mathematical model for the steam plateau agrees favorably with experimental steam plateau behavior for the runs in which pressure drop across the tube is negligibly small.

5) The proper application of the theory presented in this study can be used to determine the overall heat-transfer coefficient.

Based on the case history analysis of in-situ combustion field applications, the following conclusions summarize the second part of the study:

1) A combination of an engineering and a statistical approach to the dry in-situ combustion field case histories indicates that porosity of the formation, volume of air injected, oxygen utilization, amount of fuel burned, oil saturation at the start of the combustion, thickness of the formation and oil viscosity are important parameters to be considered in correlating in-situ combustion recovery. Depth of the formation has no discussable effect.

2) Two correlation curves have been developed for prediction of oil recovery for a dry in-situ combustion field case. The first correlation has a standard deviation of 17% with a maximum error of 21%, compared to a standard deviation of 9% with a maximum error of 14% for the second correlation at the same value of air injection. This indicates that the second is the better one to use. However, the first correlation should be preferable whenever the oil viscosity is small.

3) The oil recovery predictions for simple and rapid engineering calculations for in-situ combustion projects can be made by using these correlations.

4) Application of the correlations indicates that correlations can be used as a predictive device to calculate the relative amount of recovery from each recovery mechanism when several types of enhanced recovery mechanisms are applied in the same field simultaneously.

5) A case history analysis on pilots indicates that air injection and/or oil migration losses are important factors affecting the recovery mechanism of a pilot project. Thus in pilot projects, for the same air injection, the recovery is somewhat less than found in fieldwide cases.

6) The extension of the second correlation to pilot dry in-situ combustion projects shows that the correlation parameters used for fieldwide projects appeared to be reasonable as correlating parameters for dry pilot projects.

7) The number of wet combustion field projects are small compared to the number of dry combustion projects, therefore developing another recovery correlation for them has not been considered.

These conclusions are based on a study of only a small number of field projects. One does not like to make sweeping conclusions based on sparse data. Unfortunately in this case, these are all the data available. The three additional field results help support the correlation work but also are not conclusive. It is recommended that those correlations be tried by others who have in-situ combustion recovery results so that these correlation concepts can be tested further.

NOMENCLATURE

- A = cross-sectional area of core to fluid flow (macroscopic), ft^2
- C_p = specific heat on a mass basis, $\text{Btu}/\text{lb}\text{-}^\circ\text{F}$
- CAI = cumulative air injection, scf
- CIOP = cumulative incremental oil production, bbl
- f_s = mass fraction of steam in the gas phase
- FB = fuel burned, bbl
- h = net thickness of formation, ft
- k_h = thermal conductivity, $\text{Btu}/(\text{hr}\text{-ft}\text{-}^\circ\text{F})$
- L_v = latent heat of vaporization, Btu/lb
- L'_v = latent heat of vaporization, $\text{psi}\text{-cu ft}/\text{lb}$
- M_g = molecular weight of the steam-noncondensable gas mixture, $\text{lb}/\text{lb mole}$
- OIP = oil in place at start of combustion test, bbl
- OOIP = original oil in place, bbl
- $O_2\text{Ut}$ = oxygen utilization, fraction
- p = injection pressure, psi
- p_v = vapor pressure for steam, psi
- q = heat lost to the surroundings, Btu/hr
- r = radius of the combustion tube, ft
- R = gas constant, $\text{psi}\text{-cu ft}/(\text{lb mole}\text{-}^\circ\text{F})$
- S = saturation, fraction
- t = time, hr
- t_{ign} = time spent for ignition, hr
- T' = temperature, $^\circ\text{F}$

T_a = absolute temperature, $^{\circ}\text{F}$

T_D = dimensionless temperature, fraction

T_e = elevated pack temperature, $^{\circ}\text{F}$

T_i = temperature at the beginning of the steam plateau, $^{\circ}\text{F}$

T'_a = sum of absolute temperature and elevated pack temperature, $^{\circ}\text{F}$

u_g = air flux at steam plateau, scf/hr - sq ft

U = overall heat transfer coefficient, through annular insulation
based on radius of combustion tube, $\text{Btu}/(\text{hr-sq ft-}^{\circ}\text{F})$

v_{sp} = velocity of the beginning of the steam plateau, ft/hr

x = distance, ft

x' = distance from the beginning of the steam plateau, ft

y_s = molar fraction of steam in the gas phase

ϕ = porosity, fraction

ρ_g = density of the steam-noncondensable gas mixture, lb/cu ft

μ_o = oil viscosity, cp

$\alpha, \beta, \gamma, \epsilon, \theta$ = constant parameters defined in Equations 16, 23-26

SUBSCRIPTS

a = absolute

e = elevated

f = formation

g = gas

i = initial

o = oil

s = steam

x = x-direction

w = water

REFERENCES

1. Lauwerier, H. A.: "The Transport of Heat in an Oil Layer Caused by the Injection of Hot Fluid," Applied Science Res., Sec. A, 5 (1955), 145.
2. Marx, J. W., and Langenheim, R. H. : "Reservoir Heating by Hot Fluid Injection," Trans., AIME (1959) 216, 312.
3. Ramey, H. J., Jr. : "Reservoir Heating by Hot Fluid Injection Discussion," Trans., AIME (1959) 216, 364.
4. Ersoy, D.: "Temperature Distributions and Heating Efficiency of Oil Recovery by Hot Water Injection," Ph.D. Thesis, Stanford University, August 1969.
5. Atkinson, P.G.: "Mathematical Modelling of Single-Phase Nonisothermal Fluid Flow Through Porous Media," Ph.D. Thesis, Stanford University, May 1976.
6. Arihara, N.: "A Study of Non-Isothermal Single and Two-Phase Flow Through Consolidated Sandstones," Ph.D. Thesis, Stanford University, November 1974.
7. Holst, P.H., Karra, P.S.: "The Size of the Steam Zone in Wet Combustion," Soc. Pet. Engr. J. (February 1975), 13.
8. Chu, C.: "The Vaporization-Condensation Phenomenon in a Linear Heat Wave," Soc. Pet. Engr. J. (June 1964), 85.
9. Willman, B.T., Valleroy, V.V., Runberg, G.W., Cornelius, A.J., Powers, L.W.: "Laboratory Studies of Oil Recovery by Steam Injection," J. Pet. Tech. (July 1961), 681.
10. Szasz, S.E.: "Oil Recovery by Thermal Methods," The Mines Magazine (November 1960), 32.
11. Martin, W.L., Alexander, J.D., Dew, J.N.: "Process Variables of In-Situ Combustion," Trans., AIME (1958), 213, 28.
12. Wilson, L.A., Reed, R.L., Reed, D.W., Clay, R.R. and Harrison, N.H.: "Some Effects of Pressure on Forward and Reverse Combustion," Soc. Pet. Eng. J. (June 1963), 127.
13. Showalter, W.E.: "Combustion-Drive Tests," Soc. Pet. Eng. J. (March 1963), 53.

14. Garon, A.M., Wygal, R.J., Jr.: "A Laboratory Investigation of Fire-Water Flooding," Soc. Pet. Eng. J. (Dec. 1974), 537.
15. Parrish, D.R., Craig, F.F., Jr.: "Laboratory Study of a Combination of Forward Combustion and Waterflooding - The COFCAW Process," J. Pet. Tech. (June 1969), 753.
16. Smith, F.W. and Perkins, T.K.: "Experimental and Numerical Simulation Studies of the Wet Combustion Recovery Process," J. Can. Pet. Tech. (July-Sept. 1973), 44.
17. Boussaid, I.S., Ramey, H.J., Jr.: "Oxidation of Crude Oil in Porous Media," Soc. Pet. Eng. J. (June 1968), 137.
18. Penberthy, W.L., Ramey, H.J., Jr.: "Design and Operation of Laboratory Combustion Tubes," Soc. Pet. Eng. J. (June 1966), 183.
19. Gates, C.F. and Ramey, H.J., Jr.: "Field Results of the South Belridge Thermal Recovery Experiment," Trans. AIME (1958) 213, 236.
20. Poettmann, F.H.: "In-Situ Combustion: A Current Appraisal," World Oil, Part 1 (April 1964), 124-128; and Part 2 (May 1964), 95-98.
21. Geffen, T.M.: "Oil Production to Expect From Known Technology," Oil and Gas J. (May 7, 1973), 66-76.
22. Bleakley, W.B.: "Journal Survey Shows Recovery Projects Up," Oil and Gas J. (March 25, 1974), 69-78.
23. Farouq Ali, S.M.: "A Current Appraisal of In-Situ Combustion Field Tests," J. Pet. Tech. (April, 1972), 477-486.
24. Chu, C.: "A Study on Fireflood Field Projects," Paper SPE 5821, presented at the Improved Oil Recovery Symposium of SPE of AIME, Tulsa, Okla., Mar. 22-24, 1976.
25. Gates, C.F. and Ramey, H.J., Jr.: "Engineering of In-Situ Combustion Oil Recovery Projects," Paper SPE 7149, presented at the California Regional Meeting of SPE of AIME, San Francisco, Ca., April 12-14, 1978.
26. Sarman, A., Soliman, M.Y., Brigham, W.E.: "A Recovery Correlation for Dry In-Situ Combustion Processes," Paper SPE 7130, presented at the 1978 California Regional Meeting of SPE of AIME, San Francisco, Ca., April 12-14, 1978.
27. Stillwaugh, A.M.: "Laboratory Combustion Tube Studies of Lombardi Zone, San Ardo Oil Field," Report, Mobil Oil Co.
28. Stillwaugh, A.M.: "Laboratory Combustion Tube Studies of Tulare 700 Foot Sand, South Belridge Oil Field," Report, Mobil Oil Co.

29. Hardy, W.C.: Personal Communication, April, 1977
30. Nelson, T.W., and McNeil, J.S.: "How to Engineer an In-Situ Combustion Project," Oil and Gas J. (June 5, 1961) 59
31. Hardy, W.C.: "Deep-Reservoir Fireflooding Economics for Independents," Oil and Gas J. (Jan. 18, 1971) 60
32. Alexander, J.D., Martin, W.L., and Dew, J.N.: "Factors Affecting Fuel Availability and Composition During In-Situ Combustion," J. Pet. Tech. (Oct. 1972) 1154-1164
33. McAdams, W.H.: Heat Transmission, 3rd Ed., New York, McGraw-Hill Book Co., Inc. (1954)
34. Moore, W.J.: Physical Chemistry, 4th Ed., New Jersey, Prentice-Hall, Inc. (1972)
35. Craig, F.F., Jr., Parrish, D.R.: "A Multipilot Evaluation of the COFCAW Process," J. Pet. Tech. (June 1974) 659-666
36. Hardy, W.C., Raiford, J.D.: "High Recovery in Old Sand Boosts Fire Flood Optimism," World Oil (Jan. 1976) 80-85
37. Parrish, D.R., Pollock, C.B., and Craig, F.F., Jr.: "Evaluation of COFCAW as a Tertiary Recovery Method, Sloss Field, Nebraska," J. Pet. Tech. (June 1974) 676-686
38. Gates, C.F., Jung, K.D., and Surface, R.A.: "In-Situ Combustion in the Tulare Formation South Belridge Field, Kern County, California," Paper SPE 6554, presented at the 47th Annual California Regional Meeting of SPE of AIME, Bakersfield, April 13-15, 1977
39. Satman, A., Fassihi, M.R., Williams, R.L., Pettit P., Grim, J., Ramey, H.J., Jr., Brigham, W.E.: Laboratory Combustion Tube Studies, SUPRI TR-7, Stanford U., June 1978
40. Fassihi, M.R., Satman, A., Williams, R.L., Pettit, P., Grim, J., Ramey, H.J., Jr., Brigham, W.E.: Laboratory Combustion Tube Studies, Part II, SUPRI TR-10, Stanford U., September 1978
41. Prats, M.: "The Heat Efficiency of Thermal Recovery Processes," J. Pet. Tech. (March 1969) 323
42. Rubinstein, L.I.: "The Total Heat Losses in Injection of a Hot Fluid into a Stratum," Neft i Gaz (1959) No. 9, p. 41
43. Ramey, H.J., Jr.: "How to Calculate Heat Transmission in Hot Fluid Injection," Petr. Engr. (Nov. 1964) 110
44. Ramey, H.J., Jr.: Personal Communication, December 1978
45. Street, R.L.: Partial Differential Equations, Monterey, Brooks/Cole Pub. Co., Inc. (1973)

APPENDIX A

DERIVATION OF ENERGY BALANCE IN THE STEAM PLATEAU REGION

With reference to Fig. 1, an energy balance for a differential element of thickness dx and cross sectional area πr^2 in the steam plateau can be derived as follows.

The energy balance equation is:

$$\text{Heat In} - \text{Heat Out} = \text{Heat Accumulation} \quad (\text{A-1})$$

$$\text{Heat In} = u_g \rho_g (\pi r^2) \left\{ f_s \left[C_w (T' - T_e) + L_v \right] + (1 - f_s) C_g (T' - T_e) \right\}_x$$

$$\begin{aligned} \text{Heat Out} &= u_g \rho_g (\pi r^2) \left\{ f_s \left[C_w (T' - T_e) + L_v \right] + (1 - f_s) C_g (T' - T_e) \right\}_{x+dx} \\ &+ 2\pi r dx U (T' - T_e) \end{aligned}$$

$$\begin{aligned} \text{Heat Accumulation} &= (\pi r^2) dx \frac{\partial}{\partial x} \left\{ (1 - \phi) \rho_f C_f (T' - T_e) + \phi [S_w \rho_w C_w + S_o \rho_o C_o] (T' - T_e) \right. \\ &\quad \left. + \phi S_g \rho_g \left[f_s [C_w (T' - T_e) + L_v] + (1 - f_s) C_g (T' - T_e) \right] \right\} \end{aligned}$$

Or:

$$\begin{aligned} &- u_g \rho_g (\pi r^2) \frac{\partial}{\partial x} \left\{ f_s \left[C_w (T' - T_e) + L_v \right] + (1 - f_s) C_g (T' - T_e) \right\} - 2\pi r U (T' - T_e) \\ &= (\pi r^2) \frac{\partial}{\partial t} \left\{ (1 - \phi) \rho_f C_f (T' - T_e) + \phi (S_w \rho_w C_w + S_o \rho_o C_o) (T' - T_e) \right. \\ &\quad \left. + \phi S_g \rho_g \left[f_s \left[C_w (T' - T_e) + L_v \right] + (1 - f_s) C_g (T' - T_e) \right] \right\} \end{aligned} \quad (\text{A-2})$$

The last term on the right-hand side of this last equation is negligibly small compared to the first and second terms. Therefore, it can be dropped from the equation. Hence, it then becomes:

$$\begin{aligned}
& -u_g \rho_g \frac{\partial}{\partial x} \left\{ f_s [C_w (T' - T_e) + L_v] + (1 - f_s) C_g (T' - T_e) \right\} - \frac{2U}{r} (T' - T_e) \\
& = \frac{\partial}{\partial t} \left\{ (1 - \phi) \rho_f C_f (T' - T_e) \right. \\
& \quad \left. + \phi (S_w \rho_w C_w + S_o \rho_o C_o) (T_i - T_e) \right\} \quad (A-3)
\end{aligned}$$

Assuming constant S_w and S_o leads to:

$$\begin{aligned}
& - \frac{u_g \rho_g}{\rho_l C_l} \frac{\partial}{\partial x} \left\{ f_s [C_w (T' - T_e) + L_v] + (1 - f_s) C_g (T' - T_e) \right\} - \frac{2U}{r \rho_l C_l} (T' - T_e) \\
& = \frac{\partial}{\partial t} (T' - T_e) \quad (A-4)
\end{aligned}$$

where:

$$\rho_l C_l = (1 - \phi) \rho_f C_f + \phi (S_w \rho_w C_w + S_o \rho_o C_o) \quad (A-5)$$

APPENDIX B

TEMPERATURE DISTRIBUTION IN THE STEAM PLATEAU
UNDER ADIABATIC CONDITIONS

The temperature distribution in the steam plateau is given by Eq.

27:

$$(\beta + \gamma T_D + \epsilon T_D^2) \frac{\partial T_D}{\partial x} + \frac{\partial T_D}{\partial t} = - \theta T_D \quad (\text{B-1})$$

The term on the right-hand side represents the heat loss from the system to the surroundings. When the overall heat loss coefficient is set equal to zero, Eq. B-1 becomes:

$$(\beta + \gamma T_D + \epsilon T_D^2) \frac{\partial T_D}{\partial x} + \frac{\partial T_D}{\partial t} = 0 \quad (\text{B-2})$$

Equation B-2 describes the temperature distribution in the steam plateau in the absence of heat loss. Physically, the velocity of a convection wave in the absence of heat loss should be equal to the ratio of the total heat input rate to the total heat capacity of the formation.

The method of characteristics can be applied to solve Eq. B-2. Thus, the equations of the characteristic are:

$$\frac{dx}{(\beta + \gamma T_D + \epsilon T_D^2)} = \frac{dt}{1} \text{ and } dT_D = 0 \quad (\text{B-3})$$

Therefore, on a characteristic:

$$\frac{dx}{dt} = (\beta + \gamma T_D + \epsilon T_D^2) \text{ and } T_D = \text{constant} \quad (\text{B-4})$$

Because T_D is constant on a characteristic, dx/dt is constant also. Thus, the characteristics are straight lines.

From solution of Eq. B-4, we can write:

$$x - (\beta + \gamma T_D + \epsilon T_D^2) t = c_1, T_D = c_2 \quad (\text{B-5})$$

Or, alternatively, we can write a general solution:

$$T_D = g[x - (\beta + \gamma T_D + \epsilon T_D^2) t] \quad (\text{B-6})$$

where g is an arbitrary function of one variable. What Eq. B-6 indicates is that the temperature behind the sharp front of the steam plateau is constant at $T_D = 1$ and the temperature ahead of the front is also constant at $T_D = 0$. Therefore, $x = (\beta + \gamma T_D + \epsilon T_D^2) t$ gives the location of the front at time t where the temperature jump from 0 to 1 occurs.

The behavior of this solution is analogous to the solution describing reservoir heating by hot fluid injection, Marx and Langenheim.² They considered the total area of the heated reservoir to be at constant temperature and developed an expression for the area heated as a function of time. Equation B-5 can be used to estimate the length of the steam plateau, provided the heat loss from the steam plateau into the surroundings is neglected.

APPENDIX C

CALCULATIONS OF THE AMOUNT OF WATER VAPORIZED IN THE REGION
BETWEEN THE BURNING FRONT AND STEAM PLATEAU

Assuming a value for the temperature at the beginning of the steam plateau, T_i , the amount of water vapor in the gas phase can be determined based on the standard combustion calculations, material balance considerations, and phase equilibrium.

In the following computations, the results of combustion run 78-2, given in Table 3, will be used whenever specific values are necessary.

Let us take one cubic foot of core as a basis. The total moles of water vapor in the gas phase, $V_{w\text{ tot}}$, is the sum of the pound moles of water formed due to combustion at the burning front, $V_{w\text{ for}}$, and the pound moles of water vaporized in the region between the burning front and steam plateau, $V_{w\text{ vap}}$. The pounds of water formed per pound of fuel burned can be calculated by using the atomic H-C ratio of the fuel, as follows:

$$\text{lb water formed/lb fuel burned} = \frac{9 (\text{Atomic H-C Ratio})}{12 + (\text{Atomic H-C Ratio})} = \frac{9(0.86)}{12+0.86} = 0.60 \quad (\text{C-1})$$

So:

$$\begin{aligned} v_{w\text{ for}} \left[\frac{\text{lb mole water formed}}{\text{cu ft bulk volume}} \right] &= \left(0.60 \frac{\text{lb water formed}}{\text{lb fuel burned}} \right) \\ &\cdot \left(1.53 \frac{\text{lb fuel burned}}{\text{cu ft bulk volume}} \right) \\ &\cdot \left(\frac{\text{lb mole water}}{18 \text{ lb water}} \right) = 0.051 \quad (\text{C-2}) \end{aligned}$$

The pound moles of water vaporized can be determined as follows:

$$V_{w \text{ vap}} \left[\frac{\text{lb mole water vaporized}}{\text{cu ft bulk volume}} \right] = (\phi) (S_{w \text{ vap}}) (\rho_w) (1/18) \quad (\text{C-3})$$

Since porosity is 0.40, and the density of water at 250°F is 58.8 lb/cu ft, the pound moles of water vaporized is:

$$V_{w \text{ vap}} = (0.40) (S_{w \text{ vap}}) (58.8) (1/18) = 1.307 (S_{w \text{ vap}}) \quad (\text{C-4})$$

The pound moles of non-condensable gases per cubic foot of bulk volume can be approximated by using the air/sand ratio for the run:

$$\begin{aligned} V_{\text{NCG}} \left[\frac{\text{lb mole of non-condensable gases}}{\text{cu ft bulk volume}} \right] &= \left(\frac{11,700,000 \text{ SCF}}{\text{ac-ft}} \right) \\ &\cdot \left(\frac{1 \text{ ac}}{43,560 \text{ ft}^2} \right) \left(\frac{1 \text{ lb mole}}{380 \text{ SCF}} \right) \\ &= 0.707 \quad (\text{C-5}) \end{aligned}$$

Since the steam plateau is assumed to be under equilibrium conditions, the steam plateau temperature can be related to the molar fraction of the water vapor in the gas phase by the following relationship:

$$y_{\text{H}_2\text{O}} = \frac{(p_v)_{T_i}}{p} = \frac{V_{w \text{ for}} + V_{w \text{ vap}}}{V_{w \text{ for}} + V_{w \text{ vap}} + V_{\text{NCG}}} = \frac{0.051 + 1.307(S_{w \text{ vap}})}{0.051 + 1.307(S_{w \text{ vap}}) + 0.707} \quad (\text{C-6})$$

In Eq. C-6, $y_{\text{H}_2\text{O}}$ can be evaluated at any temperature providing the total pressure, p , and the vapor pressure of steam, p_v , at T_i are known. Various values of T_i can be used in Eq. C-4, and corresponding values of

$S_{w\text{vap}}$ can be calculated. Table C-1 shows the values of $S_{w\text{vap}}$ calculated for various T_i 's for Run 78-2.

TABLE C-1: TABULATION OF T_i VERSUS $S_{w\text{vap}}$

T_i , °F	240	245	250	255	260
$S_{w\text{vap}}$, %	0.11	0.13	0.15	0.17	0.20

Except for $S_{w\text{vap}}$ at 260°F, all other values of $S_{w\text{vap}}$ are smaller than the initial water saturation, S_{wi} . This result supports the theory, since we expect to find $S_{w\text{vap}}$ smaller than S_{wi} (=0.20). It was clear from the combustion tube such that the initial water saturation was considerably higher than the irreducible saturation. Water was the first liquid which flowed in this run. Further, a considerable volume of water was produced before any significant volume of oil was produced. Typical irreducible water saturations for sands of this type are often near 15%. In brief, these calculations indicate that the assumed initial steam plateau temperature of 250°F is reasonable.

